REPUBLIC OF TURKEY
THE GRADUATE SCHOOL OF NATURAL AND APPLIED SCIENCES OF ERCIYES UNIVERSITY
MECHANICAL ENGINEERING DEPARTMENT

LOW VELOCITY IMPACT BEHAVIOR OF GLASS FIBER AND CARBON FIBER REINFORCED COMPOSITES

Prepared by
Mohammed Mezher Jabbar AL-Rubaye

Supervisor
Prof. Dr. Zeynep Gül APALAK

Master of Science Thesis

January 2018
KAYSERI

REPUBLIC OF TURKEY
THE GRADUATE SCHOOL OF NATURAL AND APPLIED SCIENCES OF ERCIYES UNIVERSITY
MECHANICAL ENGINEERING DEPARTMENT

LOW VELOCITY IMPACT BEHAVIOR OF GLASS FIBER AND CARBON FIBER REINFORCED COMPOSITES

(Master of Science Thesis)
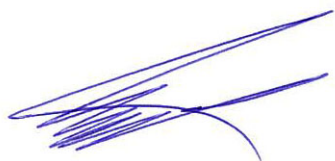

Prepared by
Mohammed Mezher Jabbar AL-Rubaye

Supervisor
Prof. Dr. Zeynep Gül APALAK

January 2018
KAYSERI

COMPLIANCE WITH SCIENTIFIC ETHICS

I hereby declare that all information in this document as been obtained and presented in accordance with academic rules and ethical conduct. I also declare that, as required by these rules and conduct, I have fully cited and referenced all material and results that are not original to this work.
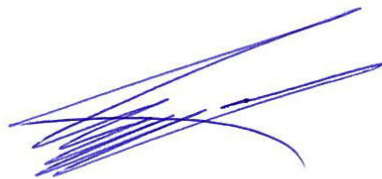
Owner of Thesis

Mohammed Mezher Jabbar Al-Rubaye

COMPLAINCE WITH GUIDELINES

This Master of Science Degree thesis entitled: "**Low Velocity Impact Behavior Of Glass Fiber And Carbon Fiber Reinforced Composites**" has been prepared in accordance with the Thesis Proposal and with the Guidelines for Writing Thesis of Erciyes University.

Thesis Prepared by   **Supervisor**

Mohammed Mezher Jabbar Al-Rubaye   Prof. Dr. Zeynep Gül APALAK

Head of Mechanical Engineering Department

Prof. Dr. Necdet ALTUNTOP

This study, entitled: **"Low Velocity Impact Behavior Of Glass Fiber And Carbon Fiber Reinforced Composites"**, which has been prepared by **Mohammed Mezher Jabbar Al-Rubaye** and supervised by **Prof. Dr. Zeynep Gül APALAK**, was accepted by the jury as M.Sc. Thesis at Erciyes University, Graduate School of Natural and Applied Sciences, Mechanical Engineering Department.

08 /01/ 2018

JURY:

Supervisor   : Prof. Dr. Zeynep Gül APALAK   ....

Juror   : Assoc. Prof. Dr. Recep EKİCİ   ....

Juror   : Assoc. Prof. Dr. Ahmet ERKLİĞ   ....

APPROVAL:

The acceptance of this thesis has been approved by the Institute's Board with the decision number 16/01/2018. and the date of 2018./03.–20

16 /01/ 2018

Prof. Dr. Mehmet AKKURT

Director of the Institute

ACKNOWLEDGEMENTS

This thesis is dedicated to my family, who gave me all the opportunities to accomplish all that I have and the drive to strive higher.

This thesis is individually dedicated to my mother and to my father, who have given me all the opportunities to have a better education and encouraged me to be independent and strong. Thank you for your guidance, encouragement, support and love over the years. To my loving wife, who has always been a big supporter to accomplish this thesis and always been there every time I needed. Thank you for your patience, encouragement and love.

I wish sincerely to thank my supervisor Prof. Dr. Zeynep Gül APALAK for her suggestions, encouragements and guidance in writing and approaching the different challenges during the thesis. She helped me to extent my academical borders and enriched my vision. Also I would like to thank Research Assist. Umut ÇALIŞKAN for all his encouragements and supports during this valuable journey.

Finally, I want to thank my colleagues for their support in completion of this thesis.

Mohammed Mezher Jabbar AL-Rubaye

January 2018

LOW VELOCITY IMPACT BEHAVIOR OF GLASS FIBER AND CARBON FIBER REINFORCED COMPOSITES

Mohammed Mezher Jabbar AL-Rubaye

Erciyes University, Graduate School of Natural and Applied Sciences
M.Sc. Thesis, January 2018
Thesis Supervisor: Prof. Dr. Zeynep Gül APALAK

ABSTRACT

Impact can be defined as a momentary external force applied on a material or structure in a very short time at low, medium or high speed.

In this study, the behaviors of glass fiber / epoxy, carbon fiber / epoxy, carbon fiber glass fiber / epoxy hybrid symmetric and non-symmetric composites under impact load were investigated experimentally and numerically. For this purpose, 8 layers of symmetric and non-symmetric specimens with dimensions of 100 x 100 mm were produced in the Mechanics Laboratory of Mechanical Engineering Department. Different ply angles have been considered to examine the effect of fiber angles on impact behavior. Low-velocity impact tests were performed on Ceast Brand Fractovis Plus test machine. Impact tests of non-symmetric hybrid composites were performed on both surfaces. 10J, 20J, 30J, 40J impact energies were applied through the composite plate. Finite element method used for numerical analyses and its results were compared with experimental results. Damage surfaces of the specimens were optically investigated. As a result of experimental and numerical studies, close results have been obtained.

Keywords: Layered composite materials, hybrid composite, impact, nonlinear finite element method.

LOW VELOCITY IMPACT BEHAVIOR OF GLASS FIBER AND CARBON FIBER REINFORCED COMPOSITES

Mohammed Mezher Jabbar AL-Rubaye

Erciyes Üniversitesi, Fen Bilimleri Enstitüsü
Yüksek Lisans Tezi, Ocak 2018
Danışman: Prof. Dr. Zeynep Gül APALAK

ÖZET

Darbe düşük, orta veya yüksek hızlarda çok kısa bir süre içinde bir malzeme veya yapı üzerinde uygulanan anlık bir dış kuvvet olarak tanımlanabilir.

Bu çalışmada, cam elyaf/epoksi, karbon elyaf/ epoksi, karbon elyaf-cam elyaf/epoksi hibridsimetrik ve simetrik olmayan kompozitlerin darbe enerjisi altındaki davranışları deneysel ve sayısal olarak incelenmiştir. Bu amaçla 100 x 100 mm boyutlarında 8 tabakalı cam elyaf/ epoksi, karbon elyaf/epoksi, karbon elyaf-cam elyaf/epoksi hibrid simetrik ve simetrik olmayan numuneler Mühendislik Fakültesi Mekanik Laboratuvarlarında üretilmiştir. Fiber açılarının darbe davranışı üzerine etkisini incelemek için farklı takviye açıları belirlenmiştir. Düşük hızlı darbe testleri Ceast Marka Fractovis Plus test cihazında yapılmıştır. Simetrik olmayan hibrid kompozitlerin darbe testinde karbon yüzeye ve cam yüzeye ayrı ayrı darbe uygulanmıştır. 10J ,20J,30J, 40J şeklinde darbe enerjileri kompozit plakalara ortadan uygulanmıştır. Sonlu elemanlar metodu kullanarak yapılan sayısal analizlerle deneysel sonuçlar mukayese edilmiş ve hasar yüzeyleri incelenmiştir. Deneysel ve sayısal çalışmaların sonucunda birbirine yakın neticeler elde edilmiştir.

Anahtar Kelimeler: Tabakalı kompozit malzemeler, hibrid kompozit, darbe, lineer olmayan sonlu elemanlar yöntemi.

CONTENTS

LOW VELOCITY IMPACT BEHAVIOR OF GLASS FIBER AND CARBON FIBER REINFORCEMENT COMPOSITES

CHAPTER ONE

OVERVIEW

CHAPTER TWO

INTRODUCTION TO COMPOSITE MATERIALS

LIST OF ABBREVIATION

(-)	Refers to the adverse result
(+)	Refers to the met of criterion
E_k	The maximum energy was applied
G^C	The fracture energy dissipated during the damage process
S^L	The longitudinal strength
S^T	The transverse shear strength
X^C	The compressive strength
X^T	The longitudinal tensile strength
Y^C	The compressive strength
Y^T	The transverse tensile strength
Y_k	Thickness of the first ply (impact side)
c_{ij}	Stiffness coefficients
d_f	The damage variables for fibre mode
d_m	The damage variables for matrix mode
d_s	The damage variables for shear failure mode
x_k	The value of proportionate decrease in thickness of successive plies of the laminate
x_1	The coefficient determining a decrease in thickness of the first laminate ply
γ_{ij}	Shear strains
δ^f_{eq}	The displacement at which the material is completely damaged in this failure mode
δ^f_{eq}	The various modes depend on the respective G^C values
δ^0_{eq}	The initial equivalent displacement at which the initiation criterion for that mode was met

$\boldsymbol{\varepsilon_{ij}}$	The strains
$\boldsymbol{\sigma_{ij}}$	Stresses in ij directions
$\boldsymbol{\tau_{ij}}$	Shear stress
DAS	Data Acquisition System for Fractovis Plus Low velocity impact tester
E	Energy
E	Constant coefficient of decrease in thickness of successive laminate plies for any impact energy
GRP	Glass-reinforced plastic
HSNFCCRT	Compression fiber criterion
HSNFTCRT	Tension fiber criterion
HSNMCCRT	Compression matrix criterion
HSNMTCRT	Tension matrix criterion
J	Joule
M	The damage operator
ms	Meter in the second
t	Time
z	The nominal thickness of the undamaged ply

LIST OF TABLES

LIST OF FIGURES

CHAPTER ONE

OVERVIEW

Computer simulations are used for design and development across many fields. In these simulations, the last step is verification. These simulations are much cheaper and easier to build than full-scale, real-life models. For aircrafts, there are various events that must be studies related to impact, such as dropping tools or debris collision on a runway. These obstacles can cause major harm to the vehicle and are often unseen. Because of loads that fluctuate during use, such as compression, the area of damage can grow and even cause complete structural collapse of the part with damage. This research deals with damage to forecast with accuracy how low velocity impacts can harm composite laminates.

Physical damage comes from stress or strain. Fractures are when the materials crack due to energy changes, as in when a crack causes lower energy within the system. In scientific terms, the energy needed to overcome the cohesive atom force equals the strain energy dissipation that the crack releases.

For homogenous metals, fractures and material damage are separate from one another. That said, they may occur at the same time, or one may cause the other. In composites, however, damage and cracks may occur concurrently. Low speed impacts will cause excessive stress to the matrix and produce micro-cracking. It may not, however, result in a fracture. It will change the distribution of loads and energy concentration, as well as produce stress at the inter-ply areas because of material stiffness variances. Cracks produce changes throughout the material, in both the section properties and load paths.

Researchers have focused on ballistic impacts over the last several years and they have built many mechanisms dealing with penetration. There are studies done analytically, as well as those done mathematically where the finite difference methods are preferred.

Pegoretti, et al. [1] studied homogenous and hybrid composites made from e-glass and PVA fibers using polyester resin. They focused on how impact effects the intra and interply composites, looking at the loading direction and stacking sequence. The experimentation showed that the e-glass and PVA hybrids outperformed the standard homogenous e-glass composites under these criteria. PVA fibers allowed for better impact energy results. The experiments also showed that cracks were more common in intraply hybrids because of the ductility.

Shi and Soutis [2] studied new modeling advances regarding low velocity impact damage in composite laminates with fiber reinforcements. They asserted that using the finite element methods are reducing reduce the necessity for long term testing of materials. Their study strengthened these models due to validating FE compared with non-destructive techniques.

Grasso, et al [3] studied the impact behaviour of thermosetting composite materials for aeronautic applications. The main goal of the experimental activity was to identify the energy level in correspondence of which penetration occurs. The initial values of the impact energy were estimated according to analytical correlations found in literature. Tests were performed on three types of composite panels: carbon fibre laminated panels, fiberglass laminated panels and hybrid panels. The technology of lamina is that of prepeg fabric with twill sequence and fibres weaving at 0°- 90° and ± 45°. The fixture used for tests is a Charpy impact test machine, which was conveniently equipped to evaluate the angular variation and the acceleration of the impacting mass. Comparisons among the results obtained for specimens made up of just one type of reinforcement (glass or carbon) and the results obtained with hybrid specimens were performed.

Nisini et al. [4] investigated tensile, flexural, interlaminater shear strength and low velocity impact properties of triple hybrids including carbon, basalt and flax fibers in an epoxy matrix. Both configurations involved the use of carbon fibers on the outside, twill basalt and flax fibers were placed internally either in a sandwich or in an intercalated sequence. They were subjected to tensile, flexural and interlaminar shear strength test, then to drop weight impact with three different energies, 12.8, 25.6 and 38.4 J, studying damage morphology and impact hysteresis cycles. Intercalation of basalt with flax layers proved beneficial for flexural and interlaminar strength. As regards impact

performance, the differences between the two laminates were quite limited: however, the presence of a compact core of flax fiber laminate or else its intercalation with basalt fiber layers had a predominant effect on impact damage features, with intercalation increasing their complexity.

Abir, et al. [5] performed Compression After Impact (CAI) tests to characterize the effect of impact damage on strength of composites. Failure during CAI was found to be triggered by local buckling, causing fiber and delamination damage growth (during compression) that leads to rapid and sudden load drop. Compressive strength, Mode I fibre compressive fracture toughness and Mode II interlaminar fracture toughness were found to be the key parameters that affect residual strength of composites. Such models can lead to a better understanding of damage growth mechanisms necessary for development of damage tolerant structures, as well as promote virtual testing, with considerable cost and time savings.

Rajesh and Jerald [6] studied how woven glass fiber composites with an epoxy matrix respond to low velocity impact using ASTM standards with a drop weight machine. They located the response and location of damage at impact velocities between 2 and 4.5 m/s and with energy levels between 3 and 15 J. They noticed a disastrous laminate response at 4.429 m/s. They discovered that failure is either from cracking or laminate perforation.

Singh, et al [7] proposed predictive models for low velocity impact of fibre reinforced composite made from epoxy and e-glass using continuum damage mechanics. They compared damage on area with minimal protection, the contact forces, and displacement occurred based on time.

Duodo, et al [8] studied how ballistic impact events for a composite of carbon fiber and epoxy, as well as structures made from steel. They used a sphere ball for the projectile in the test and the ABAQUS software for forecasting the initial response, how damage progresses, and where energy is absorbed. Their experimental data was in line with the simulation and noted that a ballistic limit of 134 m/s. The study also indicated that the carbon epoxy composite performed better than the steel structures for impact damage and energy absorption.

Liao and Liu [9] studied dynamic mechanical responses and damage mechanisms of plastic fiber-reinforced polymer matrix composite laminate under low velocity impact. First, the plastic damage model is introduced for intralaminar damage, where Puck's failure criteria and strain based damage evolution laws for fiber and matrix are used, and the bilinear cohesive model is adopted for delamination. Second, an uncoupled numerical scheme for dealing with the intralaminar plastic deformation and damage evolution by finite element analysis (FEA) is originally proposed based on the strain equivalence hypothesis, in which the effective stresses and strains are first solved using the backward Euler algorithm and then the nominal stresses and damage variables are updated independently. Finally, the proposed algorithm is implemented using ABAQUS-VUMAT by the time stepping algorithm. For two composite specimens under transverse impact, the impact force-time curve, the impact displacement-time curve and the dissipated energy at different impact energies are studied by comparing the results using experiments and FEA. Numerical results show the plastic damage model leads to higher precision than the elastic damage model as the impact energy becomes relatively large.

Fend and Aymerich [10] studied models that showcased progressive damage to forecast how the structure responds as well as what causes failure in composites with low velocity impact damage. They produced models for both intralaminar and interlaminar damage using the ABAQUS software with VUMAT subroutines programmed by the team. They next compared the models with experiments in drop weight impact and X-Ray technology. The model they devised accurately predicted damage and response time in the laminates, as well as the sequence of damage. The data between the models and testing matched, so the team then analyzed their findings to predict delamination in the interface. This analysis indicated that intralaminar damage modes are needed to simulate impact delamination patterns.

Li, et al. [11], investigated experimentally on the impact behavior of pultruded composites samples subjected to low-velocity impacts with higher impact energies ranging from 16.75 to67 J. The specimens were placed and supported according to the requirement of ASTM 7136 standard. The results of impact characteristics and performance are demonstrated and compared for different impact energy levels. The damage evaluation is also introduced to compare the failure modes of pultruded

composites subjected to different energy levels. The development and propagation of stress during the low velocity impacts are analyzed using the finite element method. The numerical predictions were found to corroborate the experimental results in terms of load-time and central deflection-time curves.

Singh and Mahajan [12] crafted a damage model for FRP composites by the use of damage progression and deformation caused by low velocity impact. They used the exponential softening model to predict damage grows in the 3D plastic. They wrote a VUMAT code and entered it into the ABAQUS software to determine the material softening using the single element model for finite element simulation.

Ahmed and Wei [13] studied the progress in dynamic and static response of composite structuressubjectedtolowvelocityimpactandquasi-staticloads.Thisreview paper focused on experimental and numerical studies done by many authors recently forthe low-velocity impact damage. For simulations of drop weight low-velocity impact damage, many researchers used software programs in order to predict the failure modes in composite structures such as ABAQUS/Explicit, LS-Dyna, and MSC. Dytran, DYNA3D, and 3DIMPACT have been commonly used. The impact response of high performance fiber composites is reviewed. An attempt is made to collect the work published in the literature and to identify the fundamental parameters determining the impact resistance of composite materials and their properties. The review concludes with detailed discussions on the damage mechanisms and failure criteria for composite structures subjected to impact loads.

Bienias, et al. [14] studied the severity of damage and where damage occurs in fiber metal laminates under low velocity impact. They tested plates of 1.5 through 3.5 mm thickness made from a composite of aluminum and epoxy glass made with autoclave. The experiments took place at room temperature with a drop-weight impact tester using 10 and 25 J impact energy. The study produced favorable results regarding internal damage and force versus time, indicating that the tested laminates have an inner structure to withstand damage. Delamination took place at the interlayers and cracks in the lower layers.

Chang, et al. [15] studied on impact damage on laminated composites from a line-nose impactor, looking at what fails after impact and why. The team focused on cracking in

the matrix as well as delamination. The team built a special facility for testing, where the rectangular barrel could be used to create equal impact from the line-nose machine. They tested T300/976 graphite and epoxy composites. They x-rayed and c-scanned each of the test items before the test and then after the impact, looking for the specific area of damage. The team also built a model to predict impact damage at certain locations. The model supported the test results and showed four things: cracks in the matrix took place first, this caused delamination, laminates with prior cracks display more damage than those without, shear and tensile stress cause matrix cracking.

Xu, et al. [16] studied scaling resulting from low velocity impact in CFRP panels with models and experimentation. They used a drop-weight impact tower for the experiment and ABAQUS's finite element solver for the simulation. Both the experiment and simulation showed that when energy passes the threshold, scaling increases, although it does not follow a regular pattern. Larger samples received more damage with scaled impact energy.

Caminero, et al. [17] investigated a major affect the efficient use of composite laminates under the effect of low velocity impact damage on the structural integrity. The aim of this study is to characterize and assess the effect of laminate thickness, ply-stacking sequence and scaling technique on the damage resistance of CFRP laminates subjected to low velocity impact. Drop-weight impact tests are carried out to determine impact response. Ultrasonic C-scanning and cross-sectional micrographs are examined to assess failure mechanisms of the different configurations. It is observed that damage resistance decreases as impact energy increases. In addition, thicker laminates show lower absorbed energy but, conversely, a more extensive delamination due to higher bending stiffness. Thinner laminates show higher failure depth. Furthermore, quasi-isotropic laminates show better performance in terms of damage resistance. Finally, the results obtained demonstrate that introducing ply clustering had a negative effect on the damage resistance and on the delamination area.

Chang, et al. [18] used the 3D progressive finite element model to study low velocity impact in scarf repaired laminates by simulation. Their model showed that patch stacking and the angle of rotation have strong effects on impact damage. However, the rotation is plays a larger role.

Lou, et al. [19] worked on a study that challenged existing theories to locate the modes of failure in both the fiber itself and the matrix, as it relates to microscales and delamination. The team used the ABAQUS software and the finite element model for CFRP. The team pin-pointed the exact moment delamination begins in the composite. The team last analyzed the computer simulation against experimental data, to see if the results agreed, to which they were.

Jagtap, et al. [20] studied the response of carbon/epoxy laminated plates subjected to low velocity impact loading. In this work impact damage is predicted at the time of initiation when maximum stress failure criteria are satisfied. 3D finite element model of composite laminate is generated. Impact simulation was performed using finite element software LS-DYNA with 3-D solid elements. Failure modes in composite laminate such as matrix cracking, delamination were studied. Force and deformation response in impact damage is estimated with varying mesh sizes. The effect of various parameters, such as clamped or simply supported boundary conditions and impactor velocity (impact energy) are examined through parametric study.

Liu, et al. [21] studied on what causes failure and the overall effect. They used various criteria to test dynamic progressive failure of laminates composites of carbon fiber: Chang-Chang, Hashin, and Puck. They created three models using these criteria in the ABAQUS software and then analyzed the specimens of various materials. The three models showed similar results, except for delamination and matrix cracking. This study indicates that the various criteria could be used in accurate simulations.

Ravandia, et al. [22] studied on the experiments of natural fiber stitches to test the impact response of a composite of woven flax and epoxy, pointing to their usage in high performance situations. They carried out both a perforated and non-perforated test in both stitched and unstitched composites. The team used flax yarn and twisted cotton for equal length laminates, as well as cross-piles of flax fibers to learn the benchmark energy absorption and fracture figures. The team learned that stitching will progress cracking, however that thicker yarns reduced energy absorption.

Antonucci, et al [23] studied on carbon fiber composites with low velocity impact, testing materials produced with pulse infusion (a new composite production method using vacuums). They used various energy levels to test complete penetration and used

the CAI tests to look for residual strength of the materials. All of the experiments noted that the new technology produces better quality materials, better suited for impact damage.

Wang, et al. [24] studied thick composite delamination with low energy impacts to predict damage. They used three materials with different stacking sequences set to specific energy levels and nondestructive testing as well as model simulations. The findings are as follows: delamination is limited to the area of impact and is less as you progress down the layers.

Tirillò, et al. [25] studied the effect of basalt fibre hybridization on carbon/epoxy laminates when subjected to high velocity impacts. In this regard, interply hybrid specimens with four different stacking sequences (sandwich-like and intercalated structures) are tested and compared to non-hybrid reference laminates made of either only carbon or only basalt layers. The response to high velocity impact tests is assessed through the evaluation of the impact and residual velocities of the projectile and the ballistic limit, calculated using experimental data, is compared with the results given by an analytical model, showing a good agreement. The damage in composite laminates is investigated by destructive (optical microscopy) and non-destructive (ultrasonic phased array) techniques. As a result of basalt hybridization, the ballistic limits of all sandwich configurations are enhanced if compared to those of carbon laminates. Therefore the observed decrease of static mechanical properties of hybrid composites is largely compensated by improved response to impact. Advantages also come in terms of cost saving, since the basalt fibre is far less expensive than the carbon one.

Boria, et al. [26] studied the results of an experimental campaign made on a fully thermoplastic composite, where both the reinforcement and the matrix are made in polypropylene. The target is to analyze its behavior under different impact loading conditions using a drop weight testing machine. The influence of the impact mass and of the velocity on the energy absorption capability of the material have been analyzed and discussed. During the tests, the material showed a ductile behavior and developed extended plasticity without a crack tip. The main observed damage mechanisms were the yarn sliding.

Camanho et al [27] studied 3D failure mechanisms in composites reinforced with fibers, related to tensors. They used the invariant theory to produce transverse and longitudinal failure mechanisms. The study noted that maximum strain is related to failures along the longitude. They were able to predict failure using a 3D kinking model that uses invariant failure criteria inspired by typical polymer failure. They noticed minimal failure in the IM7/8552 carbon fiber reinforced polymer based on shear behavior. The study compared the numerical analysis with test results, to find agreement between the two.

Daniel, et al [28] studied and characterized failure prediction methodology using fibers and matrix in a single ply and lamina material. He crafted a new theory called the NU-Daniel theory to forecast lamina strength and what causes failure at various states of multi-axial stress. This theory is specifically related to interfiber and interlaminar failure based on the matrix. This new theory allows for fast evaluation of composites without heavy experimentation.

Bienias, et al. [29] studied CARALL and GLARE type multidirectional fiber metal laminates were subjected to interlaminar fracture toughness tests by End Notched Flexure method. The critical strain energy release rates were calculated based on authors developed methodology of recent analytical Enhanced Beam Theory, and then verified by standardized experimental Compliance Calibration method. With increase of fiber orientation angle (0,45,90) at the metal composite interface, the determined critical strain energy release rate significantly decreased.

Mitchell, et al. [30] studied two structural analysis procedures for composites reinforced with fibers. Each of the models was successful at textile geometry prediction. The first model is beam-shell, which means fibers are beams and the matrix is the shell. They used the beams from their initial model to find the fabric shape after deformation. The double-orthotropic shell model was used second. Here, too shells (acting as fibers) were superimposed and in alignment with the proper direction of each fiber. These two models were then compared against the classical laminate theory and also to the data from experimentation. Through the results, the team found that the double orthotropic shell model is the better option.

Banerjee and Sankar [31] used the finite element procedure to analyze the volume of hybrid composites in one direction. The researchers presumed either hexagonal or circular fibers. They used the Halpin-Tsai equations to study both the shear and transverse elements of the fibers. The findings indicate a minimal elasticity constant and longitudinal strength between the two, but big differences in transverse strength.

Azzan and Li [32] studied two sequences of stacking to locate the three-point bending load of composite materials using an electronic universal tester. They used an optical microscope to study delamination and damage from bending, as well as the shape of damage in the composites. The first composite $[0/90/-45/45]_{2S}$, was weaker than others in fiber, splitting, and delamination, while the second $[45/45/90/0]_{2S}$, has a high curve of non linear load displacement.

Olodo, et al. [33] studied the experiment of a glass/polyester composite laminate under impact shock. Based on a thermodynamic approach, the objective is the evaluation of specific interlaminar delamination energy in a multi-layer composite material under impact loading causing damage to it by cracking. For modeling impact loading, it is used an experimental device based on the principle of Charpy test which is to measure residual energy of a mass movement following a shock at speeds generally between 1 and 4 m/s, on a test piece cut of standardized dimensions requested in bending. Some of available energy is consumed by the rupture of the test piece. The results of this work showed that for impact test, mode I fracture energy is function of impact speed and the load fall energy. These results could be useful in the design of multilayer structures in composite materials subjected to impact loads.

Reghunath et al [34] studied the experiments on woven composites with glass fiber reinforcements to find impact response based on differing volumes, hoping to find the best for impact resistance. They used vacuum bagging to make the test samples and resin burn off to establish the volume fractions. They also used a scanning electron microscope to find surface topography data. The experiments varied they impact velocity minimally. They discovered that a percentage of 43 or 44 volume fraction is optimal for resistance. This is confirmed from the SEM data, which also revealed that cracking, breaking fibers, fiber pulling, and debonding all result in failure during impact.

Mouti, et al. [35] studied the automobile components under the engine, focusing on the oil pan. Oil pans were once made from stamped steel or cast aluminum. Today, they are made with polyamide with glass fiber reinforcements. That said, these new oil pans are weak to impact loading. This often occurs when roadside stones are shot into the oil pan and cause low velocity impact. They used a gas fun and drop weight tower in the experiments. They discovered that oil pan design helps absorb shock by combining the ribbing and shape into an impact resistant design.

Bieniaś and Jakubczak [36] studied fiber metal laminates as a new kind of hybrid materials. There are good candidates for advanced aerospace structural applications due to their high specific mechanical properties. The study researches the resistance to low-velocity impact of hybrid laminates based on aluminum alloys and a carbon/epoxy composite (Al/CFRP). These are completely new materials which have higher strength properties compared to other materials of this type (GLARE, ARALL), high fatigue strength, low weight, etc. The tested laminates were prepared by the autoclave method, which provides the best possible and repeatable quality of the received components. The laminates were analyzed in terms of a comparison of their impact resistance according to different layer configurations and different energy levels. The laminates response to low velocity impact using a hemispherical tipped impactor (diameter 12.7 mm) were analyzed. The variation of the impact load as a function of force-time for different layer systems at each energy level was determined. After the tests, the damage zone was evaluated by using ultrasonic and image analysis methods. On this basis, the dependencies of the damage zone area and maximum depth of the deformation depending on the layer configurations and energy level were determined. It was noted that Al/CFRP laminates are innovative materials characterized by high impact damage resistance (at low-velocity) because of the superior properties of both metals and fibrous composite materials with strong adhesion bonding. There is a combination of high stiffness and strength from the carbon/epoxy composite layers and good mechanical, ductile properties from aluminum. Generally, specific parameters such as incipient load (Pi), peek load Pm, maximum depth and damage area increased with impact energy. For lower impact energies (up to 10 J) and the first stage of the impact process, minor matrix cracking and delamination in the polymer composite and at the aluminum/composite interface may be observed. However, as the impact energy

increased, fiber failures were observed to be the dominant damage mode. The first crack of FMLs (on the back side) related to the fiber directions in the finally layer of the carbon epoxy composite. The ply configuration (fiber directions) in Al/CFRP laminates has been particularly important for their impact resistance. The FML with (0/90) and (±45) ply sequences in the carbon fiber reinforced composite have the best behavior followed by the (0) configuration.

Nassr, et al. [37] studied an experiment to determine the damage and wave propagation characteristics in Glass Fibre Reinforced Polymer (GFRP) panels subjected to impact by steel balls at relatively low velocities up to $91 \ \mathrm{ms^{-1}}$. While maintaining the same impact energy level, the influence of ball mass onpanel response was studied. The effects of composite lay-up sequence and successive impacts were also investigated. The wave propagation characteristics, including wave types, wave velocities, wave attenuations, and strain rates, were extracted from dynamic strain records measured at various locations on the panels. The results showed that, for the same level of impact energy, the small ball mass produced larger deformation and delamination than the large ball mass. Additionally, the resistance to impact was influenced by the composite lay-up sequence of similar fiber weight fraction. Test panels subjected to successive impacts showed an increase in cumulative delamination areas, whereas the tests indicated that successive impacts had a little effect on the perforation limit of the test panels. The impact velocity showed a pronounced influence on the measured peak strains and strain rates. The flexural wave was the predominant wave system, propagating at different velocities in different directions. In proximity to the impact site, both flexural wave and indentation predominated over the transient response. In addition to the flexural wave, impact induced low amplitude tensile longitudinal waves of high velocity.

Park [38] used the finite element method to study the behavior of steel plates and a composite of graphite and epoxy under low velocity impacts. This experiment proved that the finite element model is accurate when predicting damage, specifically related to how the plates behave due to changes in weight and velocity during specific loads. The composite plate had double the performance of the steel under such impact because of the flexibility in handling the displacement for impact absorption.

Dogan and Arikan [39] studied an experiment on impact response of sandwich composite panels with thermoplastic and thermoset face-sheet. E-glass reinforced epoxy (thermoset) and polypropylene(thermoplastic) have been used to produce polymer composite face-sheets. PVC foam was used as a core material. Several low velocity impact tests were performed under various impact energies. Besides to the individual impact behavior of the thermoset and thermoplastic sandwich composites, the impact response of sandwich composites having hybrid sequences was also investigated. Along with images of damaged samples, variations of the impact characteristics such as absorbed energy, maximum contact force and maximum deflection of the samples are provided. Most particularly this study showed that sandwich composites must have the harmony between core and the face sheet material. The deformation required for core densification must be able to compensate by the face sheet material.

Salvettia, et al. [40] studied assessment of the influence of embedded optical fibres on the mechanical response of a CFRP composite laminate with a specific focus on their effect when laminates are subjected to low velocity impact and compression after impact (CAI) tests. Although several studies are present in the literature, univocal conclusions based on their results are difficult to be drawn. Indeed, impact and compressive after impact performances depend on a plethora of different parameters in addition to the typical experimental uncertainty. First, the impact behaviour of a specific specimen configuration has been studied in terms of dynamic features, such as the impact force and displacements, and the absorbed energy. Then, the impact damage is assessed through macro-scale non-destructive testing, including ultrasonic and computed tomography. Furthermore, optical microscopy and SEM imaging have been conducted at a micro-scale level for a limited number of specimens. Conclusively, CAI tests have been performed and conclusions on the variation of the compressive strength and stiffness have been presented.

CHAPTER TWO

INTRODUCTION TO COMPOSITE MATERIALS

2.1. Composite characteristics

The constituents of a composite are generally arranged so that one or more discontinuous phases are embedded in a continuous phase. The matrix is the continuous phase while the reinforcement is discontinuous [41]. When rubber hangs in a stiff rubber matrix, this represents an exception to the above and are known as rubber-modified polymers. These materials have more tough and durable reinforcements than matrices. These parts, however, cannot act independently of one another, and both are entirely necessary to carry out duties in the composite. Fibers are stronger than bulk materials. This is because during bulk production, there are a number of tiny flaws that arise that could lead to fracture. These are limited when the material is thinned out. The matrix acts as a binder that separates the fiber material. These binders are difficult to pull apart because of knots and twists in their design. They should cover the fiber completely and also remain separate from connecting fibers for ease of access and use. Composite characteristics are strongly dependent on both physical and mechanical characteristics including the geometry and constituent concentration. When reinforcement volume is increase, the overall strength of the material will increase as well. However, if the volume is too much, then there is not enough matrix between them and intermingling can occur. The composite design depends on how reinforcements are arranged around the matrix. As such, all of these characteristics must be considered when designing such materials.

Stress and strain are studied in correlation to one another using such theories as Hook's Law. Isotropic and homogenous materials are supposed to be universally uniform with identical elasticity in every direction. Under uniaxial tensile loads, materials can deform as shown by Figure 2.1. The dotted lines in the diagram represent the material without deformation. With an assumed thickness and width, the in and out-of-plane displacement are uniform. Composites are nonhomogeneous with behavior unlike isotropic materials (such as those typically used in engineering). Composites fall under either anisotropic or orthotropic.
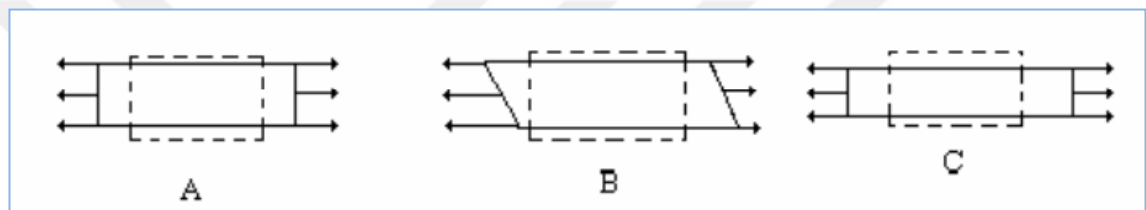
Figure 2.1. Axial Tension response for Isotropic (A), anisotropic (B), and orthotropic (C) materials.

Anisotropic materials have unique properties in each direction. Usually, after axial tension, there is coupled extension and shear deformation. Each material has unique behavior and deformation qualities. Unlike orthotropic materials (with three perpendicular planes), anisotropic materials have no shear-extension coupling. The in and out of plane displacements are different due to Poisson's ratio varying per the two directions.

2.2. Classification of Composite Materials

Composites have at least two phases that are chemically different with an interface separating them. The matrix is the continuous element and is most often found in large quantity. Within a composite, or a material made from two or more substances, the matrix can be polymeric, metal, or ceramic, and each have vastly distinct qualities. Metals are intermediate in strength and aren't brittle. Polymers are the weakest. Ceramics, then, are the strongest with durability and are very brittle.

The reinforcement is the second composite element and acts to strengthen the matrix. It is usually stronger and stiffer than the matrix. However, there is a substance known as

ductile metal that has a ceramic matrix and the reinforcement is elastic. For all reinforcements, one or more of it dimensions are very small. Its size and shape are critical in determining overall effectiveness. It can be either made from particles or fibers. Figure 2.2 shows the breakdown of a composite.
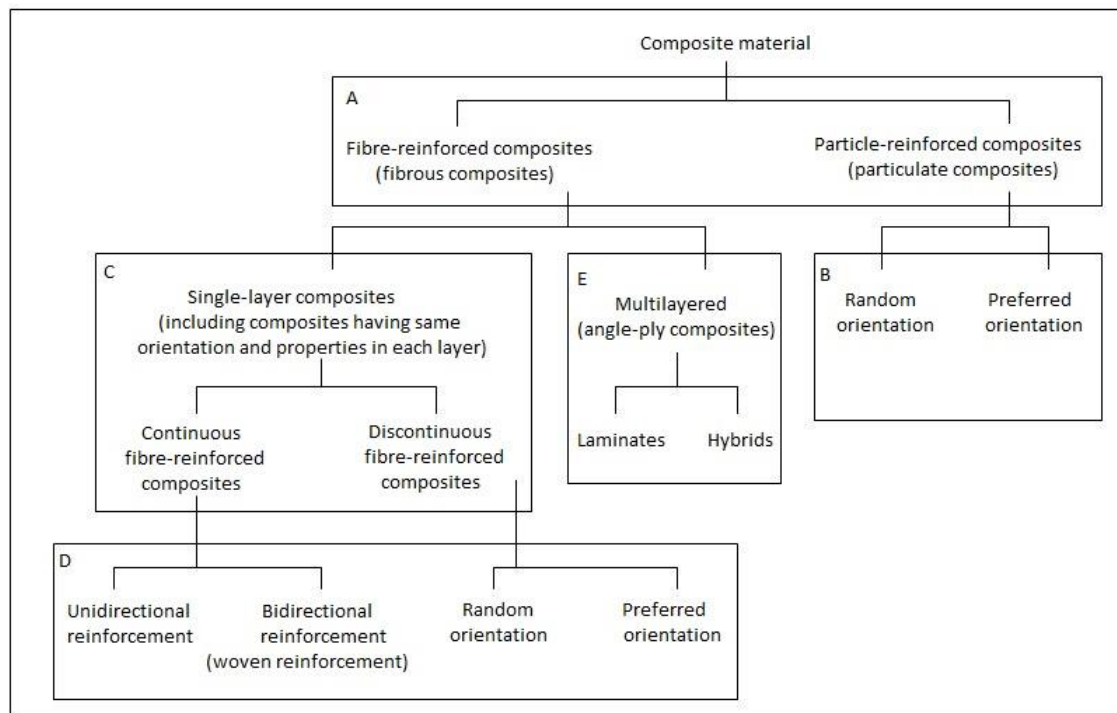
Figure 2.2. Classifications of composite materials.

Reinforcements of a particulate nature have equal dimensions and can be either spheres, cubes, or other equidistant geometries. They can have random or set arrangement, and these reinforcements are broken down into these two types. However, most are random.

Fibrous reinforcements have a length longer than the cross-sections. That said, the cross-section dimensions have a great variance. Continuous reinforcements have high aspect ratios, and discontinuous have short. They can also be random or set in arrangement. Most are unidimensional and have a bidirectional woven reinforcement to set the dimensions.

Another type of composite is multi-layer. They are the most common type and are either laminates or hybrid. Laminates are made with stacked layers in a certain order. There can be as little as four or as many as 400 layers and the fiber arrangement will vary from layer to layer. Hybrids mix fibers with either ply or at each layer and are made for the

various benefits of the properties of each material. Carbon and glass are common hybrid composites, because glass is cheap and carbon is mechanically durable.

2.3. Composite Material Terminology

2.3.1. Lamina

Laminas are either flat or curved and are an assembly of woven or unidirectional fibers hung in the matrix. They are orthotropic and the thickness is dependent on the material used in production. In models, laminas are ordered with on fiber layer to the thickness. Both types are laminas are shown in Figure 2.3 below.
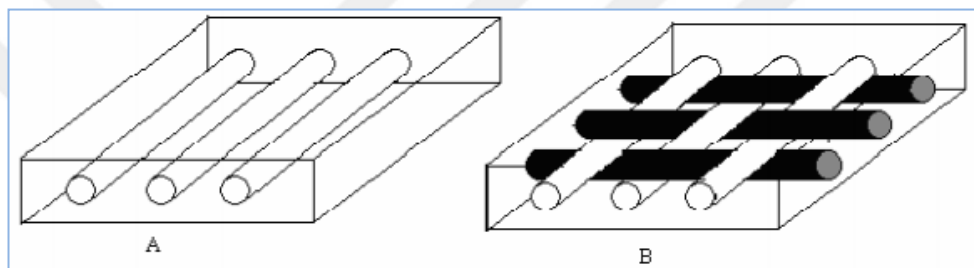
Figure 2.3. Schematic illustration of A: unidirectional; B: Woven composites.

2.3.2. Reinforcement Material

Common reinforcements include: glass, silicon carbide, titanium, boron, kevlar, and aluminum.

2.3.3. Fiber Material

Fibers are unique in that they are most often continuous and have a diameter range between three and 200 mm. They are either linear elastic or elastic perfect plastic and are much more durable than the bulk material. The frequently used fibers are: carbon, glass, Kevlar, and boron.

2.3.4. Matrix Material

The matrix, or binder, protects the fibers as well as provides support and separation with a load transfer path that is sent to the fibers if there is breakage. It is usually less dense, less stiff, and weaker than fibers. They can be plastic, elastic, ductile, or brittle and have linear or nonlinear stress-strain behavior. It should also be able to withstand force from the reinforcement when the composite is being made. Fibers are treated with chemicals

so they adhere to the matrix. Common matrix materials include: metal, ceramic, polymer, and carbon [42]. The various types are explained below.

1. Carbon endures more heat per weight and are used in rockets and aircraft brake pads.

2. Ceramic is brittle and is used in conjunction with fibers of metal, carbon, glass, or ceramic. They are used in extreme environments.

3. Glass are less elastic than their reinforcement and are often used with metal oxide and carbon fibers. Glass performs well under high temperatures and as such are used in exhaust, electrical parts, and engines.

4. Metal is also good at high temperatures. The most common metals are nickel, iron, titanium, magnesium, aluminum, and tungsten. They are broken down into three types:

    a. Class 1 have insoluble matrix and reinforcement. Boron and magnesium represent one, and aluminum and copper are another.

    b. Class 2 has some solubility that impacts the composite's characteristics after interaction. Tungsten is often found in these combinations, together with nickel, copper, and columbium.

    c. Class 3 are serious and present issues because of production. They can include silica and aluminum in one combination, and tungsten and copper in another.

5. Polymer is common and cheap because of their high frequency as pitch, resin, or amber. Early composites used cloth, fiber, and pitch. They provide decent adhesion and are low in density. Polymer is impacted by moisture, time, and temperature. They are broken down into thermoset and thermoplastic:

    a. Thermoset has polymer chains in a cross-linked pattern and is set after production. They are used in extreme temperatures.

    b. Thermoplastic are not cross-linked with chains contacting one another but not crossing. It can be molded again after production after reheating it to the forming temperature.

2.3.5. Laminate

Laminates are made from at least two laminate materials in a stack in different arrangements. There are variances in thickness and are made from different materials [43].
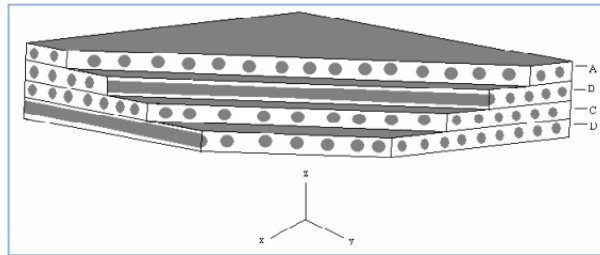
Figure 2.4. Multidirectional laminate with reference coordinate system

The material axes are different at each ply so it becomes easier to study the laminates with a fixed system using given coordinates. The ply structure is defined by the angle between the x-axis and the ply's material axis. They are measured counter-clockwise in the x-y plane. Hybrid composites have composite of more than one material. They are usually interply, [44, 45, 46].

Composites are made according to the structure, sequence of stacking, number, and type of plies. This is known as lay-up. The various lay-ups are described in Table 2.1 below, where S= Symmetric sequence, T= Total number of plies, Number subscript= Multiple of plies, K= Kevlar, C= Carbon, G= Glass fibers.

Table 2.1. Laminate designations

Unidirectional	6-ply $[0/0/0/0/0/0] = [0_6]$
Crossply	$[0/90/90/0] = [0/90]_s$ $[0/90/0] = [0/90]_s$
Angle-ply Symmetric	$[+45/-45/-45/+45] = [\pm45]_s$ $[30/-30/30/-30/-30/30/-30/30] = [\pm30]_{2s}$
Angle-ply Asymmetric	$[30/-30/30/-30/30/-30/30/-30] = [\pm30]_{4s}$
Multi directional	$[0/45/-45/-45/45/0] = [0/\pm45]_s$ $[0/0/45/-45/0/0/0/0/-45/45/0/0] = [0\ 2/\pm45/0\ 2]_s$ $[0/15/-15/15/-15/0] =[0/\pm15/\pm15/0]_T= [0/(\pm15)2/0]_T$
Hybrid	$[0_K /0_K /45_C /-45_C /90_G /-45_C/45\ _C/0_K /0\ _K]\ _T= [0_{K2}/\pm45\ _C/90\ _G]_s$

2.4.Micromechanics and Macromechanics

It is possible to study composite materials for various levels and scales based on the area of interest. Figure 2.5 shows a basic schematic used for analysis.
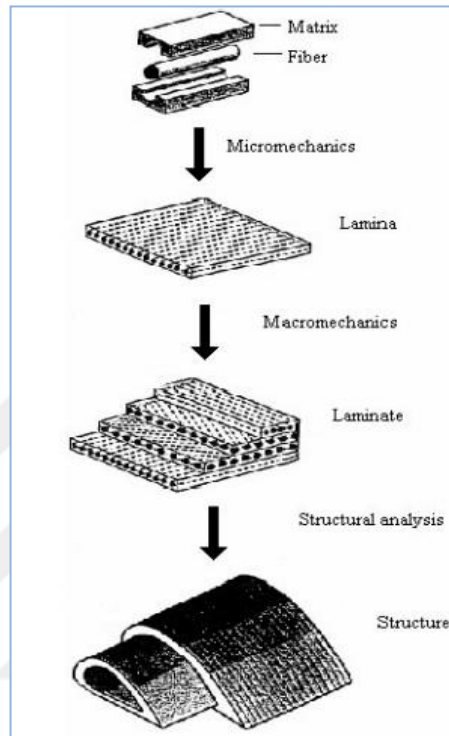
Figure 2.5. Steps of observation and types of analysis for composite materials.

When examining the materials at the constituent phase, the fiber diameter border, matrix intersections, or particle size is used. The science of micromechanics handles constituent interaction at the mircolevel and also deformation and stress, as well as local failures. These failures can be from the fiber, matrix, or interface and interphase. Figure 2.6 shows a cross section that is examined.
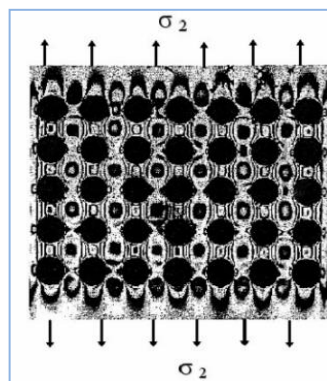
Figure 2.6. Isochromatic fringle patterns in a model of transversely loaded unidirectional composite.

This science is used for studying durability, strength, and fatigue in composite materials because these characteristics cannot be duplicated or assumed. It also forecasts how composite laminates will behave under specific conditions.

It is more beneficial for researchers to use homogenous materials in their study even if they are anisotropic. When this is done, the science is micromechanics because it uses unidirectional lamina materials with semi homogenous anisotropic materials with a common durability and rigidity. Averages stresses will determine the failure criterion, as well as the strength of the lamina, without checking other places where failure may occur. It is good to use this method when looking for elasticity or viscoelasticity. Lamination theories are used at the laminate to study behavior (as a function) and the stacking sequence in the macromechanical analysis. At the structural level, the finite element method is used with the lamination theory for a comprehensive behavior study, as well as an in-depth look at lamina stresses through various phases.

2.5. Special Features of Composites

Composites are made for high performance and low weight application and have many positives. These include:

- Part integration is possible meaning different metal elements can be used for replacement
- They can monitor themselves with sensors that are embedded, for instance in aircrafts
- They have the stiffness of steel at only 1/5 the weight and of aluminum at ½ the weight
- High density to strength ratio
- High fatigue strength
- Resistance to corrosion because of unique coatings
- Various designs are possible with the same materials
- Net shape parts (or close proximities) can be produced using composites
- The components, look, and contours are more flexible than with standard metal

- Good design for manufacturing and design for assembly (DFM and DFA) techniques

- Strong impact properties

- Have good NVH properties (noise, vibration, and harshness)

- Are extremely cost-effective under the proper design because of low temperature and pressure requirements
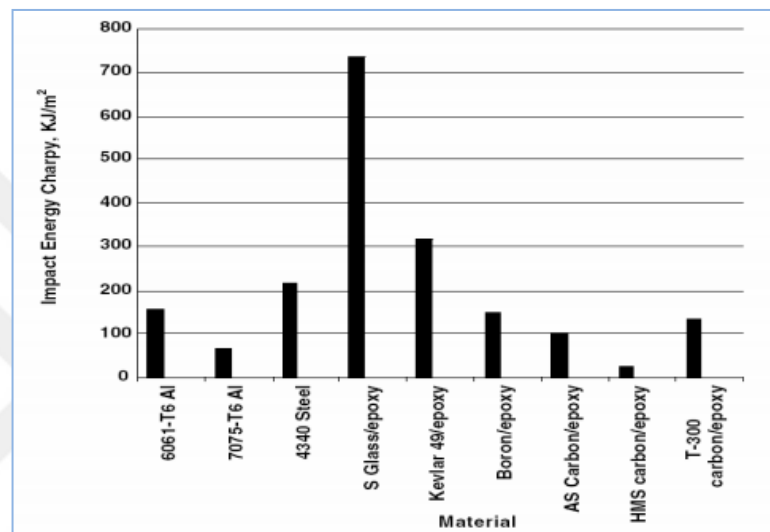
Figure 2.7. Impact properties of various engineering materials.

Unidirectional composite materials with about 60% fiber volume fraction are used.
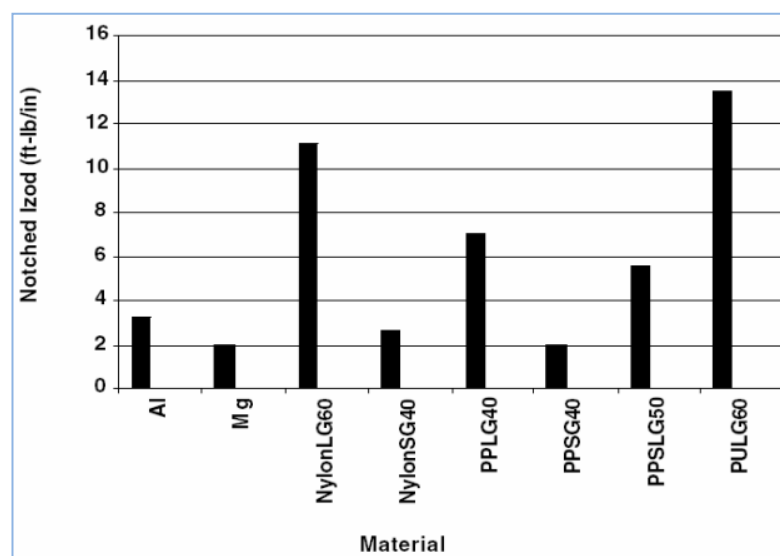
Figure 2.8. Impact properties of long glass (LG) and short glass (SG) fibers reinforced thermoplastic composites. fiber weight percent is written at the end in two digits.

2.6. Drawbacks of Composites

The benefits mentioned above are numerous, but there are several flaws as well, including:

- More expensive to produce than steel or aluminum
- Composites were made at high-volumes in the past, a process which is not possible today because of less production
- No existing training manuals or handbooks for composites, as with metals
- Temperature resistance is based on the matrix properties and can range a great deal
- Polymers dictate solvent and chemical resistance as well as cracking from stresses
- Moisture absorption changes the stability, [47, 48, 49].

2.7. Composite Manufacturing Methods

There is an assortment of methodology for composite production. All of these relate to the budget, quality, and shape of the material, as well as the experience of those producing it. All of these methods, however, can be characterized into either open or closed molding. Open molding is done with atmospheric effects, and closed molding is done in vacuum bags that block the atmosphere. Both have positives and negatives and should be carefully considered before production.

2.7.1. Hand Lay-up

The oldest composite production method is the hand lay-up way. There are low costs in this method, and it allows for specific thicknesses and complicated shapes. There are faults, however, including being slow, gaps coming during production, and changing according to the mass. Blades and boats are made using hand lay-up.

Figure 2.9. Hand lay-up, [50].

The procedure is:

1. Coat mold with gel
2. Place fibers and resins into the mold
3. Cure the material and separate it from the mold

2.7.2. Spray-up

Spray-up is another open molding method that is used for boats. Using a gel coating, this method allows for production according to specific qualities of finish. First, continuous fibers are chopped before short fibers are added and liquid resins are sprayed into the mold. The spray-up method is easy and cheap. It is shown in Figure 2.16.

Figure 2.10.Spray-up, [50].

2.7.3. Autoclave Curing

Autoclave curing is used for aerospace applications. A vessel handles temperature control and pressure. This removes air not needed for production. Temperature is used by the machine for pressure. Once cured, the material has an optimal ratio or resin to fabric and is extremely strong and durable. However, this method is very expensive. It is shown in Figure 2.17.

Figure 2.11. Autoclave curing, [51].

2.7.4. Filament Winding

Filament winding has fibers that wind around a mandrel continuously until reaching a specific thickness. It is important to cure the material afterwards to remove the mandrel. Shapes from this method can either be spheres or cylinders because of the method used. However, it is possible to apply a mass-production method for filament winding and it makes extremely strong materials. It is used for storage of water, gas, and pressure. Figure 2.18 illustrates this method.
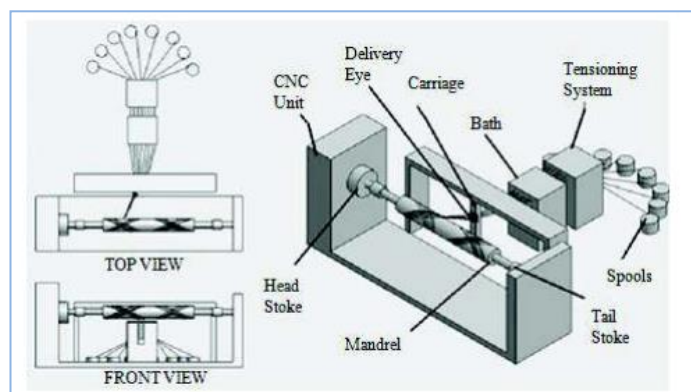
Figure 2.12. Schematic illustration of filament winding, [52].

2.7.5. Vacuum Bag Molding

Because open molding has various limitations, vacuum bag molding was invented. There are three steps. First, both the fibers and resins are inserted into the mold. Next, a supple film is placed on top. Then a vacuum is started and laminates are compressed through pressure.

There are many reasons this method is chosen over hand lay-up. It is possible to laminate efficiently using this method. Also, strength is improved because air and resin are removed. This also limits the cost because of less used resin.
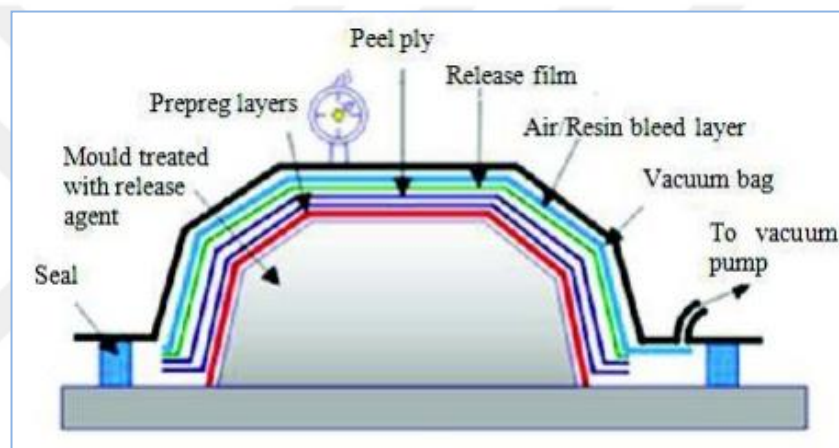
Figure 2.13.Vacuum bag molding, [53].

2.7.6. Vacuum Assisted Resin Infusion Molding

Another type of vacuum bag molding is assisted resin infusion that differs in that resin is placed into the mold after the vacuum is started. This enables proper realignment of reinforcements and limits resin usage. It is then possible to produce composites according to a specific schematic.
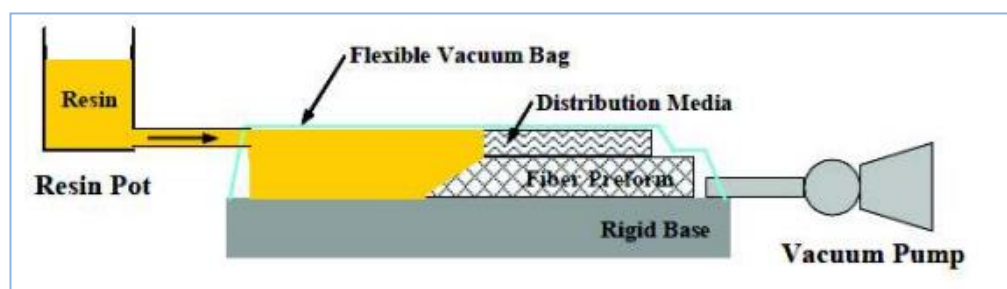
Figure 2.14.Vacuum infusion process, [54].

2.7.7. Pultrusion

Pultrusion is used to produce pipes and beams with roving fibers passing through a resin bath. An automated procedure will use several rows. Then, curing is done before the materials are cut to shape. Materials made with pultrusion are very strong and have significant fiber levels. However, this method is limited in cross-section production in that they are made universally.
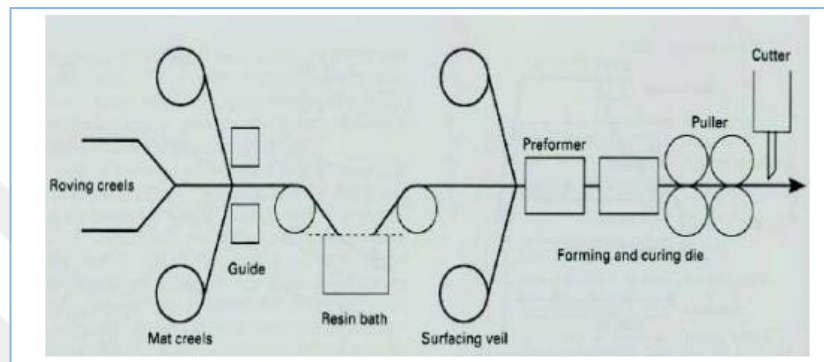
Figure 2.15.Pultrusion, [55].

2.7.8. Compression Molding

In this method, there are two molds called male and female that are managed by hydraulic or mechanical equipment. There are various types, including: bulk, sheet, liquid, and thick. It allows for complicated geometric arrangement with one or more cavities. This method is fast and automated. Still, fibers and chip and lower overall strength.
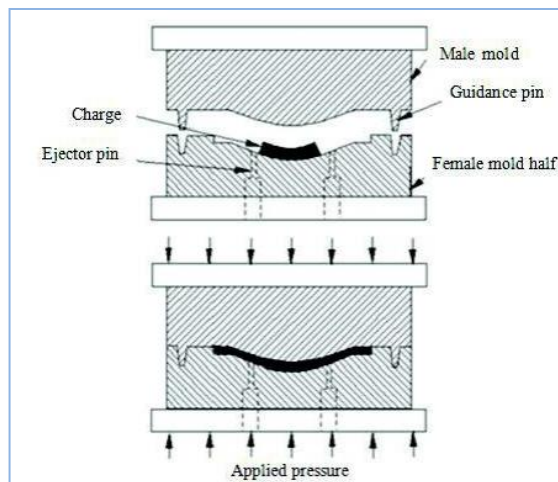
Figure 2.16.Compression molding, [56].

2.7.9. Resin Transfer Molding

In this method, two molds are used and reinforcements and resins are inserted into them. It produces complex fiber reinforcement and can be used with either mat or woven shapes. The molds are heated once resin is placed inside, before curing takes place that dries the resin. For an improved surface, gel coating is often used. This method can be mass-produced and provides a good ratio or fiber to resin with extra strength. Also, cavities allow for complicates geometries. That said, the method is expensive to run because of special tools.
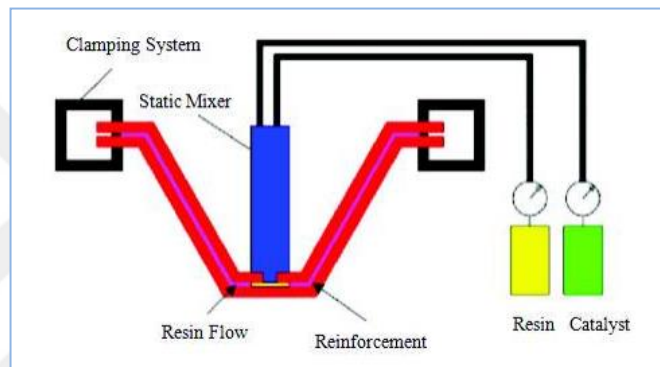
Figure 2.17. Resin transfer molding, [57].

2.7.10. Structural Reaction Injection Molding

SRIM uses short fibers that are already in the molds and two resins are placed within at high velocity. Once they are injected, the curing process takes place next. It is fast and allows for automation and isotropic material production. However, because there is a low quantity of fibers, there is also a lower strength of material using this method.
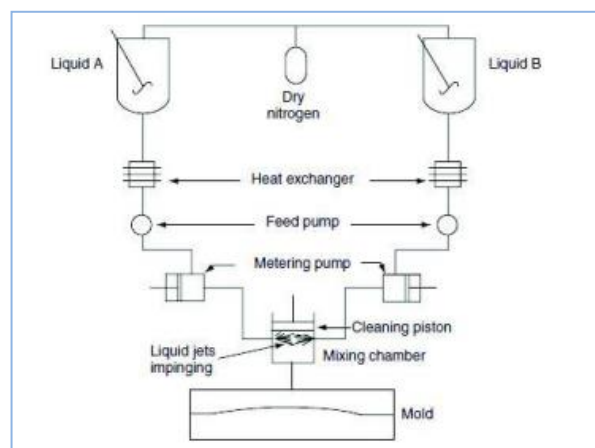
Figure 2.18. Structural Reaction Injection Molding, [58, 59].

2.8. Behavior of Unidirectional Composites

Composites reinforced with fibers have been used across many fields because they have high structural potential. Composite structural components or laminates of fiber have multiple layers, often from the same material. Still, these layers can differ from each other in three ways:

1. Material volume
2. Reinforcement form (continuous or discontinuous; woven or unwoven)
3. Fiber structure related to a given axis

Also, hybrids can have varying fibers or matrix materials in each layer, causing vastly differing directions. In order to analyze and design a structural component, one must have thorough understanding of each layers' properties. Unidirectional composites have a matrix with parallel fibers and can be used for basic laminate building. This chapter covers unidirectional composites, including their properties and behavior.

2.8.1. Nomenclature
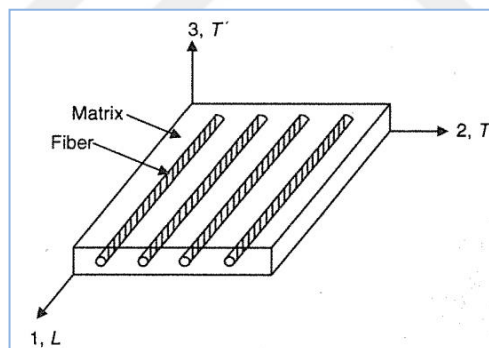
Axis 1, L - longitudinal direction/Axis 2, T - transverse direction to lamina/
Axis 3, T- transverse direction perpendicular to lamina.
Figure 2.19. Unidirectional composite.

Figure 2.19 above shows a unidirectional composite with unidirectional layers stacked in such a way that it can produce certain stiffness and strength requirements. Each of these layers can be called layers, plies, or laminas. Axis 1 is the longitudinal direction and runs parallel to the fibers. The transverse direction runs axis 2-3 and runs perpendicular. The figure above shows a single fiber at the ply thickness. In real materials, only fibers with large diameters will have such a design. Other plies will have many fibers through the thickness.

2.8.2. Volume and Weight Fractions

One of the most important factors determining the properties of composites is the relative proportions of the matrix and reinforcing materials. The relative proportions can be given as the weight fractions or the volume fractions. The weight fractions are easier to obtain during fabrication or by one of the experimental methods after fabrication. However, the volume fractions are used exclusively in the theoretical analysis of composite materials. It is thus desirable to determine the expressions for conversion between the weight fractions and volume fractions.

2.9. Longitudinal Behavior of Unidirectional Composites

Composite materials are largely dependent on constituent properties and arrangement, as well as interactions both physical and chemical. It is possible to find these properties through rigorous experimentation or through simple testing. If a system variable changes, then the test must be readapted to the changes. As such, it is useful to use theoretical models in place of testing, to save time, money, and energy. These models help to locate a wide array of variables. Although models are not always useful because of the transverse properties of unidirectional composites, it is possible to study the longitudinal properties with great accuracy.

2.10. Transverse Stiffness and Strength

2.10.1. Constant-Stress Model

Composite transverse properties can be studied using simple numerical models. Within these models, fibers are thought to be identical in terms of diameter and properties, run parallel to one another, and continuous. The transverse direction bears the stress. Layers constitute fibers and matrix materials. The layers run perpendicular to loading and have identical area to the loading zone. Through this, each layer has identical loads and stress. This is shown in Figure 2.20 below.
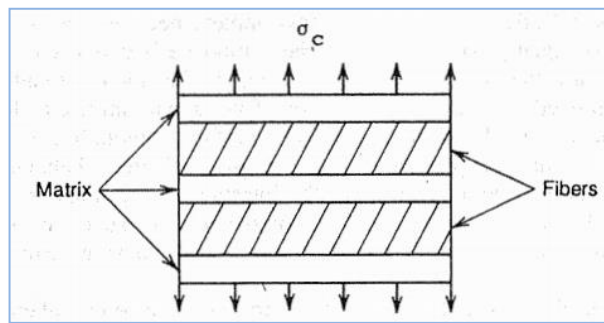
Figure 2.20. Model for predicting transverse properties of unidirectional composites.

2.10.2. Elasticity Methods of Stiffness Prediction

There are three techniques to predict composite stiffness with elasticity principles:

1. Bounding
2. Exact solutions
3. Self-consistent method

Bounding uses energy theories to find elastic property bounds. The lower bound is found with the minimum-complementary-energy theory while the upper bound is found using minimum-potential-energy. Several researchers have used this technique, including Paul [60] and Hashin and Rosen [61]. Paul's bounds are too far apart to be of much practical utility, particularly at intermediate fiber volume fractions. The bounds obtained by Hashin and Rosen are much improved. A comparison of their predictions with experimental data shows that the experimental results on the transverse modulus lie close to the upper bound.

2.10.3. Halpin-Tsai Equations for Transverse Modulus

Equations from Halpin and Tsai [62] estimate micromechanics analyses in an easy manner. The simplicity of use makes them accessible to various design schemes. Beyond this, they provide accuracy when there is no nearness to the fiber volume fraction.

2.10.4. Transverse Strength

So far in this discussion it is seen that the composite longitudinal strength and stiffness and transverse stiffness are improvements over the corresponding matrix properties

owing to the presence of fibers. The longitudinal strength and stiffness are improved because of the predominant role played by the fibers. The response of composites to longitudinal loading is determined by the fact that the load common between the matrix and fibers. However, because of their higher strength and stiffness, fibers carry a major portion of the load and thus cause composite properties that are significantly improved over the matrix properties. If unidirectional composites face transverse loads, fibers cannot handle a high percentage of the load (like in longitudinal loading) because of their shape. The high-modulus fibers serve restraint matrix deformation, which causes the transverse composite modulus to be higher than the matrix modulus. There are only small differences unless there is a high fiber volume fraction.

2.10.4.1. Micromechanics of Transverse Failure

Failure is a process that, is initiated by localized conditions. State of stress is the most important condition influencing initiation of failure. The failure of structures and components generally is initiated at the locations of highest stress produced by geometric or material discontinuities. Geometric discontinuities result from the shape of the structure or from holes and cutouts made for assembly pm poses. These geometric discontinuities reduce the strength of structures on macroscopic level as a result of the stress concentrations produced by the discontinuity.

2.10.4.2. Prediction of Transverse Strength

There are two ways to predict composite tensile strength: strength-of-materials and advanced elasticity (that uses numerical solutions). Both methods require the assumption that transverse strength is governed by matrix ultimate strength. It is also presumed that composite strengths are lower than matrix strength by S (strength reduction factor). This is dependent on fiber properties and the matrix volume fractions.

2.11. Prediction of Shear Modulus

The in-plane shear modulus of a unidirectional composite may be forecast using the transverse modulus model section 2.3.1, as shown by Figure 2.21 fiber and matrix shearing stress are identical. The total shear deformation of the composite Δ_c is the sum of the shear deformations of the fibers Δ_f and the matrix Δ_m.
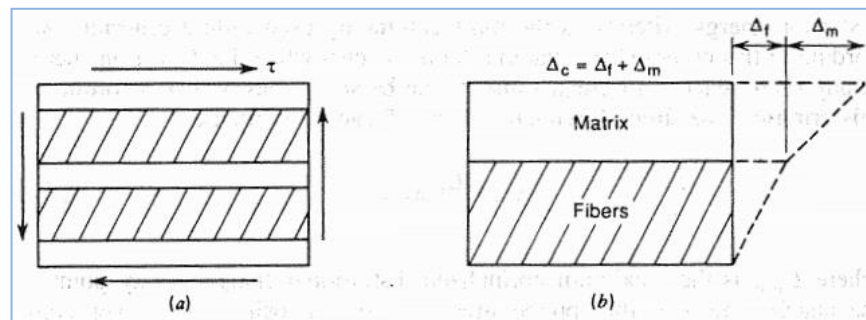
Figure 2.21. (a) Shear modulus prediction and (b) shear deformations in the model.

2.12. Prediction of Poisson's Ratio

For in-plane loading of a unidirectional composite, two Poisson ratios are defined. The first of these relates the longitudinal stress to the transverse strain · It is normally referred to as the major Poisson ratio. The second one, called the minor Poisson ratio, relates the transverse stress to the longitudinal strain. However, the load is applied parallel to the fibers, that is, parallel to the layers in the model. Transverse strains in the fibers, matrix, and composite can be written in terms of longitudinal strains and the Poisson.

2.13. Failure Modes

Structural parts fail when they no longer perform as expected. Because of the broad nature of this definition, failure will mean something different to each application. A miniscule deformation could be considered a failure in some applications. For composites, there is generally a long-standing internal failure long before such failure is visibly present. This failure can occur at multiple sites, either in conjunction or separately. They include: matrix cracking, fiber breakage, debonding, or delamination.

2.13.1. Failure Under Longitudinal Tensile Loads

In a unidirectional composite (consisting of brittle fibers) subjected to increasing longitudinal tensile load, failure initiates by fiber breakage at their weakest cross sections. As the load increases, more fibers break. Variation in the cumulative number of fiber breaks is shown as a function of applied load in Figure 2.22 for a model representing a unidirectional composite [63]. It can be observed that the individual fibers break at less than 50% of the ultimate load. Breaking of the fibers is a completely

random process. As the number of broken fibers increases, some cross section of the composite may become too weak to support an increased load, thus causing a complete rupture of the composite. The interfaces of broken fibers may become debonded because of stress concentrations created at the fiber ends and thus may contribute to the separation of the composite at a given cross section. In other cases, cracks as different cross sections of the composite may join up by debonding of the fibers along their length or by shear failure of the matrix. Therefore, a unidirectional composite can fail in at least three modes under longitudinal tensile load. These modes are (1) brittle, (2) brittle with fiber pullout, and (3) brittle failure with fiber pullout and (a) interface-matrix shear failure and (b) constituent debonding (i.e., matrix breaking away from the fibers).
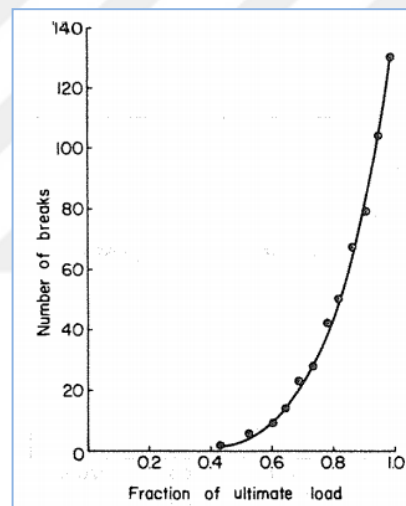
Figure 2.22. Cumulative number of fiber breaks with increasing longitudinal load.

2.13.2. Failure Under Longitudinal Compressive Loads

Fiber microbuckling can happen if composites face compressive loads and are possible even if matrix stress is within the elastic range for composites with low fiber volume. That said, at the fiber volume fraction of ($V_f > 0.40$), matrix yield and debonding with microcracking will precede microbuckling. Compressive failure can start from splitting of composite failure within unidirectional composites [64, 65]. In other words, strain from the Poison ratio effect can go beyond the composite's ultimate transverse strain and cause interface cracks. Shear failure is also caused by compressive loads in the longitudinal direction. Failure modes with a compressive load can fail in three ways:

1. Transverse tensile failings

2. Microbuckling

    a. With elastic matrix

    b. After matrix yielding

    c. After debonding

3. Shear failure

2.13.3. Failure Under Transverse Tensile Loads

Fibers that are perpendicular to the direction of loading work to concentrate stress to the matrix and interface. Because of this, unidirectional composites under tensile loads can fail because the matrix fails under tensile stress. That said, they can also sometimes fail because of tensile failings in the transverse direction if the fibers in that direction are weak. As such, composite failure modes are either from matrix tensile failure or debonding and splitting of fibers.

2.13.4. Failure Under Transverse Compressive Loads

Matrix shear failure is the most common cause of unidirectional composite failure under compressive loads. This can be in conjunction with debonding or crushing of fibers. Researcher Collings [66] studied plastics reinforced with carbon fiber and noticed that failure originates from a shear direction normal to the fibers on parallel planes under compressive loads. Figure 2.23 shows two pictures of the mode of failure. Scientists have proposed that failings of the bond between fiber and resin exacerbate this failure. As such, compressive strength in the transverse direction is lower than the longitudinal direction. It is also possible to produce similar strength in the two directions with constraints that prevent deformation. This is because failure will then originate from fiber shear failure, that have higher strength that the matrix or bonds. When this occurs, transverse compressive strength increases alongside fiber volume fractions.
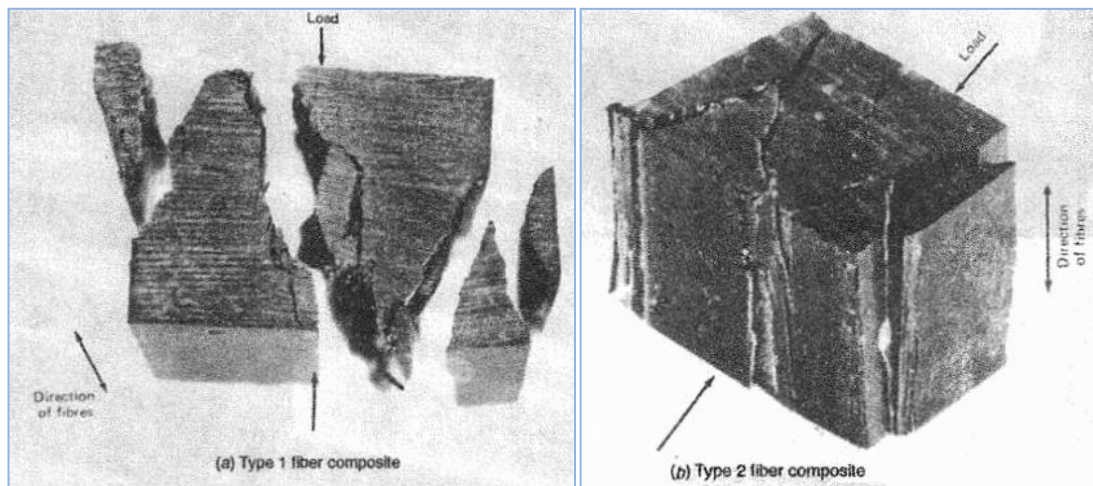
Figure 2.23. Photographs showing shear failure of unconstrained unidirectional carbon-fiber reinforced plastics subjected to transverse compressive loads, [66].

2.13.5. Failure Under In-Plane Shear Loads

In this situation the failure could happen as a result of matrix shear failure, constitutive debonding, or a cooperation of the two. So the failure modes are (1) the failure of matrix shear, (2) the failure of matrix shear in addition to constitutive debonding, and (3) constitutive debonding.

2.14. Typical Unidirectional Fiber Composite Properties

The preceding discussions on property-prediction methods and failure modes should be of use in comparing various physical properties of unidirectional composites. It is also valuable to appreciate the difference between different types of fiber composites and their respective properties. From the known values of fiber and matrix properties, the interested reader can try to predict the properties shown in Table 2.2. A few points should be made concerning the data presented in Table 2.2. The measured compression strength in the fiber direction of a unidirectional composite generally is less than the tensile strength.

Table 2.2. Typical properties of unidirectional-fiber-reinforced epoxy resins.

Property	Fiber type		
	E-Glass	Kevlar 49	Graphite (Thornel 300)
Fiber volume fraction	46	60–65	63
Specific gravity	1.80	1.38	1.61
Tensile strength, 0° (MPa)	1104	1310	1725
Tensile modulus, 0° (GPa)	39	83	159
Tensile strength, 90° (MPa)	36	39	42
Tensile modulus, 90° (GPa)	10	5.6	10.9
Compression strength, 0° (MPa)	600	286	1366
Compression modulus, 0° (GPa)	32	73	138
Compression strength, 90° (MPa)	138	138	230
Compression modulus, 90° (GPa)	8	5.6	11
In-plane shear strength (MPa)	—	60	95
In-plane shear modulus (GPa)	—	2.1	6.4
Longitudinal Poisson ratio (ν_{LT})	0.25	0.34	0.38
Interlaminar shear strength (MPa)	31	69	113
Longitudinal coefficient of thermal expansion (10^{-6}/°C)	5.4	−2.3 to −4.0[a]	0.045
Transverse coefficient of thermal expansion (10^{-6}/°C)	36	35[b]	20.2

[a] −79 to +100°C.
[b] −195 to +120°C.

Since compression strength of this type of composite is so difficult to measure, the reported value often is merely a reflection of the quality of the test technique. Occasionally one sees values reported in the literature that might exceed the value of the tensile strength, and in such cases, the compression test fixture is often such that it prevents certain failure modes, perhaps producing artificially large values of strength. The very low value of compression strength for the Kevlar composite is caused by the exceptionally low shear and transverse tensile strength of the highly oriented Kevlar fiber, which initiates failure in the composite when subjected to compression, [67].

CHAPTER THREE

EXPERIMENTAL RESULTS OF LOW SPEED IMPACT BEHAVIOR

3.1. Introduction

In recent years, low speed impact in composite laminates and their adverse effects on composites have led to an increase in their research. Composite materials reinforced with fibers high specific strength, so they are used in aircrafts and other lightweight applications. Still, these laminates carry a high concern for impact from external objects that produce internal damage that reduces strength and intensifies under loads. This damage is also hard to notice. Aircrafts are privy to all sorts of impact, including tools left on the runway, debris raised by the tires, or other flying objects such as birds.

This chapter elaborates on experimentation and numerical analyses from low velocity impacts on glass, carbon, and hybrid fiber plates with an epoxy matrix. How these impacts effect using different impact energies is analysied, and studying the damage in the laminates after impact using Fractovis Plus Low velocity impact tester [68,69]. Different kinetic energies were used for the drop dart test through changing the height of dropping. Because of this, the velocity will be different in each test and the materials face different rates of deformation.

Carbon fiber-reinforced plastic is expensive, although it is strong and light. It is comparable to fiberglass and often called carbon fiber based on the name of its reinforcement. The fiber is strong for its size because of how the crystals are aligned. A yarn is formed from thousands of twisted fibers and the material can be used alone or woven into fabrics.

Glass-reinforced plastic (GRP) has a plastic matrix with fine glass as the reinforcement. It is light, strong, and used across numerous industries for building: pipes, roofing, cars, boats, water tanks, and more. It is also possible to control the stiffness and strength properties of this composite through layering fibers atop each other, [70].

Hybrid composites have multiple materials used to reinforce it that are connected to the same matrix. This gives way to materials produced for specific needs. Hybrids can combine the effects of multiple materials and limit the negative aspects of each. Hybrids are also often much cheaper than the single material because of lower percentages [2].

3.2. Manufacturing Steps

3.2.1. Steps Involved in Preparing Specimen

Unidirectional layers of dry E-glass fibers, carbon fibers arranged symmetrically relative to the mid plane of the plate and hybrid fibers (symmetrical and unsymmetrical) were stacked layer by layer of about 8 layers, Figure 3.1 to attain the specimen thickness about 2 mm., Table 3.1 shows plies orientation and stacking sequences of manufactured specimens. Bonding agent (epoxy resin) is applied to create. The epoxy resin (MGS L 160) was mixed with the hardener (MGS H 160) with the stoihiometric ratio of 100:50

Figure 3.1. Specimens preparing: (a) carbon fibers, (b) E-glass fibers, (c) hybrid.

Table 3.1. Ply orientation- stacking sequence of manufactured specimens.

Specimen	Plies orientation sequence	Plies stacking sequence
E-glass laminate	[0/90/±45]s	[G/G/G/G/G/G/G/G]
Carbon laminate	[0/90/±45]s	[C/C/C/C/C/C/C/C]
Hybrid laminate-symmetrical	[0/90/±45]s	[C/G/C/G/G/C/G/C]
Hybrid laminate-unsymmetrical	[0/90/±45]2	[C/G/C/G/C/G/C/G]

The composite laminates discussed in this research were made using the innovative vacuum assisted technology (pulse infusion), as shown in Figure 3.2. This method uses two bags with an oriented pressure distribution machine controlling vacuum pressure to produce a pulsed transverse action for thicker resins. It uses fewer materials and has less waste than other methods also fiber reinforcement are oriented as desired
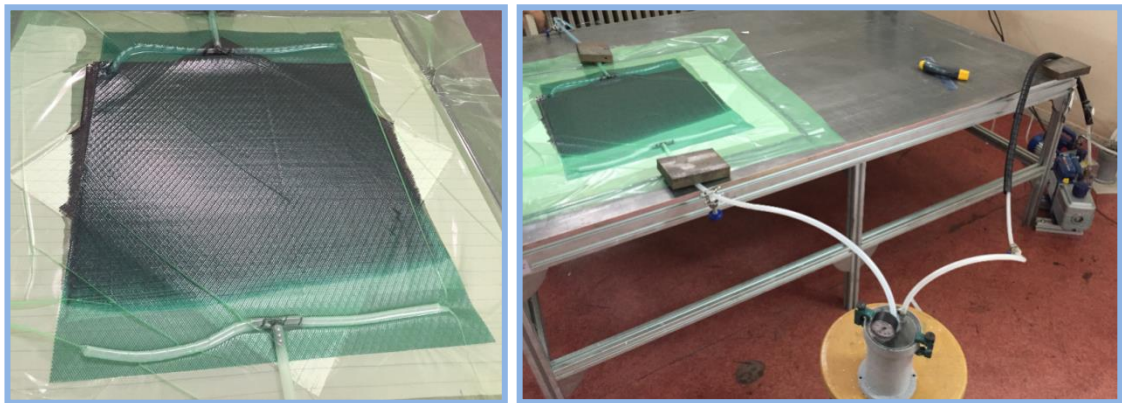
Figure 3.2. Pulsed infusion apparatus.

- Curing is controlled by temperature and resin compounds. It can last a few minutes or a few hours. It is possible to cure some materials with heating, while others need a specific amount of time and a certain temperature.
- Vacuuming removes air traps present between layers.
- The process takes roughly three hours.

- Afterwards, post-curing is necessary to prepare the material for use.

When vacuuming and curing are complete, the post-curing process involves the plates placed into an oven at 100 ^{0}C for two hours. Then, the material is cut to size and shape. This process is shown in Figure 3.3.
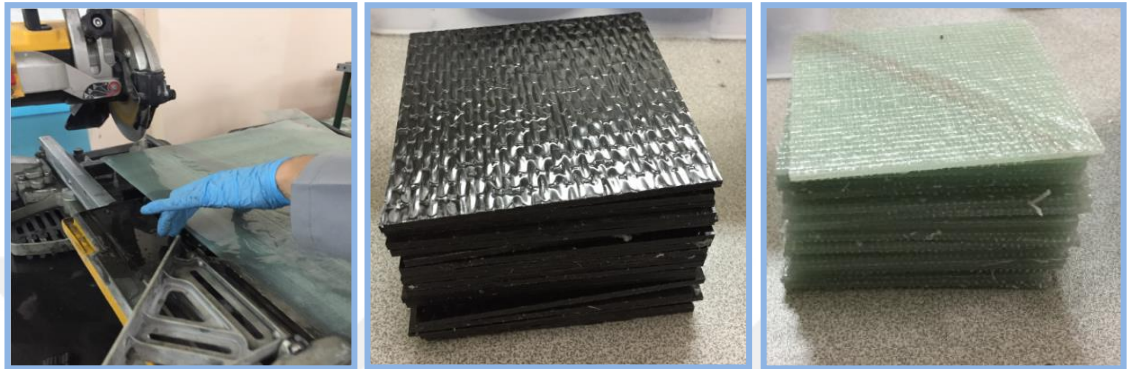
Figure 3.3. The specimen cutting to obtain the required size.

3.2.2. For Impact Test Specimen

The test samples used in this research were made of e-glass and carbon fibers that weight 200 g/m^2 using a polyester resin. After curing, the panels were cut into 100×100 mm pieces with 2 mm thickness.

In this study, the characterization and assessment of the effect ply-orientation, and ply-stacking sequence, Table 3.1, on the damage response of laminates subjected to low velocity impact loading are examined. Four multidirectional laminates have been analysed using two different scaling techniques: symmetrical and unsymmetrical.

3.3. Experiment Method - Impact Test Machine and Test Conditions

The Fratovis Plus machine and the weight drop method were used in this study on every sample. Figure 3.4.a shows the machine and Figure 3.4.b shows the testing schematic. There are three elements on the machine: a crosshead that drops down, an impactor rod 20 mm diameter and connected to crosshead, and nose. The experiments also used the piezoelectric striker that is heavy for testing thick materials such as the composites used. The force transducer has a 22.24 kN capacity and set on the front of the striker. It was covered by a sphere nose. The experiment used a constant drop height of 30-1100 mm for a steady 0.75 - 4.6 m/s.
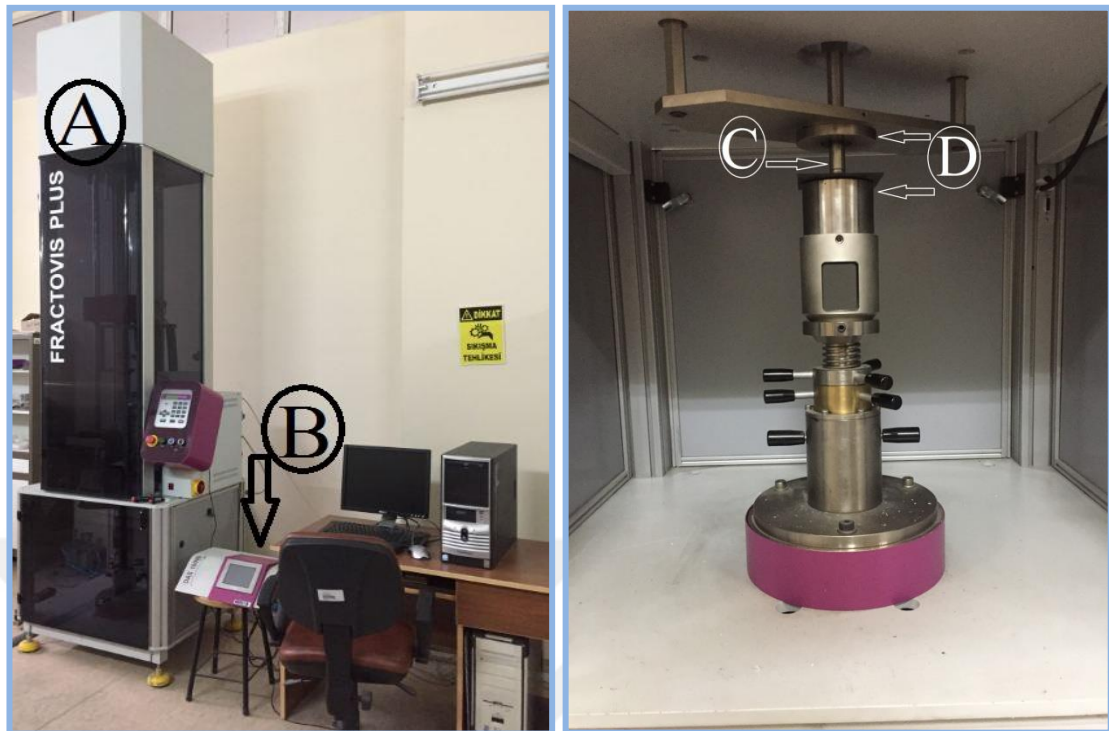
Figure 3.4. (a) Fractovis Plus Low velocity impact tester (b) Data Acquisition System (DAS), (c) The tester equipments; impactor nose and (d) The specimen clamp mechanism.

The impactor had a mass between 2 and 70 kg that caused a 0.6 to 755J impact energy. It also has heating and cooling as part of the machine that are controlled by a computer. The composites used in the test had a 100×100 mm dimension. Central impact was performed in the test by the impactor connecting with the composite's middle.

As a result, the history of the contact force is found with the time history. As well the history of kinetic energy is found with the time history. It is then possible to find the impactor's velocity history using the first impact velocity. Again, this allows for the finding of the displacement history. With a rigid impactor and losing energy at contact.

3.4. Experimental Results

The impact response of unidirectional cross-ply carbon, E-glass and hybrid/epoxy laminates were inserted in different stacking and angle orientation sequences under low velocity impact with various energy levels has investigated. Using the Fractovis Plus machine at room temperature. The nose has a 20 mm diameter. The force transducer has a 22.24 kN capacity. The tested materials have 100×100 mm square geometry. The

mass of the impactor is 5.045 kg. Four impact energies are tested as 10, 20, 30, and 40J. The four impact velocities are: 2m/s, 2.81m/s, 3.44m/s, 4m/s.

Table 3.2. Experiment specs.

Specimens	Test -1	Test -2	Test -3	Test -4
■ Carbon fiber, ■ Glass fiber, ■ Hybrid-symmetrical, ■ Hybrid- unsymmetrical.	5.045kg- 10 Joule- (2 m/s)	5.045kg- 20 Joule- (2.81 m/s)	5 .45kg- 30 Joule- (3.44 m/s)	5.045 kg- 40 Joule- (4 m/s)

Based on Table 3.2 there are 16 experiments to carry out. Each were done for a specific reason and were recorded in tables, figures, diagrams, and explanation. The various impact energies were tested and measured to compare with the data from numerical models. This was done to see the possibility of predicting impact energy and residual strength.

3.5. Failure Mode After Impact Test

Providing damage mechanism are critical to understand the areas of damage. There are several damage modes after composites are impacted. These include cracking in the matrix, delamination, and breaking of fibers. They can occur individually or in conjunction. Figure 3.5 shows delamination together with matrix cracking. Visual inspection was performed to investigate the damage progressive in surface of polymer composites. The four samples were contrasted after impact and visual damage was noticed. There was, however, a marked dent to the face after 10 J impact test. After increasing the force to 20J, deformation and crack was noticed. At 30 J impact test, it was easy to notice deformation and there was a serious crack at the base. At 40 J impact test, beyond a major mark of impact, there was visible splitting and breaking of fibers, as well as cracks in the matrix. For all plates, the damage was more visible at the rear end than at the impact area.

Visual observations suggest that cross/plus marks are formed on the front face of laminates, while damage has been created in the shape of pyramid/trapezium the rear side for the perforated specimen. Two distinct regions are observed on zone at the rear side of the laminate. First, there is a fractured area where the complete debonding between the fiber and the matrix has been observed. The second region is in transverse direction to the impact where the delamination between the plies is observed. When impact energy is increased, the visible damage at the face of impact increases. The lowest layers show high delamination after all levels of impact energy because of bending and fractures in the fibers. After studying the results of the experiments, it is noted that carbon fiber reinforced composites have less absorbed energy than those of fiber glass, and also more elastic energy.

When studying the hybrid samples, it becomes clear that damage is similar to that of the carbon samples. They showed the same levels of: splitting, indentation, and cracks. At 40 J, the hybrid behaves similar to fiber glass. E- glass fiber / epoxy laminate undergoes failure through matrix cracking, fiber breakage. At hybrid (carbon/ E-glass) fiber laminates could enhance the impact-resistance performance of composites significantly, in addition to positive correlation. Laminate perforation thresholds are enhanced.

laminate	face	10J	20J	30J	40J
(a) Carbon fiber	front				
	back				
(b) E-glass fiber	front				
	back				
(c) Hybrid fiber	front				
	back				
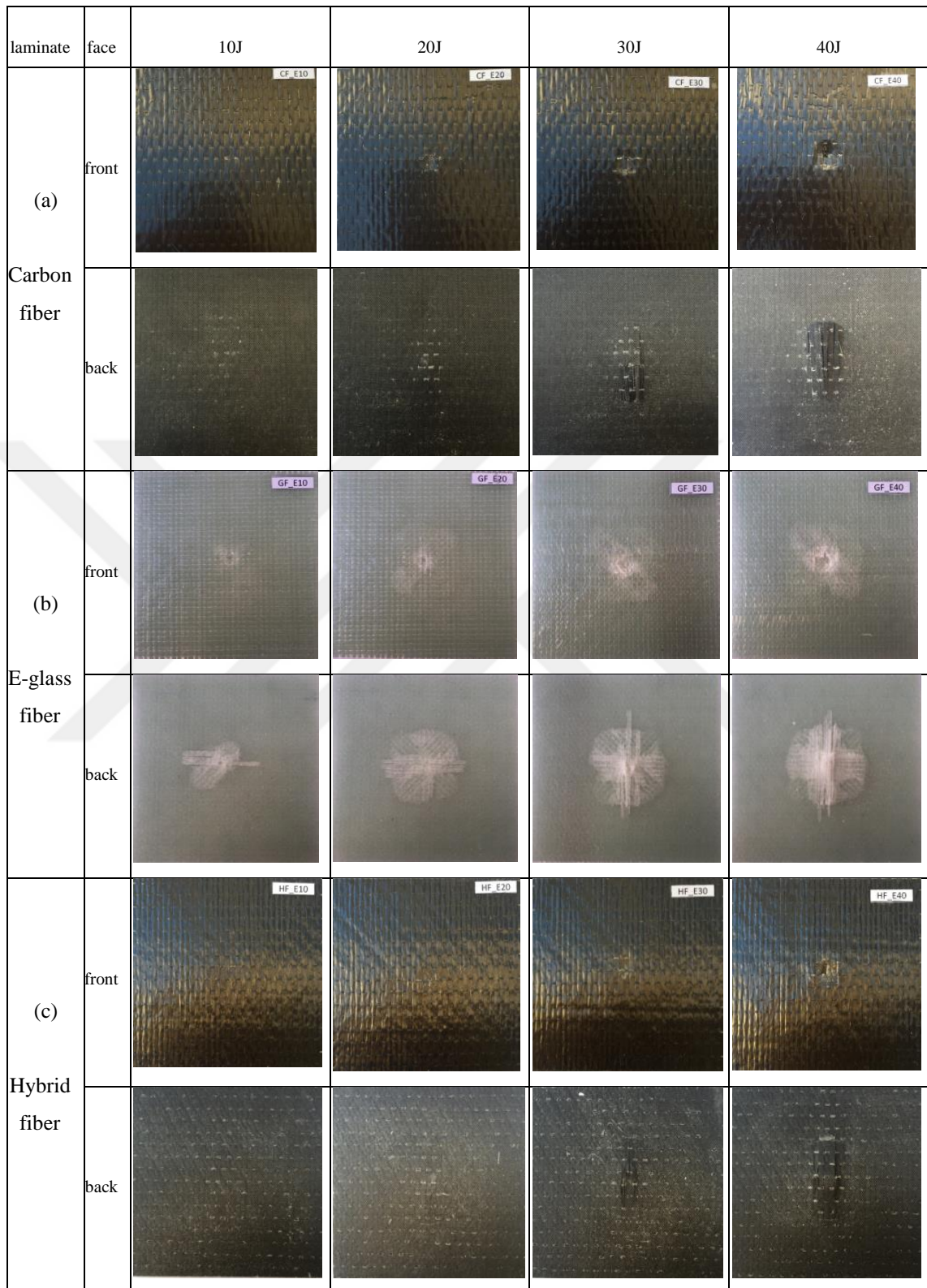
Figure 3.5. The photographs of damaged samples on the contact side and back side after impact (a) carbon fiber, (b) E-glass fiber and(c) hybrid (symmetrical) laminate.

Figure 3.6 shows the impact damage area of front face and back face of unsymmetrical hybrid laminates (a) impacted from carbon side and (b) impacted from E-glass side. 5.045 kg impactor mass is applied to the specimens with different impact energy levels, the orientation angle of plies is [0/90/±45]. After comparing the stacking sequence of unsymmetric hybrid laminates there was a little change in impact response of composites. On the other hand, the rotation angle plays an important role in the impact response.

laminate	face	10J	20J	30J	40J
(a) Hybrid fiber	front				
	back				
(b) Hybrid fiber	front				
	back				
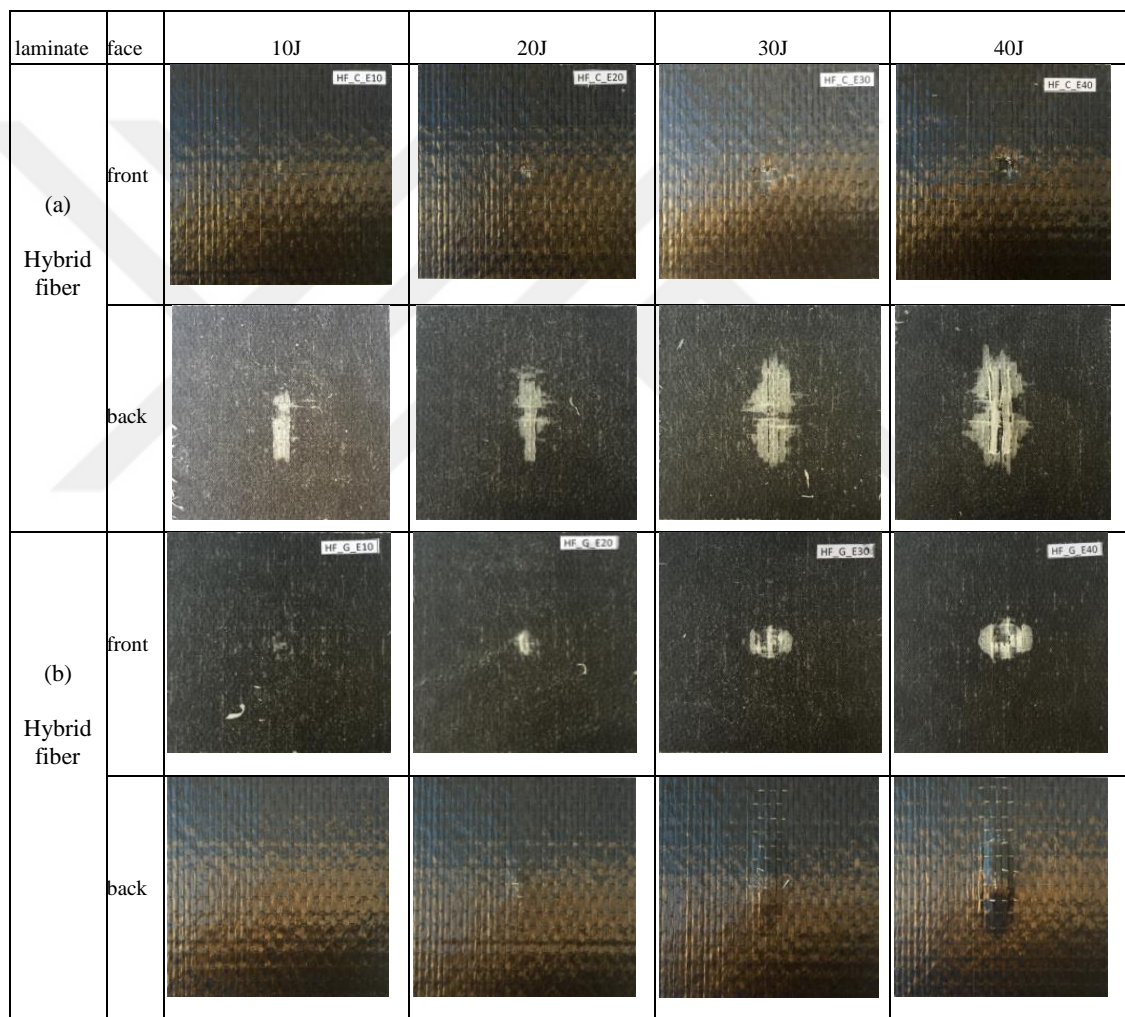
Figure 3.6. The photographs of damaged samples on the contact side and back side after impact of unsymmetrical hybrid laminates (a) impacted from carbon side, (b) impacted from E-glass side.

In this work, carbon, E-glass and hybrid laminated specimens have the same thickness and dimensions. The orientation angle of plies here was [0/90/±45]s. The comparison of contact force-time curves between specimens for 10, 20, 30 and 40J impact energy, respectively, are shown in Figures 3.7. a-d.

The contact force increases by increasing impact energy, the peak force also increases. The peak force is more sensitive to the impact energy at low-impact energy range.

It is visible that curves behave similarly under various impact levels for all test samples. At the start, impact force fluctuates through a gradual increase. After, they rise with more impact force and the curve range becomes slightly less until the peak impact force. During rebound, the curves show smooth declinations. At the end, there is no impact load after punch and sample are separated.

For instance, the carbon fiber specimen delivered a higher peak load than hybrid and E-glass specimens for 10J impact energy level examined, in the impact energy case shown in Figure 3.7. a, it is noted that the average peak load of carbon fiber specimen was 7.9 kN which is 3% higher than the average peak load, 7.6 kN, for the hybrid specimen and 7% higher than the average peak load, 7 kN, for the E-glass specimen. For the contact time presented by carbon fiber, hybrid fiber and E-glass fiber laminated specimens is 5.13 ms , 5.57 ms and 6 ms, respectively.

The peak contact forces under 20J impact energy were measured as 9.8, 10.6 and 10.7 kN for carbon fiber, hybrid fiber and E-glass fiber respectively, while they were 9.5, 11.4 and 12 kN for carbon fiber, hybrid fiber and E-glass fiber respectively, at 30J impact energy. The peak contact forces under 40J impact energy were measured as 10.3, 11.9 and 12.9 kN for carbon fiber, hybrid fiber and E-glass fiber respectively.

The curves of hybrid and E-glass specimens gave almost a similar peak load and higher than carbon fiber specimen for 20J impact energy level. The maximum contact forces are obtained for E-glass laminate at 40J impact energy. The experimental test series showed an increased deflection for carbon composite plates, which led to higher extent of material damage as compared to glass fiber laminates with energy absorption capacity being lower in carbon fiber laminates as compared to E-glass fiber laminates. The peak contact forces for symmetrical hybrid were measured as 7.7, 10.6, 11.4 and

11.8 kN under the present impact energies, while they were 7.5, 9.8, 10.9 and 10 kN for unsymmetrical hybrid at the same impact energies.

From the above results the carbon fiber has less impact strength than E-glass fiber laminates. The E-glass fiber composites behave in a purely elastic mod until approximately 20% of the maximum impact load for all impact events, and the number of linear increases of load inelastic regime matches the number of roving layers.

With respect to the parameters governing the damage resistance, the effects of impact energy were significant. The results showed higher values of peak deformation and absorbed energy and more extensive delamination as impact energy increased. Laminates showed higher failure depth and permanent damage due to a lower bending stiffness resulting in more severe through thickness damage.
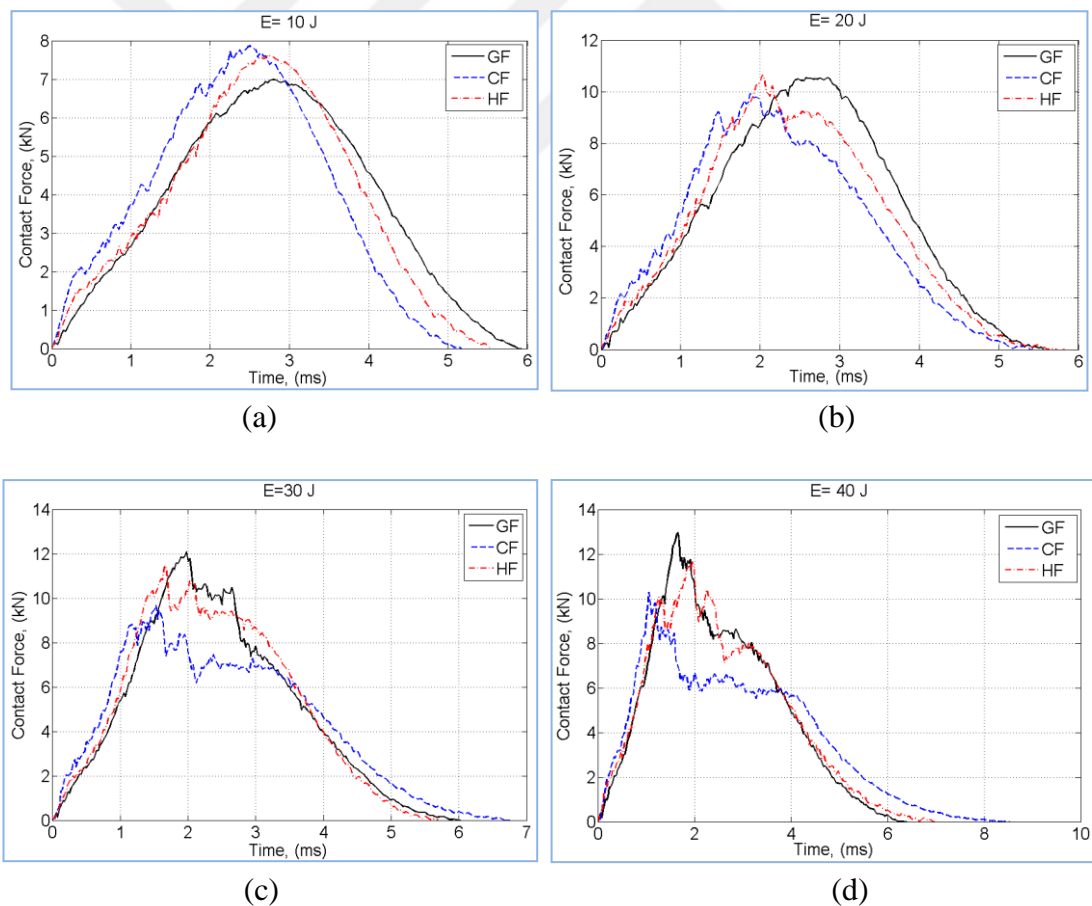
Figure 3.7. Experimental test results analysis - contact force history of different specimens at various energy levels (a) 10, (b) 20, (c) 30 and (d) 40J.

Figure 3.8 shows the experimental test results analysis- contact force history of symmetrical and unsymmetrical hybrid specimens at various energy levels (a) 10, (b) 20, (c) 30 and (d) 40J. The peak contact forces for symmetrical hybrid were measured as 7.7, 10.6, 11.4 and 11.8kN under the present impact energies, while they were 7.5, 9.8, 10.9 and 10 kN for unsymmetrical hybrid at the same impact energies.

Comparatively, stacking sequence has greater effect than rotation angle on impact properties of laminates. The stacking sequence should be severely controlled in design and operation process.
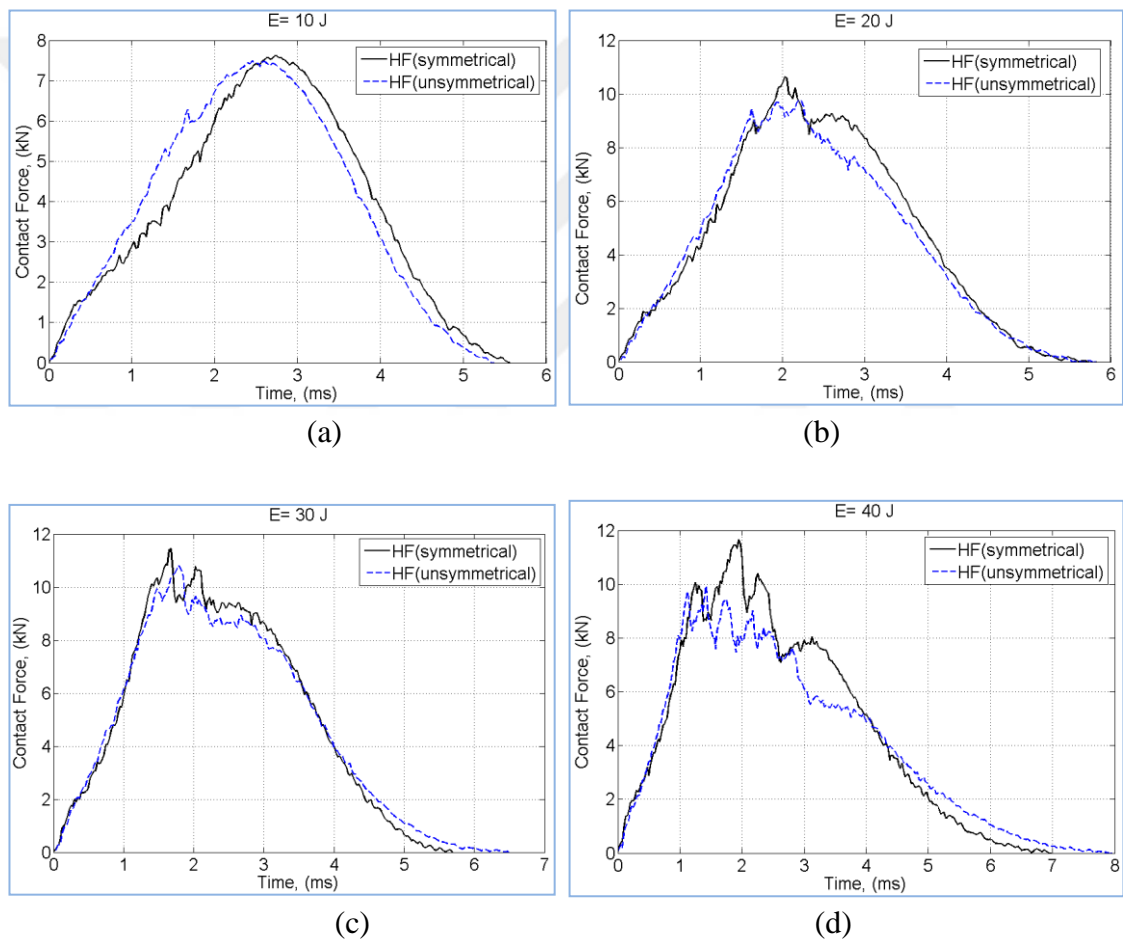
Figure 3.8.   Experimental test results analysis-contact force history of symmetrical and unsymmetrical hybrid specimens at various energy levels (a) 10, (b) 20, (c) 30 and (d) 40J.

CHAPTER FOUR

NUMERICAL ANALYSIS OF LOW SPEED IMPACT BEHAVIOR

4.1. Finite Element Method Simulation

Finite element analysis have been carried out using ABAQUS/ Explicit software. Numerical results were compared with experimental results. Hashin's failure criterion was used to predict failure in composite laminates. After thorough comparison, it was found that the finite element model is best at analysing composite behavior. They are accurate, cheap, and take minimal time. Hybrid composites have better impact absorption and resistance. Because of this, the experiments were performed on e-glass and carbon fibers, as well as hybrids to see where failure begins in the composites. The ABAQUS/ Explicit software was used to carry out the simulations. Because composite laminates are shells, the problem cannot be easily solved. The experiment used the finite element method for simulating failure in the composites under impact. The Hashin methodology was also used.

4.2. Geometry and Boundary Conditions

The ABAQUS software predicted the low-velocity impact response and progression of damage of fiber reinforced laminated composite plates. Four cases unidirectional laminates 16 target plates of equal dimensions were studied; carbon fiber/epoxy laminate, E-glass fiber/epoxy laminate arranged symmetrically relative to the central plane of the plate and E-glass/carbon hybrid laminate (symmetrical , unsymmetrical) with 100×100 mm in dimension with an average thickness of 2 mm were used for the model . The composite laminate is a 8-layer with stacking sequence and the interfaces between plies with different fiber orientations sequence were similar for those in

experimental work in chapter four, Table 3.1, for example Figure 4.1 shows the modeling of layers orientations sequence.

		Ply Name	Region	Material	Element Relative Thickness	CSYS	Rotation Angle	Integration Points
1	✔	Ply-1	(Picked)	carbon	0.125	<Layup>	0	3
2	✔	Ply-2	(Picked)	carbon	0.125	<Layup>	90	3
3	✔	Ply-3	(Picked)	carbon	0.125	<Layup>	45	3
4	✔	Ply-4	(Picked)	carbon	0.125	<Layup>	-45	3
5	✔	Ply-5	(Picked)	carbon	0.125	<Layup>	-45	3
6	✔	Ply-6	(Picked)	carbon	0.125	<Layup>	45	3
7	✔	Ply-7	(Picked)	carbon	0.125	<Layup>	90	3
8	✔	Ply-8	(Picked)	carbon	0.125	<Layup>	0	3

Figure 4.1. Modeling of layers orientations sequence in ABAQUS program.

A hemispherical projectile of diameter 20 mm and 5.045 kg of mass, with impact energy of 10, 20, 30 and 40J, is used in the experimental setup. The boundary condition was assigned to the projectile prescribed in z-direction with all degrees of freedom constrained to zero to replicate experimental conditions. Rigid elements discretized the impactor, top and bottom apparatus. The supporting base was set in every direction in order to simulate the conditions of the experiment. A displacement boundary condition is prescribed at the top edge clamp of Ux=0, Uy=0, Uz=-Uz . The impact event was simulated by imposing the appropriate initial velocity v_o at the instant of contact to the impactor. Figure 4.2 shows the simulation of the experimental setup.
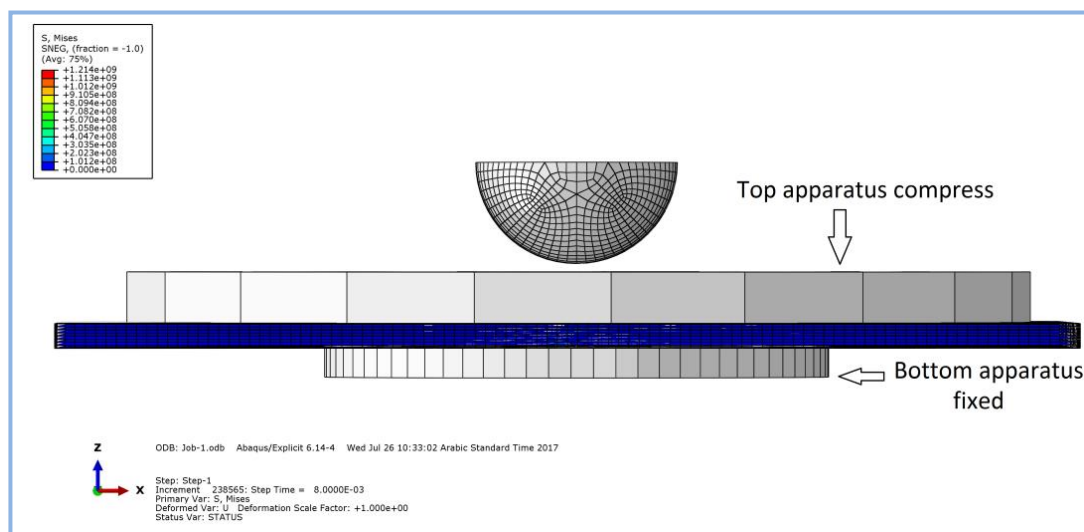
Figure 4.2. Simulation of the experimental setup.

The plate is simply free while the bottom apparatus has fixed supported Ux=Uy=Uz= 0. The plate was finely meshed with elements 0.5 × 0.5 mm size, while a coarser mesh built with 1 × 1 mm elements was used for the impactor. A surface-to-surface contact pair was used to define the interaction response between the target plate and the projectile which were also applied to simulate the contact between the laminate panel and the supporting base. Thus, contact between the projectile and plate as well as each contact ply was defined by the general contact algorithm within ABAQUS/ Explicit, Figure 4.3.
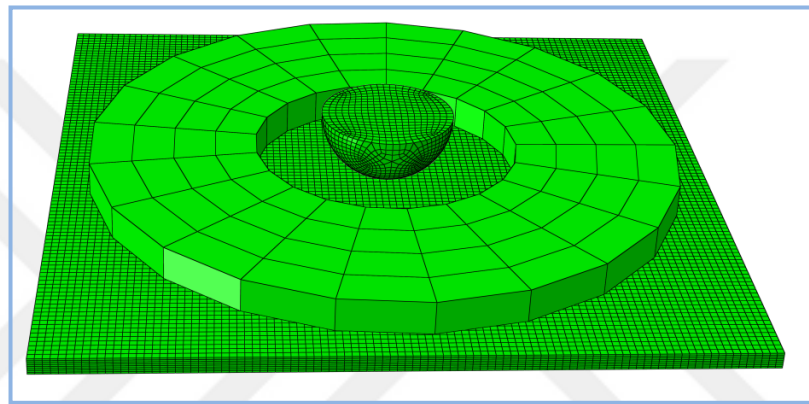
Figure 4.3.Meshing model.

A frictionless model was included in the contact property and for input file usage, the elastic, and density properties values were used in the finite element model, they were obtained by a series of experimental tests or gathered from the literature. The values of the main properties adopted in the analyses are summarized, Figure 4.4.
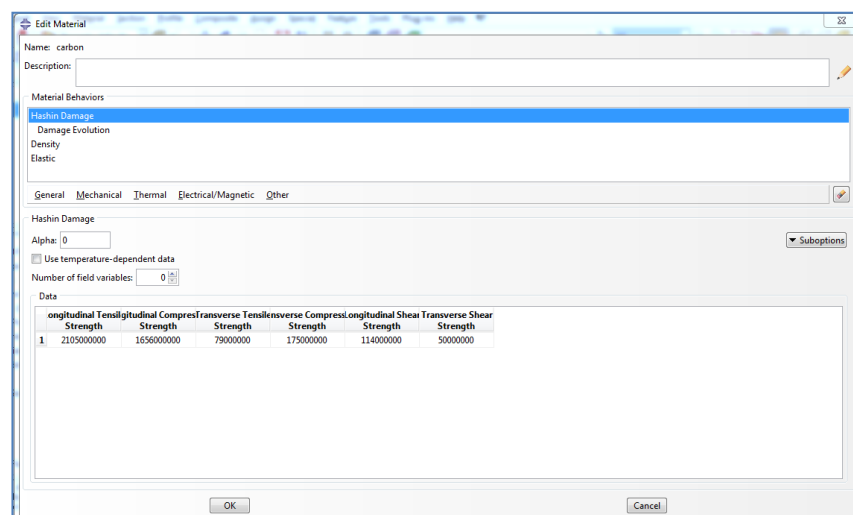
Figure 4.4. Modeling properties.

Orthotropic material properties are given for carbon/epoxy and e-glass/epoxy composite layers, Table 4.1. These material properties are used in finite element simulations.

Table 4.1. Mechanical properties of the specimens

Mechanical properties	Carbon fiber/epoxy composite plate	E-glass fiber/epoxy composite plate
Density, ρ	1580 kg/m^3	18300 kg/m^3
Longitudinal modulus, E_1	143.4 GPa	40.51 GPa
Transverse modulus, E_2	92.7 GPa	13.96 GPa
Poison ratio, v_{12}	0.31	0.22
In plan shear modulus, G_{12}	3.8 GPa	3.10 GPa
In plan shear modulus, G_{31}	3.8 GPa	3.10 GPa
Out-of-plane Shear Modulus G_{23}	3.2 GPa	3.10 GPa
Longitudinal tensile strength, X_t	2945 MPa	783.30 MPa
Longitudinal compression strength, X_c	1650 MPa	298 MPa
Transverse tensile strength, Y_t	54 MPa	64 MPa
Transverse compression strength, Y_c	240 MPa	124 MPa
In-plan shear streangth, S_{12}	114 MPa	69 MPa

Experimental results from literature [78,79] were used to compare the results of the models.

4.3. Damage Initiation For Fiber-Reinforced Composites

The material damage initiation capability for fiber-reinforced materials:

- requires that the behavior of the undamaged material is linearly elastic ;
- is based on Hashin's theory (Hashin and Rotem, 1973 [72], and Hashin, 1980 [71]);
- takes into account four different failure modes: fiber tension, fiber compression, matrix tension, and matrix compression; and
- can be used in combination with the damage evolution model.

4.3.1. Simplified Impact Damage Model

The study first used low velocity impact testing on carbon, E-glass, and hybrid fiber multi-ply plates at 10, 20, 30, and 40J impact energy using a drop weight system having 20 mm impactor diameter and weight of 5.045 kg. The damage is dependent on the energy levels. A simple damage model was used to simulate the real damage. It presumed that gradients are less based on thickness. The thickness of the ply decreases as the force moves towards the impact side. The employed modeling procedure required performing several calculations for a specific impact energy E_k , here, the maximum energy was applied, (E_k = 40 J) to confirm the highest possible corroboration between the experiment and simulations. The calculations produced a method for finding ply thickness in the region of impact. The results helped determine a thickness of the first ply Y_k (impact side) for the energy E_k, shown with:

$$y_k = z - (x_1 E_K), \tag{4.1}$$

where: z is the nominal thickness of the undamaged ply, x_1 is the coefficient determining a decrease in thickness of the first laminate ply, which, after transformation (1), is expressed as:

$$x_1 = \frac{y_k - z}{-E_K} \tag{4.2}$$

The calculation of the energy E_k also led to determination of a constant value of x_k, describing the value of proportionate decrease in thickness of successive plies of the laminate. The results helped establish a relationship that describes the constant coefficient of decrease in thickness of successive laminate plies for any impact energy E, expressed as:

$$x_2 = \frac{x_k}{E_K}. \tag{4.3}$$

Once the relationships between equations 4.1 through 4.3 are generalized, the technique used for damage modelling allows an easy discovery of ply thickness and for impact energy (E) as:

- Ply 1 thickness:

$$y_1 = z - (x_1 E),$$

(4.4)

- Thickness for following plies:

$$y_n = y_{n-1} - (x_2 E).$$

(4.5)

The studied composite damage determination model is easy yet thorough in that it finds the proper decrease in strength after damage.

4.3.2. Composite material damage model

Damage in composite materials is complicated because there are various modes of failure including damage to the matrix, fibers breaking or buckling, delamination, or combinations of these. They are hard to elaborate upon in depth because existing research only deals with composite damage. Although there are models, these models must be backed up with lab experiments for verification. This research used the progressive damage criteria formed by Lapczyk and Hurtado [75] that deals with the relationship between the effective stress $\sigma\hat{}$ and the nominal stress σ is described by the damage operator M, shown as:

$$\sigma\hat{} = M\sigma = \begin{bmatrix} \frac{1}{(1-d_f)} & 0 & 0 \\ 0 & \frac{1}{(1-d_m)} & 0 \\ 0 & 0 & \frac{1}{(1-d_s)} \end{bmatrix} \sigma.$$

(4.6)

where: d_f, d_m and d_s are the damage variables for fibre, matrix, and shear failure modes, respectively, which are derived from the damage variables d_f^t, d_f^c, d_m^t and d_m^c, corresponding to the above four failure modes as follows:

$$d_f = \begin{cases} d_f^t \; if \; \sigma\hat{}_{11} \geq \; 0, \\ d_f^c \; if \; \sigma\hat{}_{11} < \; 0, \end{cases}$$

(4.7)

$$d_m = \begin{cases} d_m^t \; if \; \sigma\hat{}_{22} \geq \; 0, \\ d_m^c \; if \; \sigma\hat{}_{22} < \; 0, \end{cases}$$

(4.8)

$$d_s = 1 - (1 - d_f^t)(1 - d_f^c)(1 - d_m^t)(1 - d_m^c).$$

(4.9)

Before damage begins and progresses, the damage operator (M) equals the identity matrix. Thus, $\sigma\hat{} = \sigma$. Using this system, the onset of damage is based on Hashin's theory [71, 72], which means that surface failure is shown by possible stress space. Hashin considers four change devices: fiber tension and compression; matrix tension and compression. These criterions can be shown by:

Fiber tension $(\sigma\hat{}_{11} \geq 0): F_f^t = \left(\frac{\sigma\hat{}_{11}}{X^T}\right)^2 + \alpha \left(\frac{\tau\hat{}_{12}}{S^L}\right)^2.$ (4.10)

Fiber compression $:(\sigma\hat{}_{11} < 0): F_f^c = \left(\frac{\sigma\hat{}_{11}}{X^C}\right)^2.$ (4.11)

Matrix tension $(\sigma\hat{}_{22} \geq 0): F_m^t = \left(\frac{\sigma\hat{}_{22}}{Y^T}\right)^2 + \left(\frac{\tau\hat{}_{12}}{S^L}\right)^2.$ (4.12)

Matrix compression $(\sigma\hat{}_{22} < 0): F_m^c = \left(\frac{\sigma\hat{}_{22}}{2S^T}\right)^2 + \left[\left(\frac{Y^C}{2S^T}\right)^2 - 1\right]\frac{\sigma\hat{}_{22}}{Y^C} + \left(\frac{\tau\hat{}_{12}}{S^L}\right)^2.$ (4.13)

where: X^T, X^C are the longitudinal tensile and compressive strengths, respectively; Y^T, Y^C are the transverse tensile and compressive strengths; and S^L and S^T are the longitudinal and transverse shear strengths, respectively. The coefficient α in equation 4.10 regulates the contribution of the shear stress to the fiber tensile initiation criterion. When the damage initiation criterion is satisfied, the composite undergo degradation, which leads to a progressive decrease in stiffness of the material. Damage evolution is described here by means of an energy criterion which is a generalization of the Camanho and Davil theory [76] for the modelling of delamination by cohesive elements. The description of damage evolution after satisfying the damage initiation criterion is based on the fracture energy dissipated during the damage process, G^C, figure 4.5.a. After damage initiation (i.e., $\delta_{eq} \geq \delta_{eq}^0$) for the behaviour shown in figure 4.5a, the damage variable for a particular mode is given by the following expression:

$$d = \frac{\delta_{eq}^f(\delta_{eq} - \delta_{eq}^f)}{\delta_{eq}(\delta_{eq}^f - \delta_{eq}^0)},$$ (4.14)
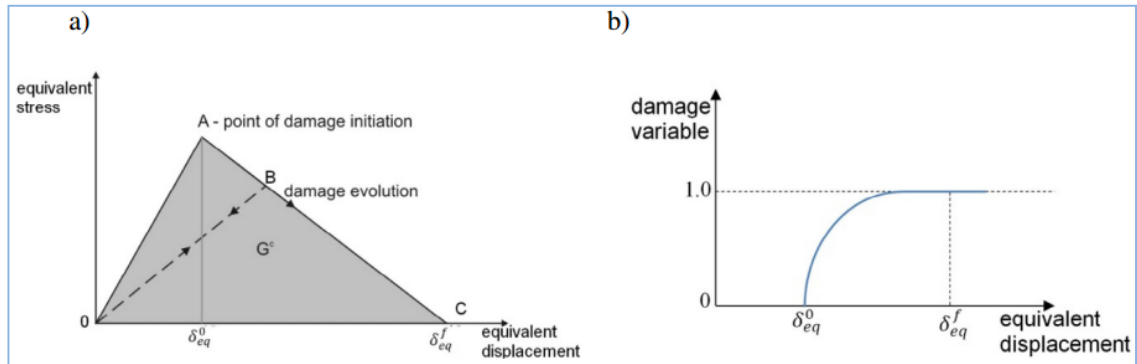
Figure 4.5. Damage evolution law: (a) linear damage evolution, (b) damage variable as a function of equivalent displacement, [73].

Where δ_{eq}^0 is the initial equivalent displacement at which the initiation criterion for that mode was met (d = 0) and δ_{eq}^f is the displacement at which the material is completely damaged in this failure mode (d = 1) – Figure 4.5.b. For each failure mode it is necessary to determine the energy dissipated due to failure, G^C, which corresponds to the area of the triangle OAC in Figure 4.5.a. The values of δ_{eq}^f for the various modes depend on the respective G^C values. Unloading from a partially damaged state, such as point B in Figure 4.5.a, occurs along a linear path toward the origin in the plot of equivalent stress vs. equivalent displacement (this same path is followed back to point B upon reloading as shown in the figure).

4.3.3. Finite element analysis for damage model

ABAQUS was used to perform the numerical simulation within the non-linear range. The analysis was carried out for the samples with damage caused by impact from varying energy levels. This is shown in Figure 4.6. A simple damage model was used to indicate where composite materials were damaged. The ply thickness decreases from impact energy, and this agrees with the process discussed in section 4.3.1.
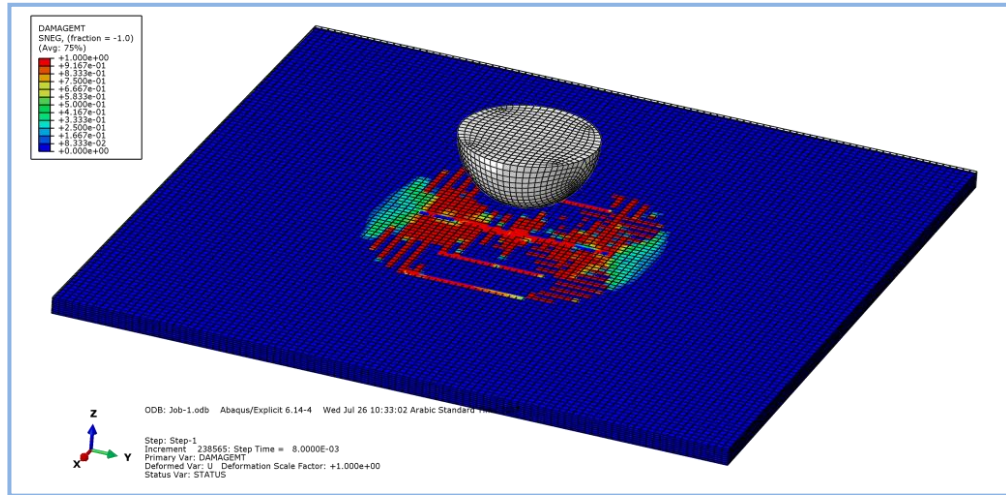
Figure 4.6. Impact simulation.

The numerical analysis was performed on a composite plate consisting of 8 plies of unidirectional carbon, E-glass fiber and hybrid /epoxy laminate, in a symmetric arrangement compared to the plate's central plane as [0/90/±45]s, in addition to hybrid (unsymmetrical) laminate arranged as [0/90/±45]2. The single ply thickness was 0.125 mm, with a total plate thickness of 2 mm. A single ply laminate model was established for plain stress. For undamaged and elastic orthotropic laminates, the stress –strain relationship in plane stress can be written:

$$\begin{Bmatrix} \sigma_{11} \\ \sigma_{22} \\ \tau_{12} \end{Bmatrix} = \frac{1}{D} \begin{bmatrix} E_1 & -v_{21}E_1 & 0 \\ -v_{12}E_2 & E_2 & 0 \\ 0 & 0 & DG_{12} \end{bmatrix} \begin{Bmatrix} \varepsilon_{11} \\ \varepsilon_{22} \\ \gamma_{12} \end{Bmatrix} \qquad (4.15)$$

Where σ_{ij} are stresses in ij directions, c_{ij} are stiffness coefficients, ε_{ij} are strains, τ_{ij} are shear stress and γ_{ij} are shear strains and D is defined as:

$$D = 1 - v_{12}v_{21} \qquad (4.16)$$

As the above information stated, equation 4.15 allows for calculation of laminate stresses from a 3D load. Behavior is completely elastic in the initiate loading phase. This relates to the damage variable from equation 4.14: d=0. After meeting the onset of damage criteria from Hashin's theory, equations 4.10-13 establish the gradual decrease in stiffness until there is none remaining and d=1. The stiffness matrix is written as:

$$\begin{Bmatrix} \sigma_{11} \\ \sigma_{22} \\ \tau_{12} \end{Bmatrix} = \frac{1}{D} \begin{bmatrix} (1-d_f)E_1 & (1-d_f)(1-d_m)v_{21}E_1 & 0 \\ (1-d_f)(1-d_m)v_{12}E_2 & (1-d_m)E_2 & 0 \\ 0 & 0 & D(1-d_s)G_{12} \end{bmatrix} \times \begin{Bmatrix} \varepsilon_{11} \\ \varepsilon_{22} \\ \gamma_{12} \end{Bmatrix} \qquad (4.17)$$

where damage variables d_f, d_f and id_f are described by equations 4.7–9, and D equation 4.16. The criteria for the onset of must be used with elements with a plane

stress formulation. These include the elements of: plane stress, shell, continuum shell, and membrane. Using the above variables to note if damage has begun, a value less than 1 shows there is not sufficient satisfaction of the criteria. Values of 1 or higher show that the criteria is met. For any model, the maximum value of this variable does not exceed 1.0. However, if we didn't define a damage evolution model, this variable can have values higher than 1.0, which specifies by how much the criterion has been exceeded, [74, 77].

4.4. Simulation results and discussion

4.4.1. Impact study

The model is effective because the results from the numerical analysis and experiments agree based on impact loads and damage features. After analysing the patch stacking sequence and angle of rotation, the results show that the model used the Hashin failure criteria to compare damage in composites after impact. There was agreement between the simulation and experiment for the three stacking sequences. The model for progressive failure made using ABAQUS is usable for failure prediction for interply hybrids with glass and carbon unidirectional composites. The experiment and simulation results agree. The results from the experiment and finite element method of impact velocity are extremely close. The contact force error in ABAQUS is small at the onset and then grows based on the function of contact time. Any differences between the software's results and those from the experiment can be understood as: there is no element model for the beginning of impact so contact exists between the top surface and impactor. Then, there is agreement between the two. That said, because the impactor is rigid body, absorbed energy is ignored. Because of this, stiffness lessens faster at higher energy levels and longer periods of contact. Also, curves are less as the element fails.

Figure 4.7.a, b, c and d show force–time histories of E-glass/epoxy specimens 10, 20, 30 and 40J impact energy levels, respectively. As seen in these figures, the peak contact forces for numerical results were measured in ABAQUS as 6.9, 9.2, 12.05 and 13.6 kN under the present impact energies, respectively. In the laboratory the experimental results were measured as 7, 10.6, 12 and 13.7 kN under the present impact energies, respectively. The contact force takes maximum value 13.7 kN for numerical results under 40J impact energy. Also, it was observed that the contact force and time increased

with the increase of the impact energy level. The experiment revealed that damage begins in the e-glass at the area of contact because of high compression. Delamination is visible after extended indentation and this decreases the contact force. This is explained due to stiffness and delamination. The increase and decrease of force time explains that delamination arises from longer periods. There are two stages of impact: pre-rebound and rebound. During the former, contact forces increases despite rises and falls until impactor velocity reaches zero at top contact force. During the latter, there is a steady decrease in contact force until there is a complete drop-off between plate and impactor. The results display incongruity of 20 to 30 percent in the force time history during the rebound stage for both laminate types. These figures reveal the effect of epoxy, which does not have a place in modelling.

(a)

(b)

(c)

(d)

Figure 4.7. Comparison of experimental and numerical results analysis- contact force history E- glass/epoxy fiber specimens at various energy levels (a) 10, (b) 20, (c) 30 and (d) 40J.

Figure 4.8 shows the curves of contact force for carbon fiber specimens at 10, 20, 30 and 40J ,energy levels, respectively. The peak contact forces for numerical results were measured in ABAQUS as 7.92, 9.8, 10.3 and 10.5 kN under the present impact energies, respectively. In the experimental results were measured in the laboratory as 7.9, 10, 9.8 and 10.2 kN under the present impact energies, respectively. They reveal a maximum force for numerical results as 10.5 kN and this is more than the experimental data by 5.8 percent.
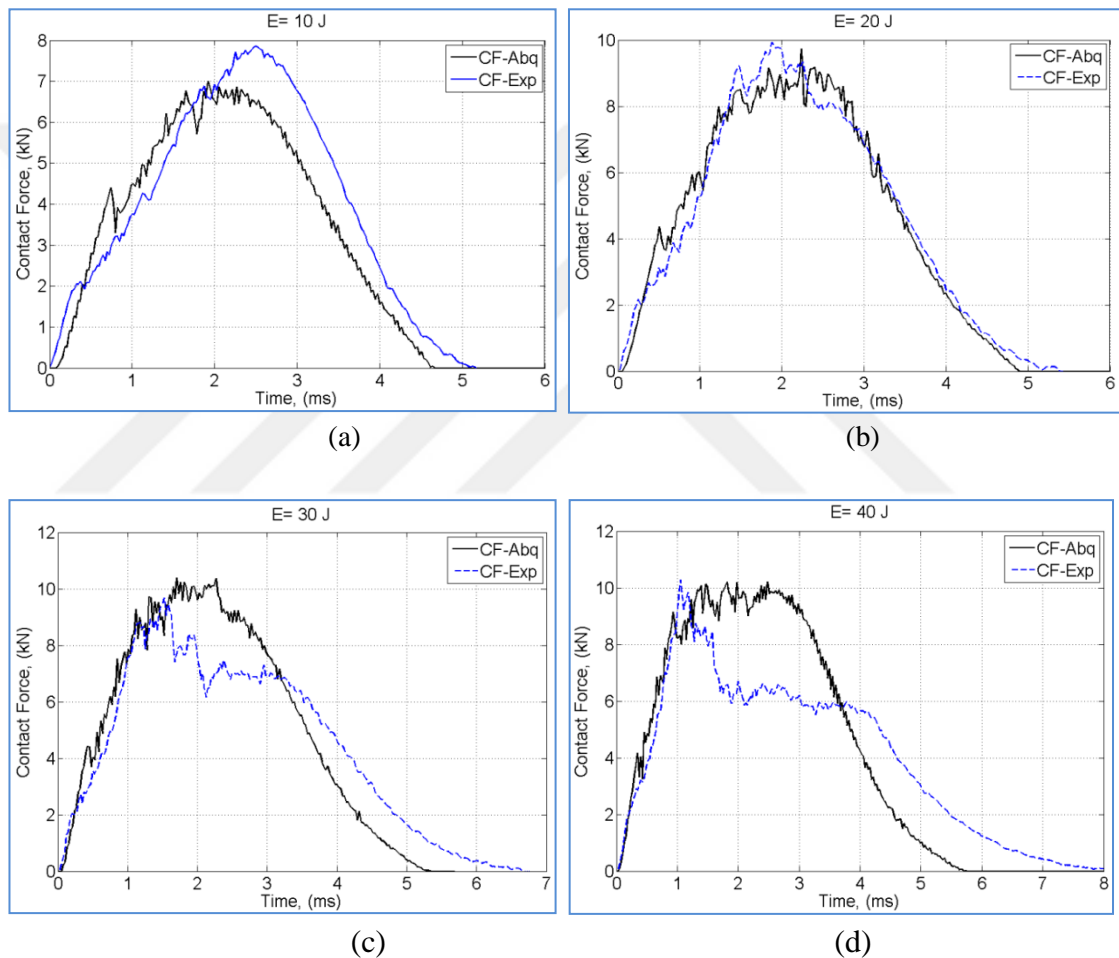
Figure 4.8. Comparison of experimental and numerical results analysis- contact force history carbon fiber specimens at various energy levels (a)10, (b) 20, (c) 30 and (d) 40J.

Figures 4.9 displays the simulation for symmetrical hybrid laminates at different energies 10, 20, 30 and 40J as a function of time of contact. The peak contact forces for experimental results were measured in the laboratory as 7.7, 10.9, 11.4 and 11.8 kN under the present impact energies, respectively. While, the peak contact forces for

numerical results were measured in ABAQUS as 6.8, 9.8, 12 and 12.5 kN under the present impact energies, respectively. It is known that hybrid composites deform more at longer periods of contact until rebounding happens at E= 20J. It increases when the hybrids are fully penetrated at E = 30J. At the first, damage begins at t = 4.7ms. They are half perforated at t = 5.2 ms. The laminate damage increases quickly after E = 40J.
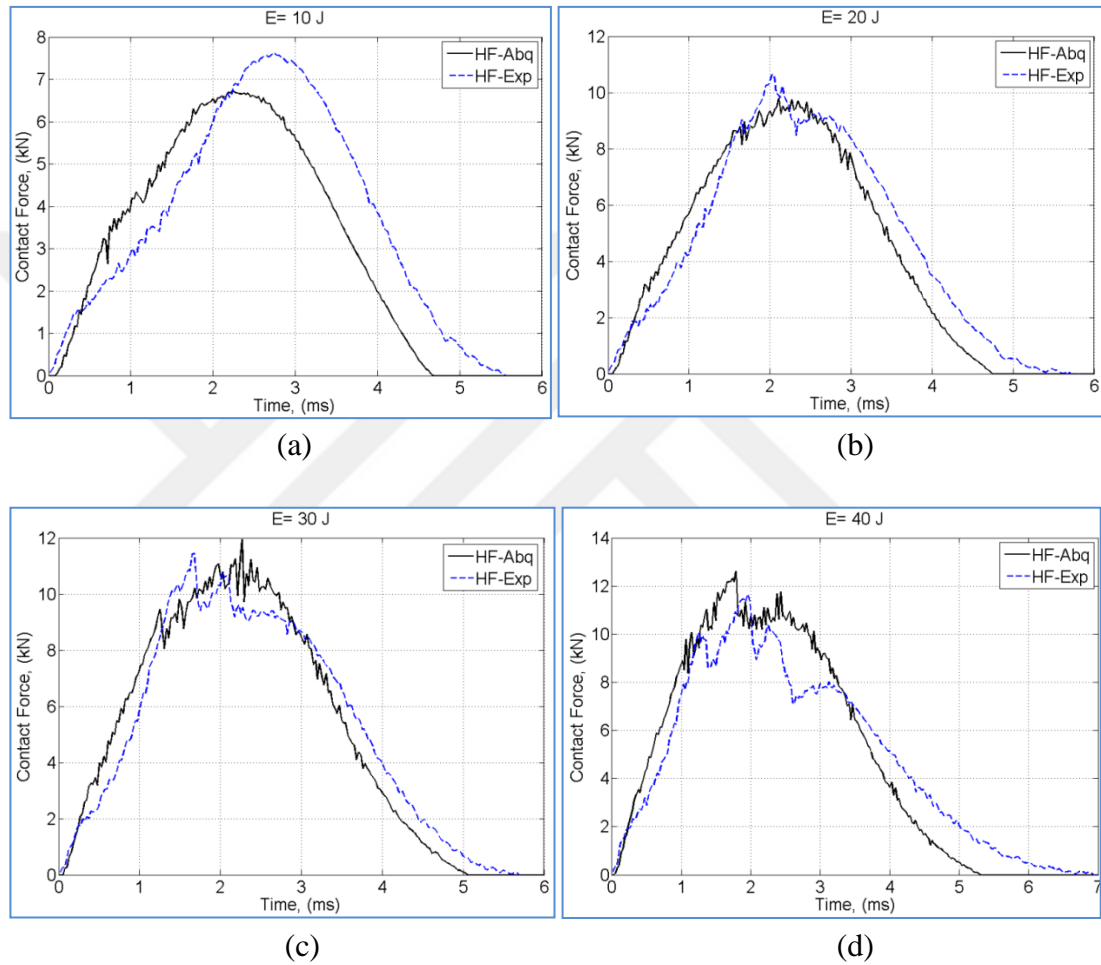
Figure 4.9. Comparison of experimental and numerical results analysis- contact force history of symmetrical hybrid fiber specimens at various energy levels (a)10, (b) 20, (c) 30 and (d) 40J.

Figure 4.10 shows comparison of experimental and numerical results analysis - contact force history of unsymmetrical hybrid fiber specimens at various energy levels (a) 10, (b) 20, (c) 30 and (d) 40J. The peak contact forces for numerical results were measured in ABAQUS as 7.5, 9.9, 10.9 and 10.5 kN under the present impact energies, respectively. While, the peak contact forces for experimental results were measured in the laboratory as 6.9, 10.3, 11 and 11.8 kN under the present impact energies, respectively.

The numerical results are compared and verified with experimental results, a reasonably good agreement is achieved in terms of load-time curves. The numerical simulations using the proposed damage model effectively forecast low velocity impact behavior of carbon, E-glass and hybrid laminates. Simulation results indicate that E-glass/epoxy laminate show bigger peak loads, lower contact time values and smaller ultimate central damage under the same impact energy. As such, E-glass fibers / epoxy deserves more research because it has better impact resistance than the others.
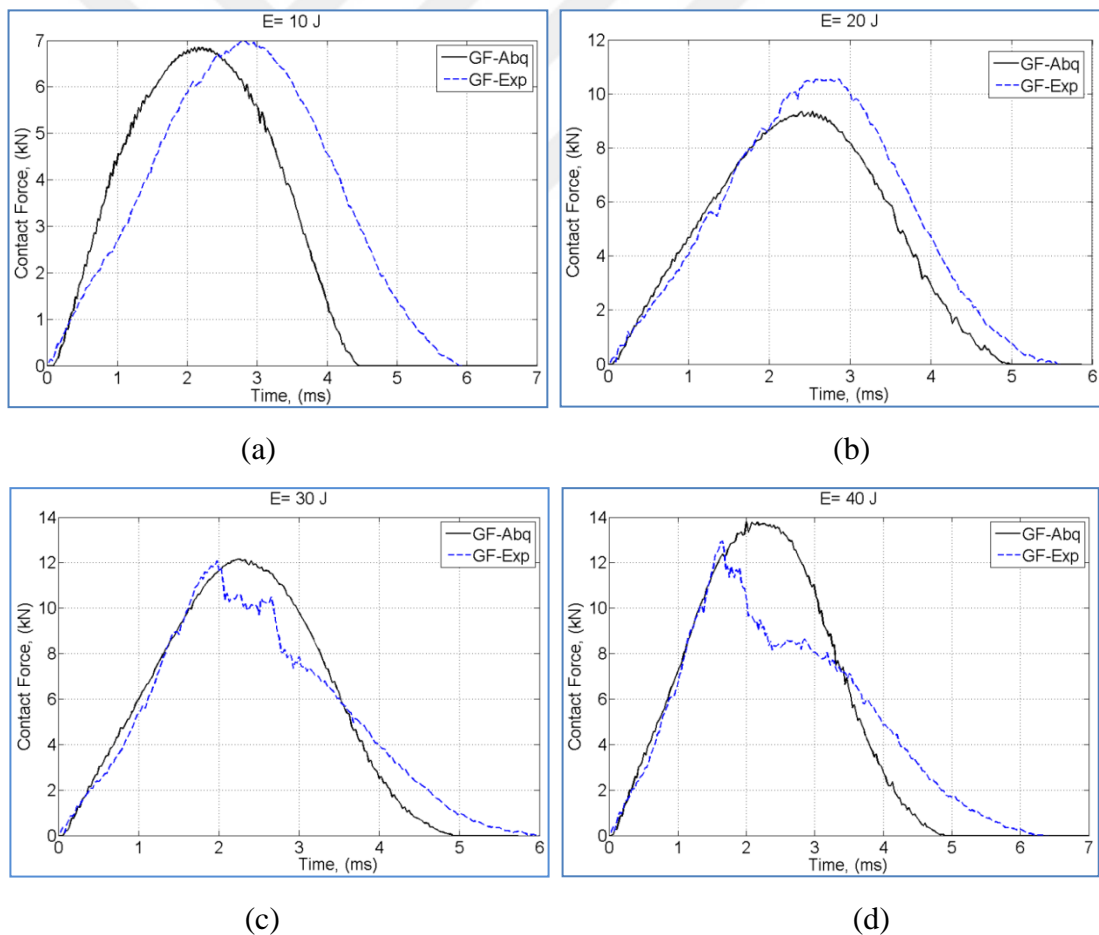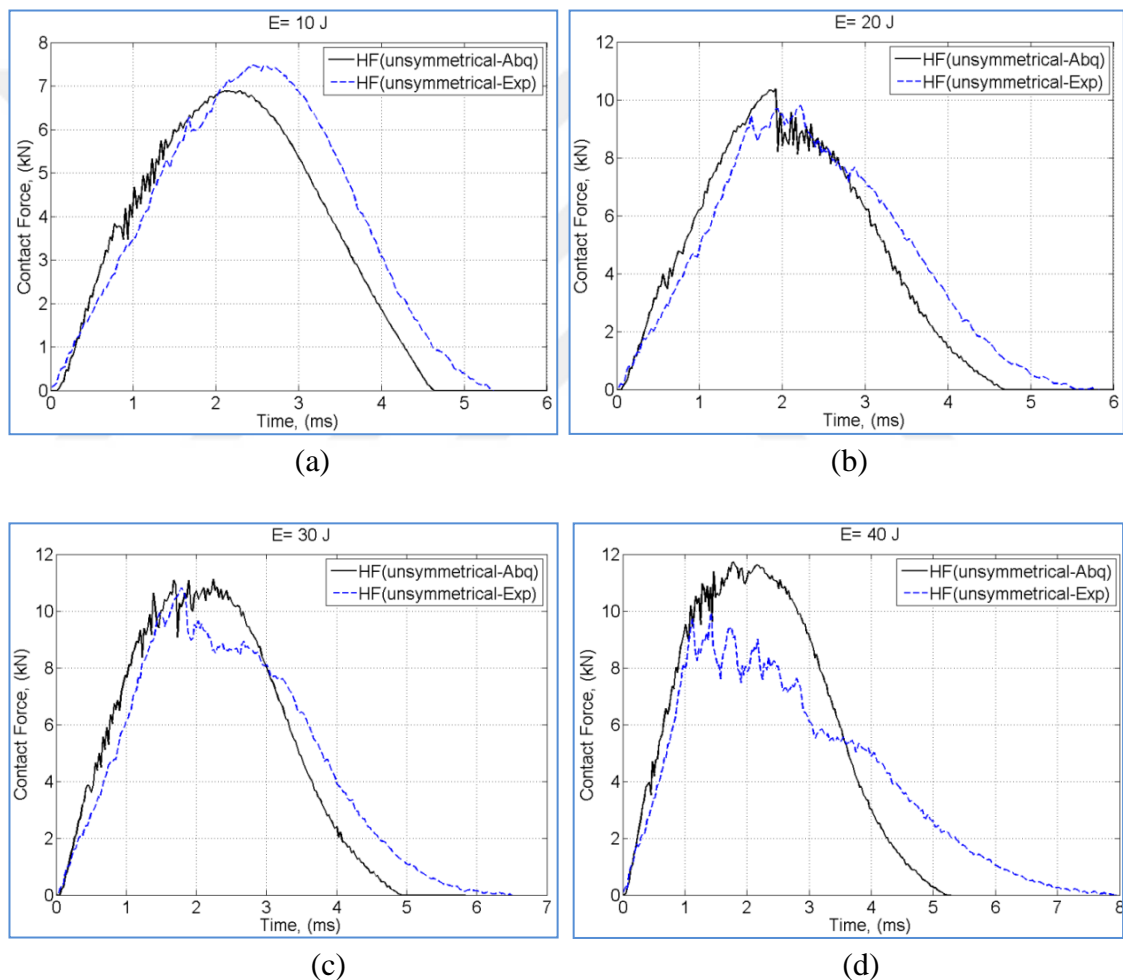

Figure 4.10. Comparison of experimental and numerical results analysis - contact force history of unsymmetrical hybrid fiber specimens at various energy levels (a) 10, (b) 20, (c) 30 and (d) 40J.

The transferred energy from the impactor to the hybrid composite plates, is depicted in Figure 4.11 vs. time for different impact energies. These curves are representative of the performed tests and show the typical behavior for composite specimens. The absorbed

energy levels are approximately the same curve line shape. They are characterized by an increase in the energy up to a maximum value, followed by a drop. The minimum energy occurs when the impactor is completely stopped by the composite plate. At this instant, all kinetic energy of the impactor is transferred to the composite specimen. Once the minimum energy is reached, the transferred energy tends to an asymptotic value which corresponds to the energy absorbed by the composite plate.

The absorbed energy and the normalized absorbed energy increase as the impact energy increases until fail . The composite plates almost absorbed the total kinetic energy of the impactor at impact energies 10J and 20J. At 30J and 40J test conditions the composite specimens are penetrated by the impactor, as shown in Figures 3.5.c and 3.6.a.
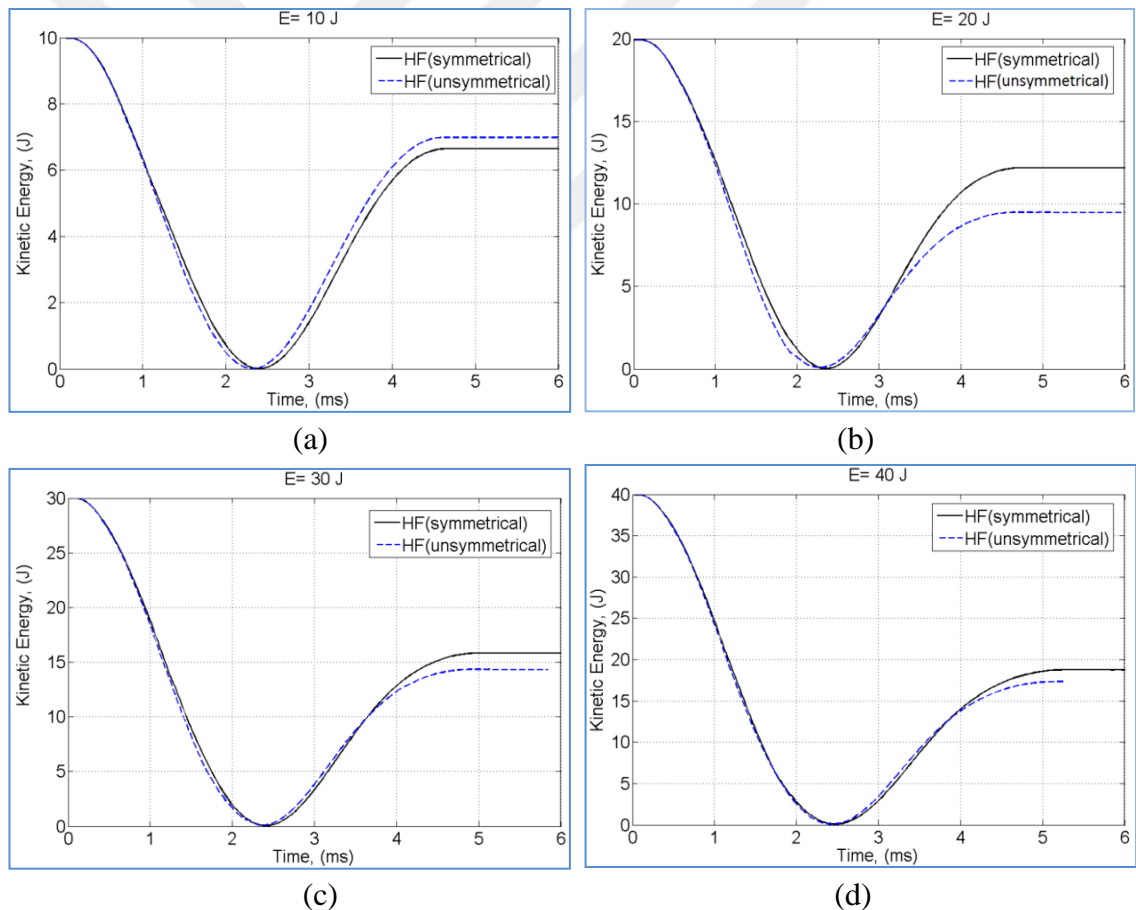
Figure 4.11. Comparison of numerical results analysis - Kinetic energy history of symmetrical and unsymmetrical hybrid fiber specimens at various energy levels (a) 10, (b) 20, (c) 30 and (d) 40J.

Figure 4.11 displays how impactor kinetic energy changes over time and that there is more kinetic energy with higher levels of impact energy. The symmetrical and

unsymmetrical (the impact from carbon side), for hybrid laminates are in strong agreement, excluding those calculated with the finite element model. Here, it is more at 10J and less for 20 and 30J. At 40J it is the closest. Delamination is the suspected culprit of these variations.

The diagrams in Figure 4.12, present the time history distribution of kinetic energy in the target structures for E-glass ,carbon and hybrid fiber laminate sat various energy levels. In all cases, the impact energy of the hemispherical projectile suddenly declines as penetration duration increases. The diagrams compare the absorbed energy prediction of the three structures and observe that the absorbed energy increases proportionally to the corresponding duration.

(a)   (b)

(c)   (d)
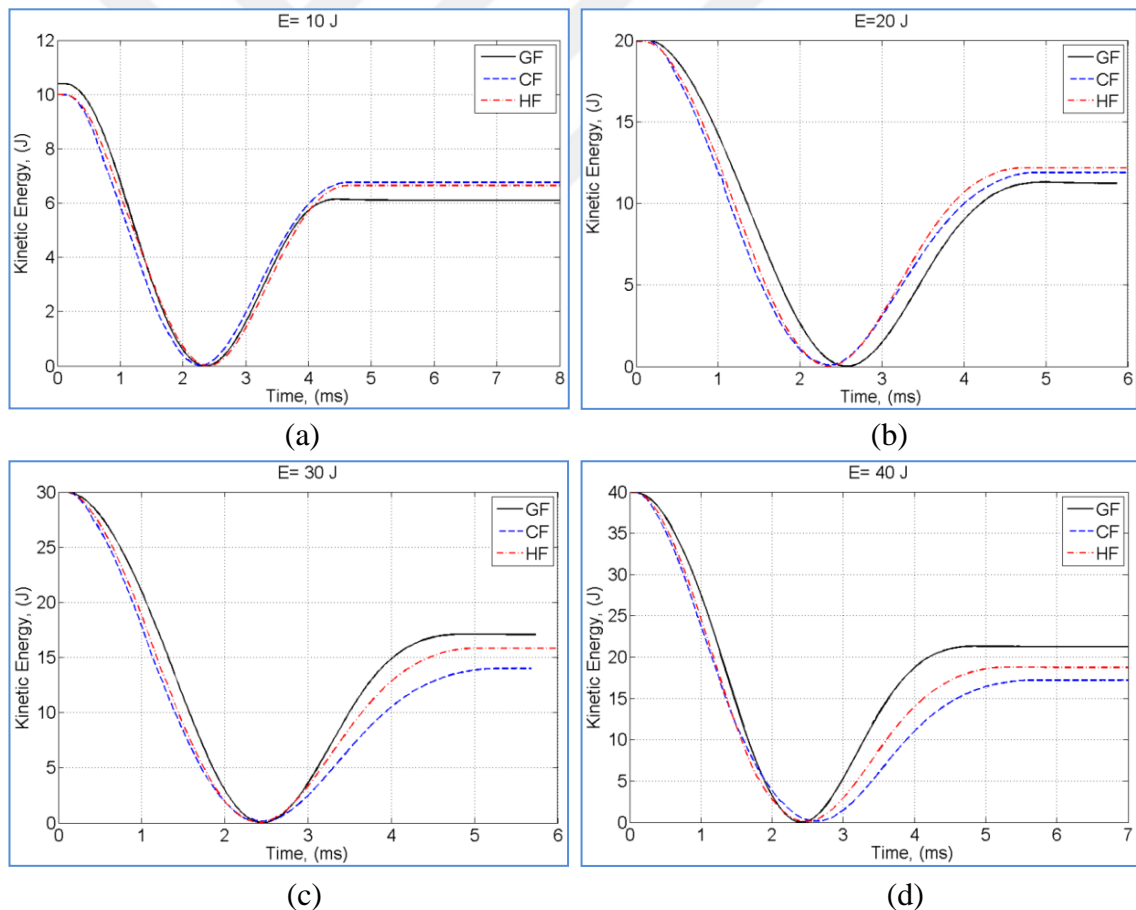
Figure 4.12. Numerical results analysis-Kinetic Energy and time histories of E-glass, carbon and hybrid fiber laminates at various energy levels (a) 10, (b) 20, (c) 30, (d) 40 J.

In the plot of Figure 4.12.a, E-glass with an impact velocity of 2 m/s, numerical result in the composite plate increases slightly to about 6 J within 4.15s. Also, the carbon laminate and the hybrid curves grows swiftly corresponding to about 6.9 J within 4.4s and maintains this variability mode to accomplish the propagation of the energy absorbed (significant difference of 20.68%). Once again, when the projectile is impacted at 2.81 m/s, the absorption tendency continues as shown in the diagram of Figure 4.12.b, The predicted energy of the E-glass composite plate increases marginally at a constant energy of 12J within 4.5s and then moves speedily to17J at 3.44 m/s and finally completes the event with 22J at 4 m/s with constant trajectory. Also, the carbon and hybrid plate numerically predicts a slight rise in energy at 12.55 J from onset and maintains the level constantly to conclude the trajectory incident, a difference of 2.2J. Similar trend is noted in the 4 m/s impact velocity as displayed in the graph of Figure 4.12.d. Numerically, it is evident that absorbed energy threshold of composite plate increases intermittently to about 22J within 4s and continuously maintains the threshold to mode to complete propagation (a significant difference of about 30%).

In all cases, the simulation result confirms that the carbon structure absorbed more energy than the other composites structures except in the 2m/s impact velocity. This tendency suggests that the increase in the impact energy reduces the strength and stiffness properties of the composite plate.

4.4.2. Damage Initiation– Progressive Damage Evolution

The first numerical examination was done on unidirectional composites of carbon and epoxy with a symmetrical arrangement and similar stiffness. Because of this, the analysis was furthered through progressive damage study. Equations 4.10 through 4.13 explain how damage begins in composite materials through the piles of compressed plates. Based on the Hashin theory, damage is initiated when a value of 1 reaches: fiber compression, tension, or matrix compression or tension. Based on these equations and the found results, it is found that damage begins when the matrix and fibers are damaged because of compression. The maps showcase the exact point where damage begins.

Constitutive model based on continuum damage mechanics for the prediction of the beginning and increase of damage is offered computationally, the experimentally exact

light projected damage area is checked aligned with the whole damaged area from simulations. This means that the following criteria are satisfied: compression matrix criterion (HSNMCCRT > 1) and tension matrix criterion (HSNMTCRT > 1), compression fiber criterion (HSNFCCRT > 1) and tension fiber criterion (HSNFTCRT > 1). This indicates that lay-up is impacted where laminates are damaged after impact. After analyzing the plates, the results are listed in the Table 4.2, (+) refers to the met of criterion; (-) refers to the adverse result.

Table 4.2. Results of damage initiation criterion.

Energy	HSNFTCRT	HSNFCCRT	HSNMTCRT	HSNMCCRT
10J	+	+	+	+
20J	+	+	+	+
30J	+	+	+	+
40J	+	+	+	+

Matrix and fiber damage cause damage to begin. The results also show that this is more complex than it sounds because many modes of damage occur simultaneously. Damage spreads are the plates are first impacted, as shown in equation 4.14. This occurred after the damage reached 1, and stiffness then started declining. Figures 4.14, 4.15, 4.16 and 4.17 show the Hashin compressive and Hashins tensile, failure criteria evolution of the carbon fiber, E-glass fiber and hybrid fiber laminates at 10, 20, 30 and 40J for impact energy levels, respectively. Four Hashin variables (or called status variables) in ABAQUS are defined for Compressive fiber, Tensile fiber, Compressive matrix and Tensile matrix, 8 plies are selected for analysis. The damage evolution of composites can be divided into four stages; carbon fiber , E-glass fiber, hybrid (symmetrical and unsymmetrical), respectively. There is a minimal fiber breaking at low-velocity impact but large presence of cracks to the matrix. Damage to the matrix is causes by compressive stress at the top and tensile stress at the bottom. The prediction of the response and modes of failure from Finite element method agree with the experimentation. The main mode of failure is tension to the matrix which starts at the base and moves to the direction of the fiber. Matrix compression begins at the top and also moves towards the fiber. However, matrix compression that starts in the middle presents the biggest threat. Impact energy does not have a strong effect on initial load of

damage. Lost energy because of composite damage and dynamic friction increases because of impact velocity and energy.

Through the Finite element method analysis, Hashin's criteria is revealed for strong application of impact analysis, especially using ABAQUS software. Such an application can benefit those considering a proper method for measuring damage based on cost. Matrix cracks at the interface of the fiber and matrix are pushed back along the interface. Compressive and tensile failures are impacted by the shape of the fiber, the materials of the fiber and matrix, defects in the fiber and matrix, and interaction between these two components. The matrix presents a more serious issue to damage control than the fiber. Matrix fails in a similar way at the various energies used (10, 20, 30, and 40J), as shown in Figure 4.14. a, b, c and d. Compressive matrix failure progresses from layer 1 through 8 (top to bottom). This indicates that matrix failure at the bottom is because of tensile concerns and at the top because of compression. Also, matrix tensile and compressive failure are often found together in the same layer. It is also revealed that tensile failures impact the entire laminate while compression only impacts the top layers.
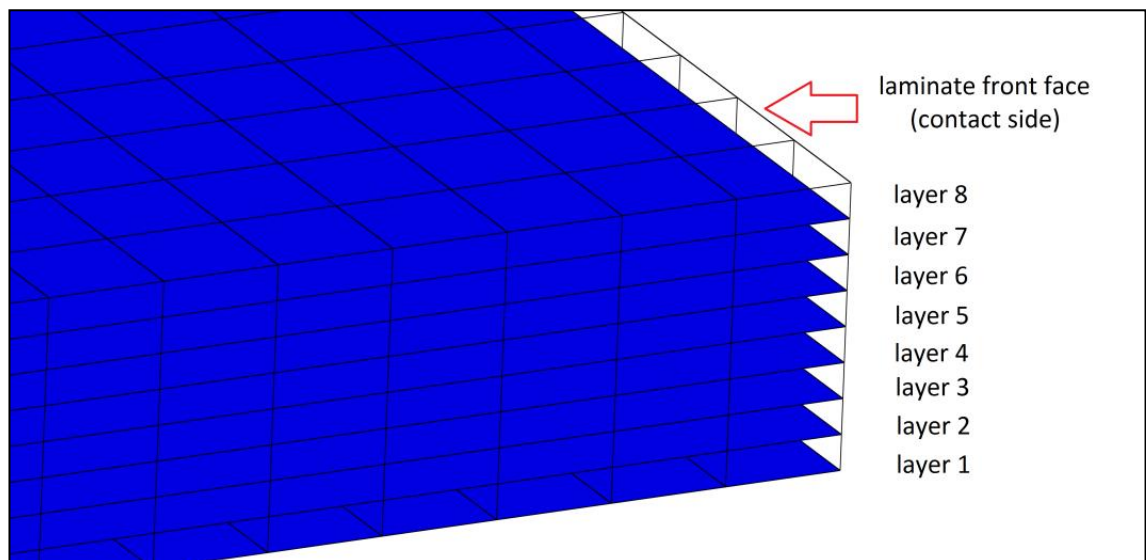
Figure 4.13. Shows the arrangement of layers in the laminate.

Compressive fiber	[1] 0	[2] 90	[3]+45	[4] -45	[5] -45	[6]+45	[7] 90	[8] 0
Tensile fiber	[1] 0	[2]90	[3]+45	[4]-45	[5]-45	[6] +45	[7]90	[8] 0
Compressive matrix	[1]0	[2]90	[3]+45	[4] -45	[5] -45	[6]+45	[7]90	[8] 0
Tensile matrix	[1]0	[2]90	[3]+45	[4]-45	[5] -45	[6] +45	[7] 90	[8] 0

Figure 4.14. (a) Hashin fiber and matrix failure evolution criteria of carbon fibers specimen predicted by Finite Element model under 10 J impact energy load.

Compressive fiber	[1] 0	[2] 90	[3]+45	[4] -45	[5] -45	[6]+45	[7] 90	[8]0
Tensile fiber	[1] 0	[2] 90	[3]+45	[4] -45	[5] -45	[6]+45	[7] 90	[8] 0
Compressive matrix	[1] 0	[2] 90	[3]+45	[4] -45	[5] -45	[6]+45	[7] 90	[8] 0
Tensile matrix	[1] 0	[2] 90	[3]+45	[4] -45	[5] -45	[6]+45	[7] 90	[8] 0

Figure 4.14. (b) Hashin fiber and matrix failure evolution criteria of carbon fibers specimen predicted by Finite Element model under 20 J impact energy load.

Compressive fiber	[1] 0	[2] 90	[3]+45	[4] -45	[5] -45	[6]+45	[7] 90	[8] 0
Tensile fiber	[1] 0	[2] 90	[3]+45	[4] -45	[5] -45	[6]+45	[7] 90	[8] 0
Compressive matrix	[1] 0	[2] 90	[3]+45	[4] -45	[5] -45	[6]+45	[7] 90	[8] 0
Tensile matrix	[1] 0	[2] 90	[3]+45	[4] -45	[5] -45	[6]+45	[7] 90	[8] 0

Figure 4.14. (c) Hashin fiber and matrix failure evolution criteria of carbon fibers specimen predicted by Finite Element model under 30 J impact energy load.

Compressive fiber	[1] 0	[2] 90	[3]+45	[4] -45	[5] -45	[6]+45	[7] 90	[8] 0
Tensile fiber	[1] 0	[2] 90	[3]+45	[4] -45	[5] -45	[6]+45	[7] 90	[8] 0
Compressive matrix	[1] 0	[2] 90	[3]+45	[4] -45	[5] -45	[6]+45	[7] 90	[8] 0
Tensile matrix	[1] 0	[2] 90	[3]+45	[4] -45	[5] -45	[6]+45	[7] 90	[8] 0

Figure 4.14. (d) Hashin fiber and matrix failure evolution criteria of carbon fibers specimen predicted by Finite Element model under 40 J impact energy load.

In order to understand e-glass impact results, the experiments were compared with the simulation. The ply area corresponds to an entirely damaged region in the simulation and are calculated accordingly and superimposed to find the complete damage profile. Through comparison, there is a noticeable match between keeping the shape. The simulation is best used for prediction of lower velocities. A computer was used to produce a model for continuum damage mechanics that predict the onset and growth of damage for low velocity impacts. They were carried out for e-glass epoxy plates in one direction. The history curves of the force time were contrasted to the experimental data. This information pointed to the requirement of adding plastic into the epoxy model. They had a strong match in results. The extent of damage on both front and back surfaces increases monotonically with the increased impact energy. Multiple shear damage modes occur when E-glass fiber/ epoxy composites are subjected to higher level of impact energy, Figure 4.15. a, b, c and d.

| Compressive fiber | [1] 0 | [2] 90 | [3]+45 | [4] -45 | [5] -45 | [6]+45 | [7] 90 | [8] 0 |

| Tensile fiber | [1] 0 | [2] 90 | [3]+45 | [4] -45 | [5] -45 | [6]+45 | [7] 90 | [8] 0 |

| Compressive matrix | [1] 0 | [2] 90 | [3]+45 | [4] -45 | [5] -45 | [6]+45 | [7] 90 | [8] 0 |

| Tensile matrix | [1] 0 | [2] 90 | [3]+45 | [4] -45 | [5] -45 | [6]+45 | [7] 90 | [8] 0 |

Figure 4.15. (a) Hashin fiber- matrix failure evolution criteria of E-glass fibers specimen predicted by Finite Element model under 10J impact energy load.

72
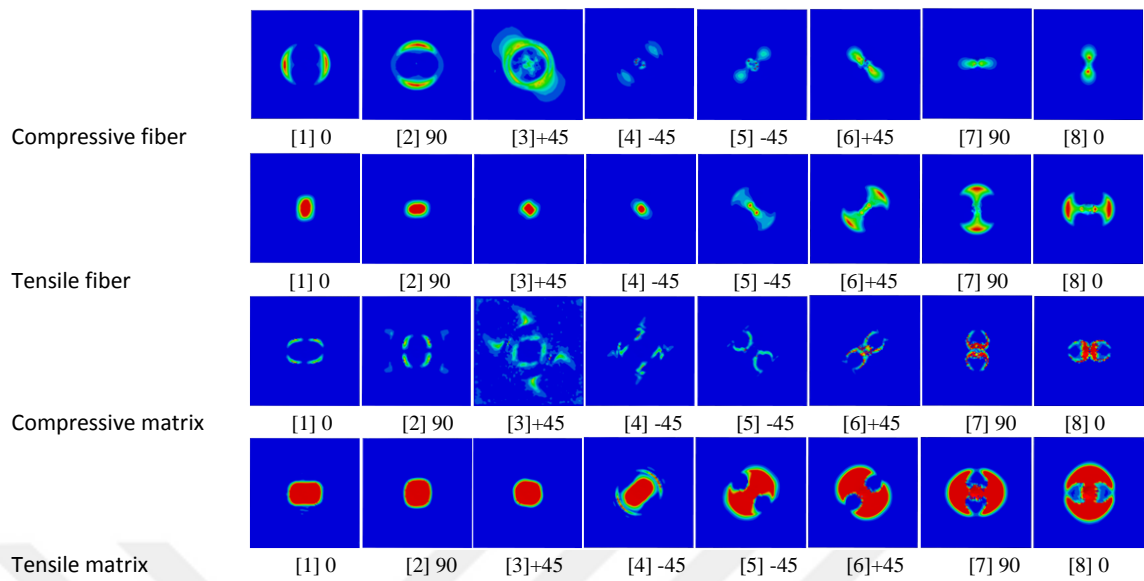
Figure 4.15. (b) Hashin fiber- matrix failure evolution criteria of E-glass fibers specimen predicted by Finite Element model under 20J impact energy load.
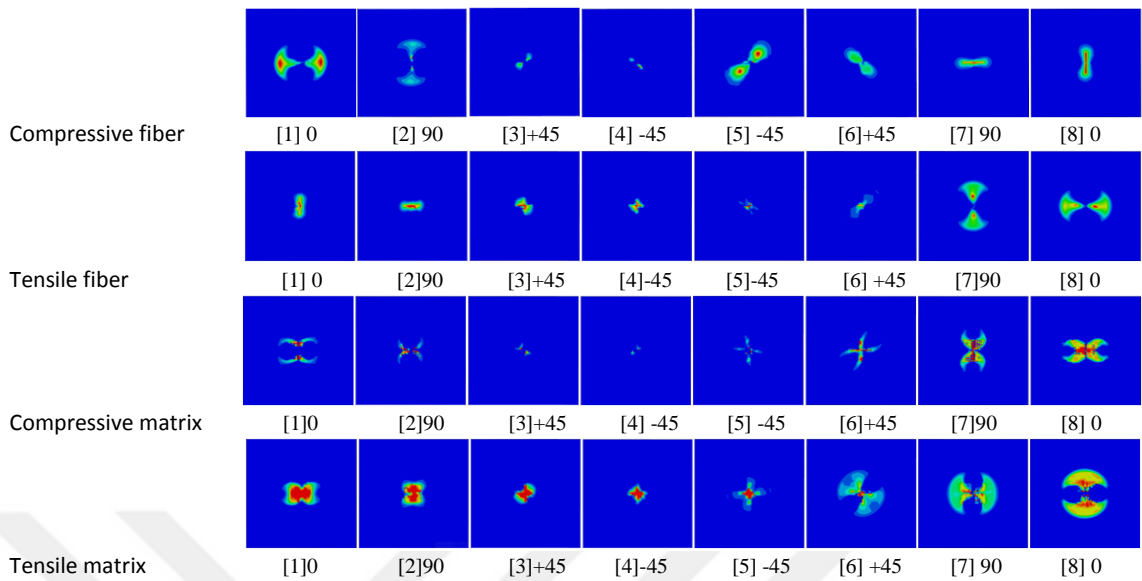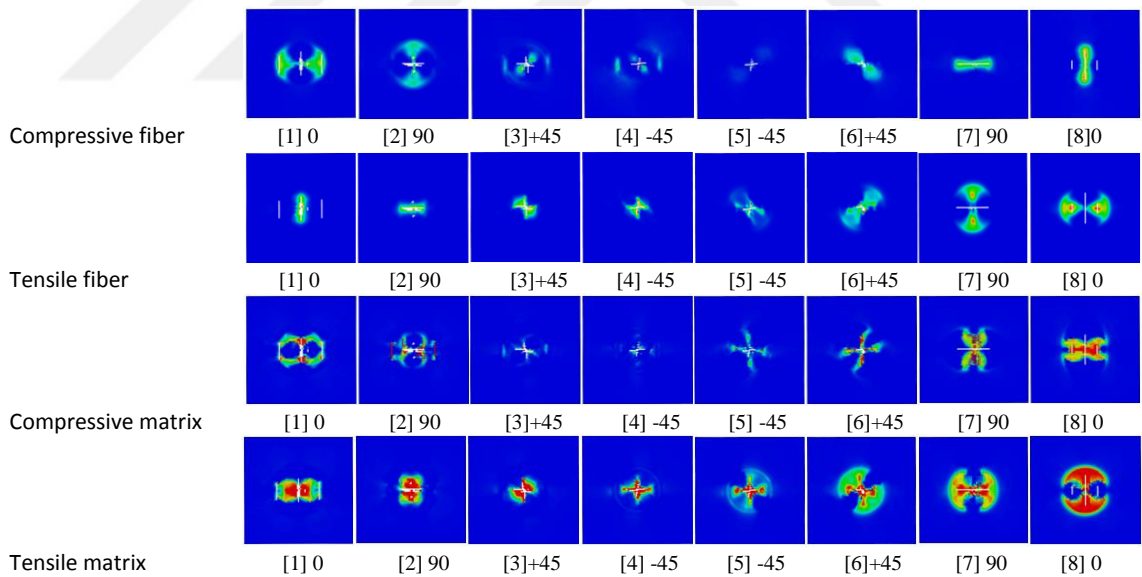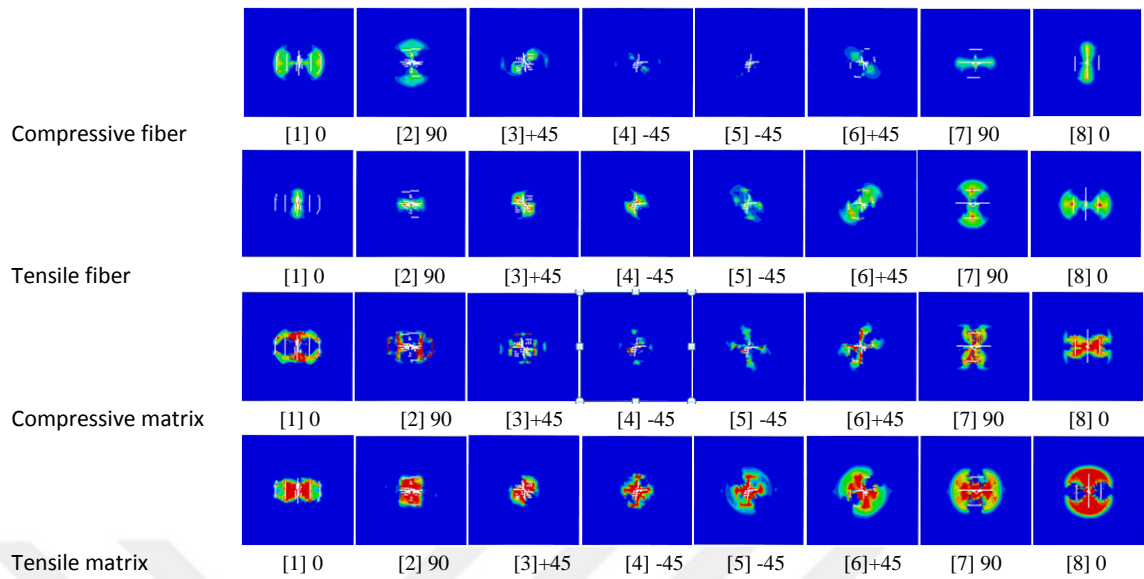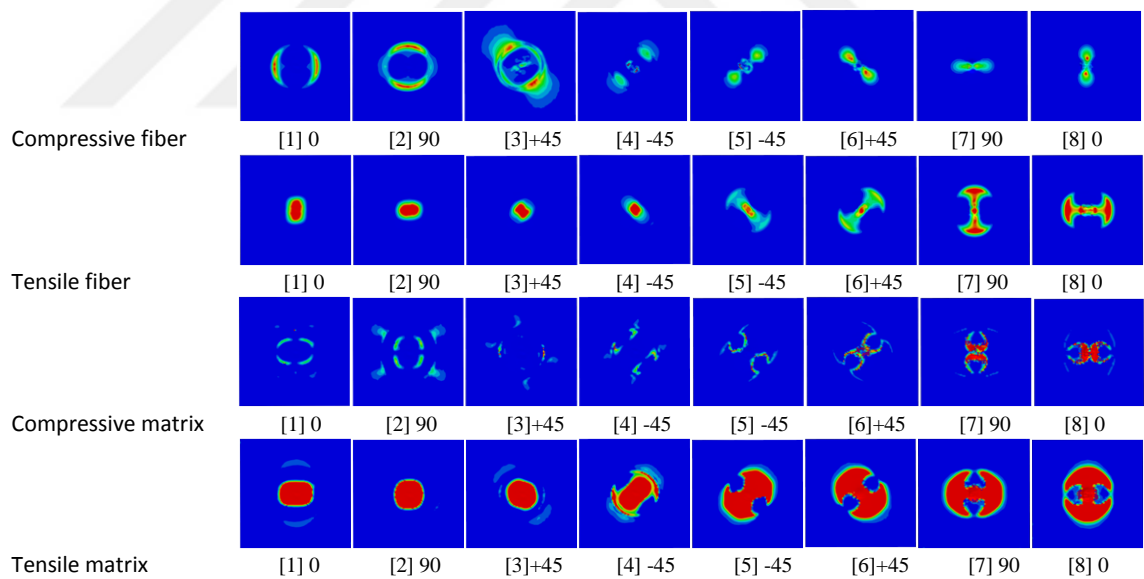

Figure 4.15. (c) Hashin fiber- matrix failure evolution criteria of E-glass fibers specimen predicted by Finite Element model under 30J impact energy load.

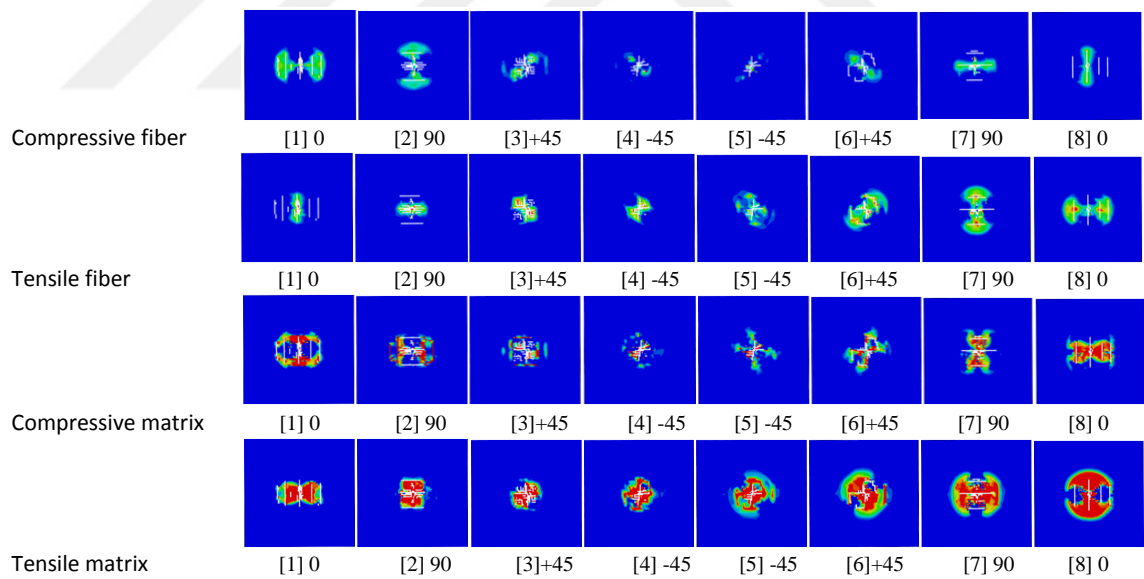|	[1] 0	[2] 90	[3]+45	[4] -45	[5] -45	[6]+45	[7] 90	[8] 0
Compressive fiber								

Figure 4.15. (d) Hashin fiber- matrix failure evolution criteria of E-glass fibers specimen predicted by Finite Element model under 40J impact energy load.

Figure 4.16 - 4.17 a, b, c and d show, Tensile fiber, Tensile matrix, Compressive fiber and Compressive matrix of the laminate at 10J , 20J, 30J and 40J impact load, respectively. Four damage variables in ABAQUS/ explicit are defined for hashin failure criteria hybrid (symmetrical and unsymmetrical) laminate.
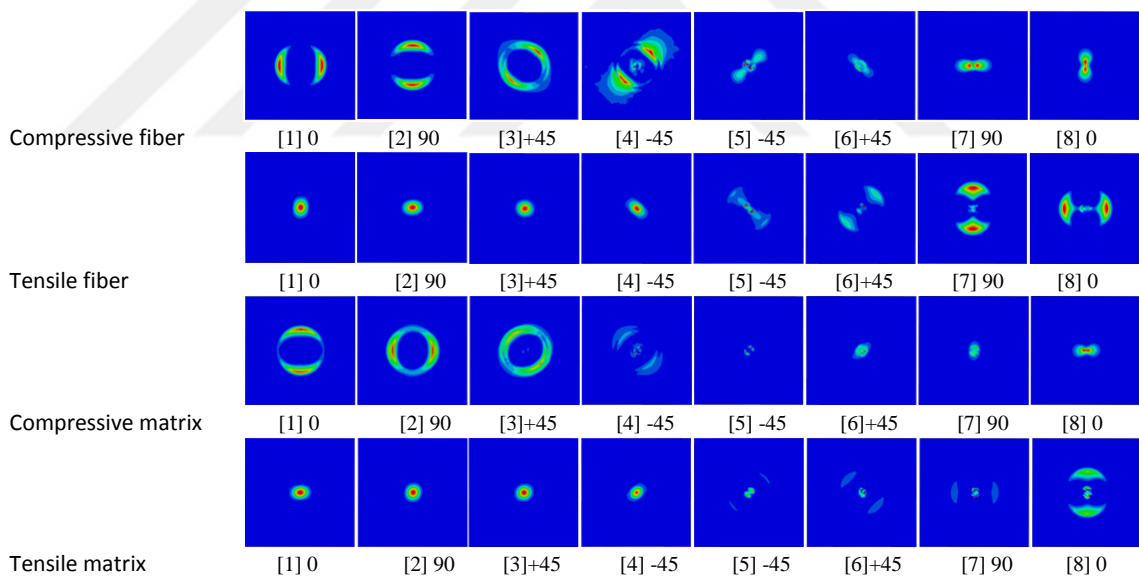

Figure 4.16. (a) Hashin fiber- matrix failure evolution criteria of hybrid symmetrical specimen predicted by Finite Element model under 10 J impact energy load.

	[1] 0	[2] 90	[3]+45	[4] -45	[5] -45	[6]+45	[7] 90	[8] 0
Compressive fiber	[1] 0	[2] 90	[3]+45	[4] -45	[5] -45	[6]+45	[7] 90	[8] 0
Tensile fiber	[1] 0	[2] 90	[3]+45	[4] -45	[5] -45	[6]+45	[7] 90	[8] 0
Compressive matrix	[1] 0	[2] 90	[3]+45	[4] -45	[5] -45	[6]+45	[7] 90	[8] 0
Tensile matrix	[1] 0	[2] 90	[3]+45	[4] -45	[5] -45	[6]+45	[7] 90	[8] 0
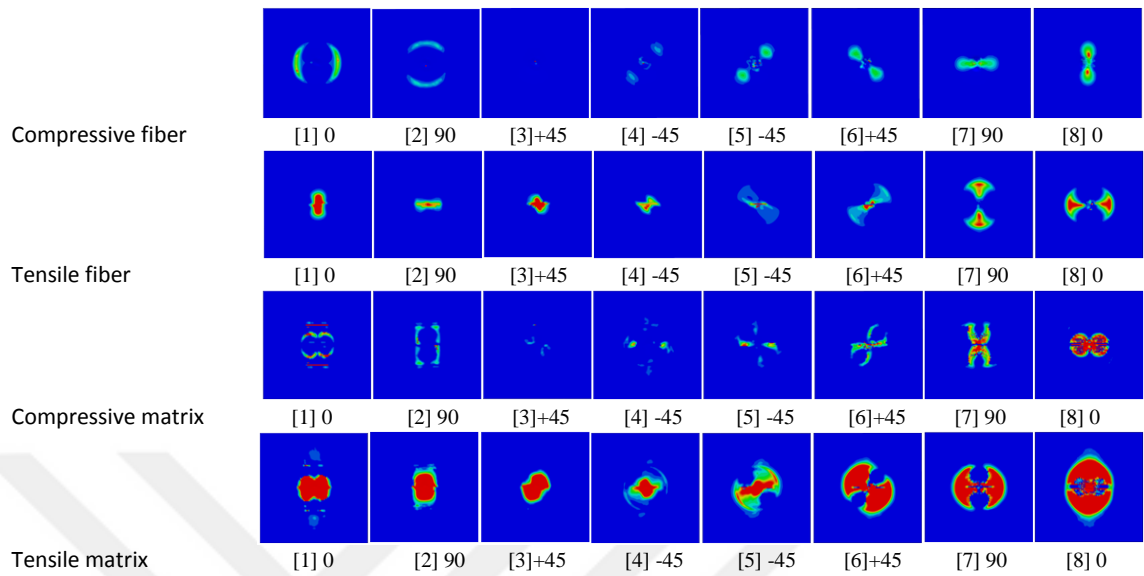
Figure 4.16. (b) Hashin fiber- matrix failure of hybrid symmetrical specimen predicted by Finite Element model under 20 J impact energy load.

|	[1] 0	[2] 90	[3]+45	[4] -45	[5] -45	[6]+45	[7] 90	[8] 0
Compressive fiber	[1] 0	[2] 90	[3]+45	[4] -45	[5] -45	[6]+45	[7] 90	[8] 0
Tensile fiber	[1] 0	[2] 90	[3]+45	[4] -45	[5] -45	[6]+45	[7] 90	[8] 0
Compressive matrix	[1] 0	[2] 90	[3]+45	[4] -45	[5] -45	[6]+45	[7] 90	[8] 0
Tensile matrix	[1] 0	[2] 90	[3]+45	[4] -45	[5] -45	[6]+45	[7] 90	[8] 0
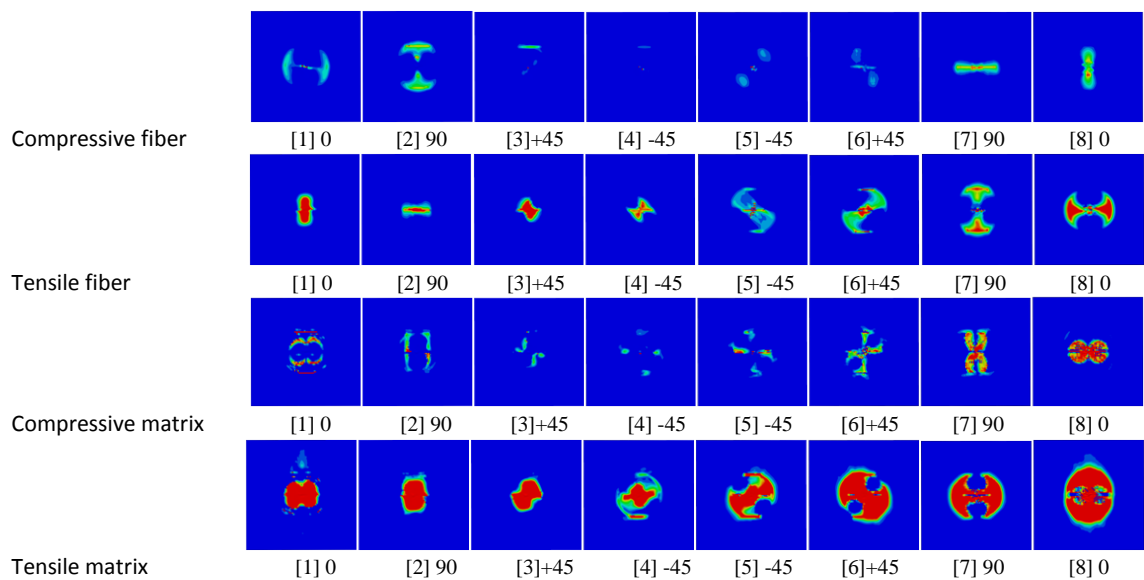
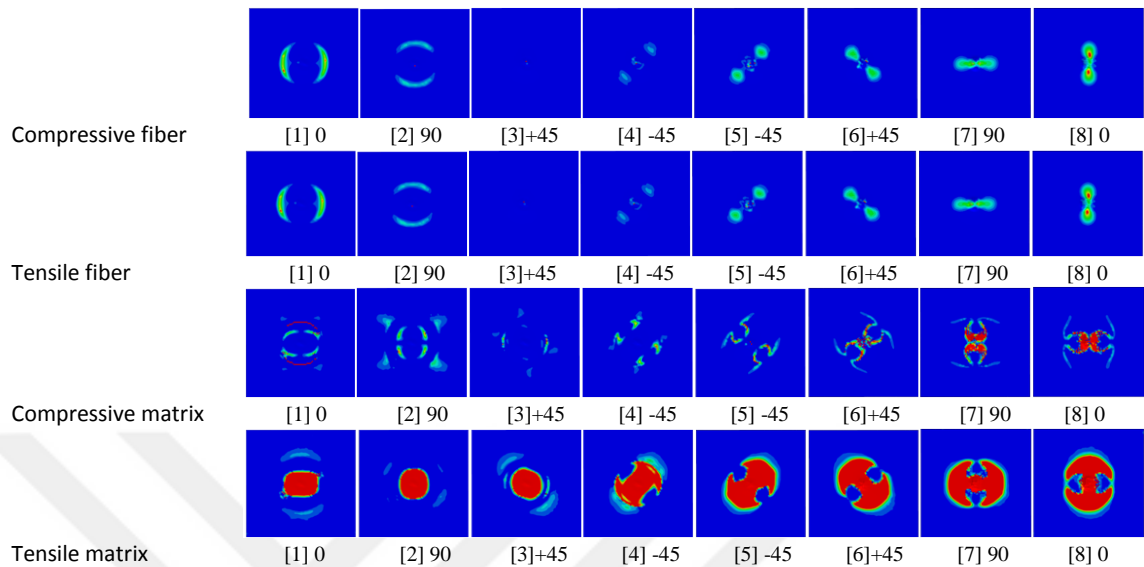Figure 4.16. (c) Hashin fiber- matrix failure of hybrid symmetrical specimen predicted by Finite Element model under 30 J impact energy load.
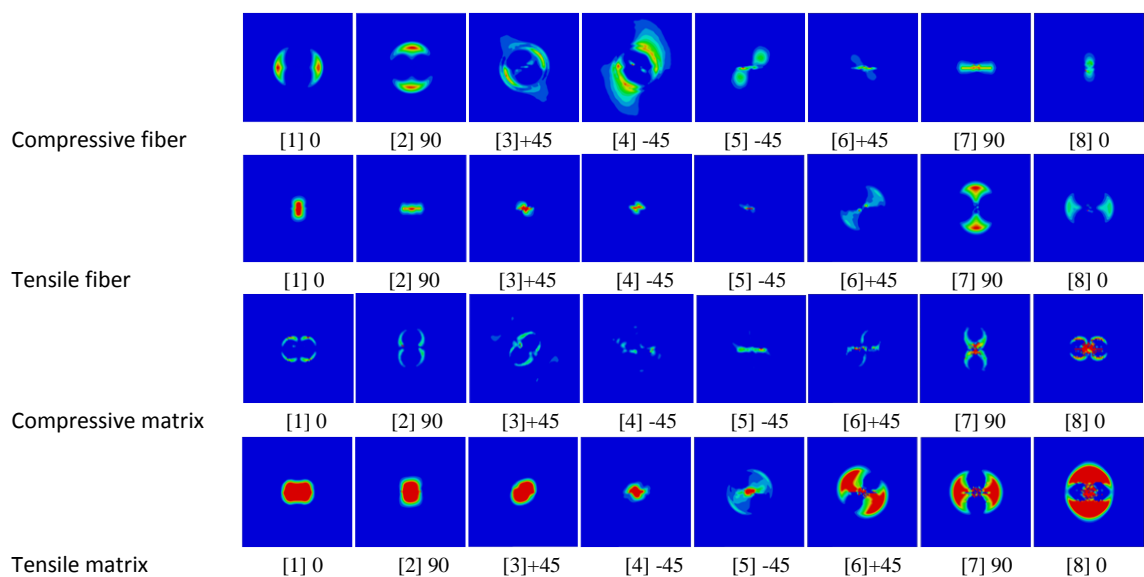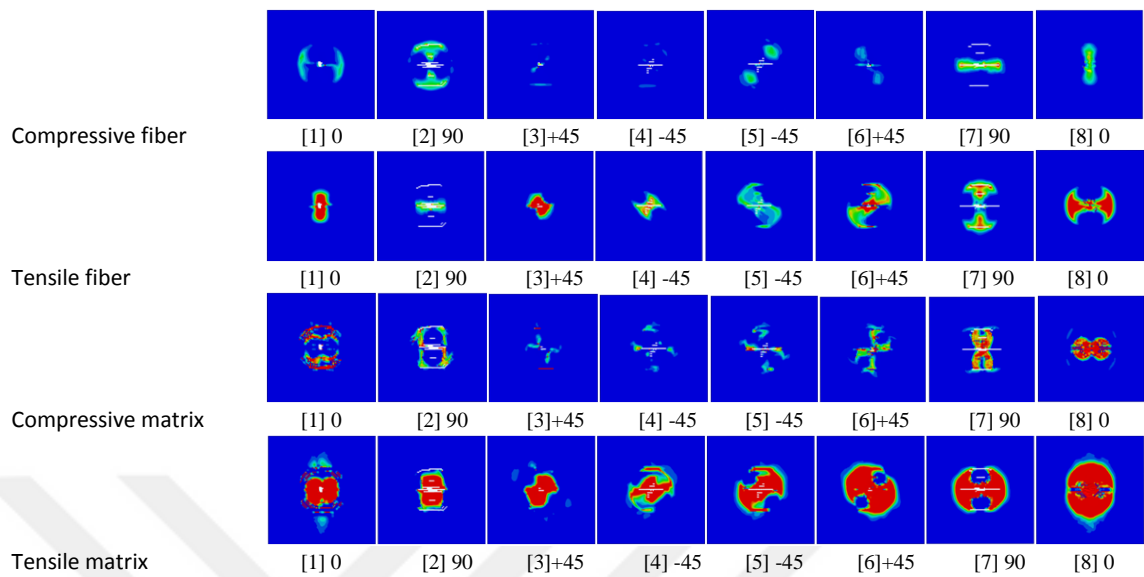
Figure 4.16. (d) Hashin fiber- matrix failure of hybrid symmetrical specimen predicted by Finite Element model under 40 J impact energy load.

In this section, a fresh model was presented that mixes the benefits of micromechanics and modelling to predict modes of failures and how structures respond. This was focused around a hybrid composite reinforced with plastic under low velocity impact. The new theory explained the fiber and matrix components and the impactor force. The study compared results from impacts of 10, 20, 30, and 40J.

The signs of shear damage on top surface show that the matrix cracking is initiated during the impact testing, and the numerical simulation also shows the tensile stress on transverse direction of top layer exceed the limitation after the elastic stage and satisfy the damage initiation criteria of progressive damage model.

Compressive fiber [1] 0 [2] 90 [3]+45 [4] -45 [5] +45 [6] -45 [7] 90 [8] 0

Tensile fiber [1] 0 [2] 90 [3]+45 [4] -45 [5] +45 [6] -45 [7] 90 [8] 0

Compressive matrix [1] 0 [2] 90 [3]+45 [4] -45 [5] +45 [6] -45 [7] 90 [8] 0

Tensile matrix [1] 0 [2] 90 [3]+45 [4] -45 [5] +45 [6] -45 [7] 90 [8] 0

Figure 4.17. (a) Hashin fiber- matrix failure evaluation of hybrid unsymmetrical (the impact from carbon layer side) specimen predicted by Finite Element model under 10J impact energy load.

Compressive fiber [1] 0 [2] 90 [3] +45 [4] -45 [5] +45 [6] -45 [7] 90 [8] 0

Tensile fiber [1] 0 [2] 90 [3] +45 [4] -45 [5] +45 [6] -45 [7] 90 [8] 0

Compressive matrix [1] 0 [2] 90 [3] +45 [4] -45 [5] +45 [6] -45 [7] 90 [8] 0

Tensile matrix [1] 0 [2] 90 [3] +45 [4] -45 [5] +45 [6] -45 [7] 90 [8] 0

Figure 4.17. (b) Hashin fiber- matrix failure evaluation of hybrid unsymmetrical (the impact from carbon layer side)specimen predicted by Finite Element model under 20J impact energy load.

Compressive fiber	[1] 0	[2] 90	[3] +45	[4] -45	[5] +45	[6] -45	[7] 90	[8] 0
Tensile fiber	[1] 0	[2] 90	[3] +45	[4] -45	[5] +45	[6] -45	[7] 90	[8] 0
Compressive matrix	[1] 0	[2] 90	[3] +45	[4] -45	[5] +45	[6] -45	[7] 90	[8] 0
Tensile matrix	[1] 0	[2] 90	[3] +45	[4] -45	[5] +45	[6] -45	[7] 90	[8] 0

Figure 4.17. (c) Hashin fiber- matrix failure evaluation of hybrid unsymmetrical (the impact from carbon layer side) specimen predicted by Finite Element model under 30J impact energy load.

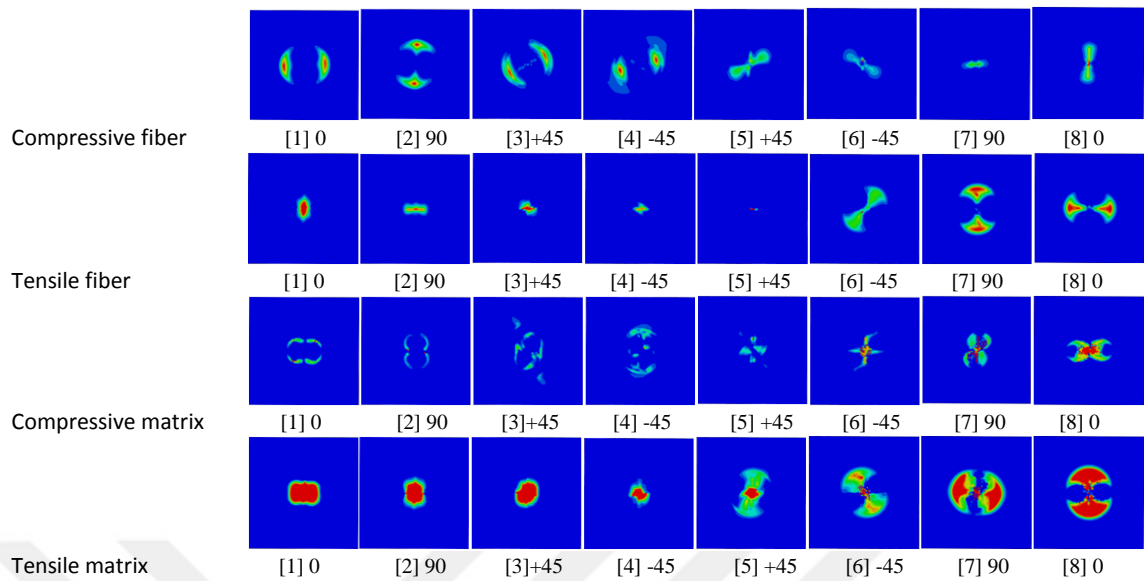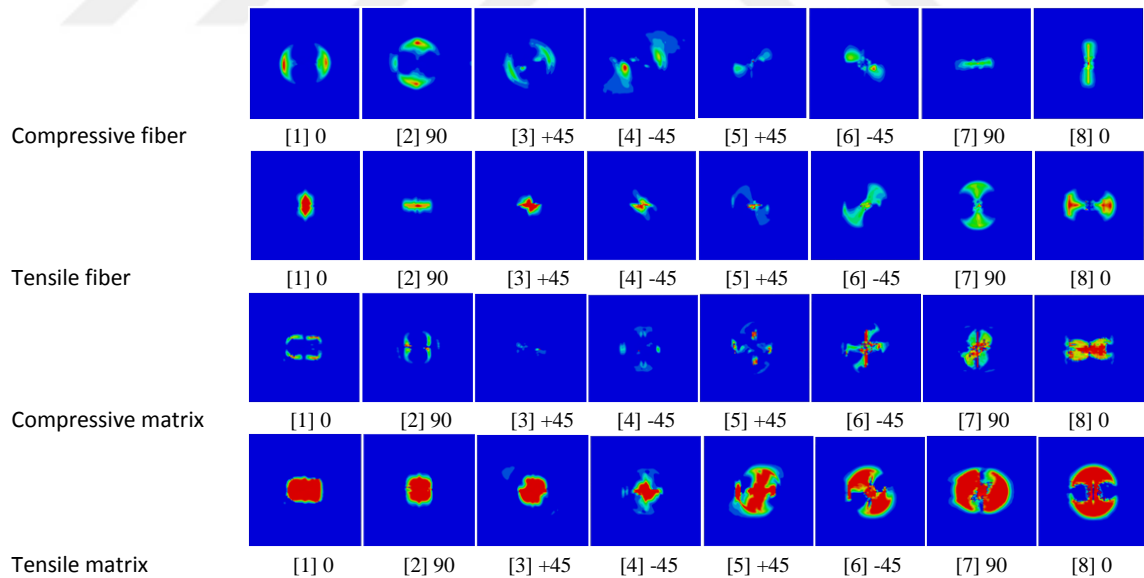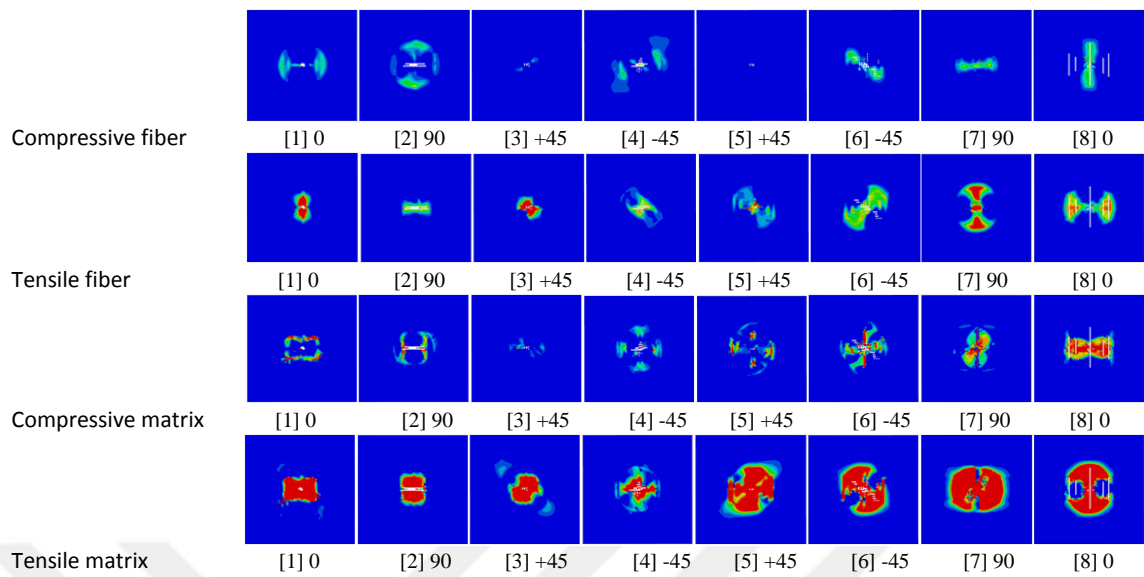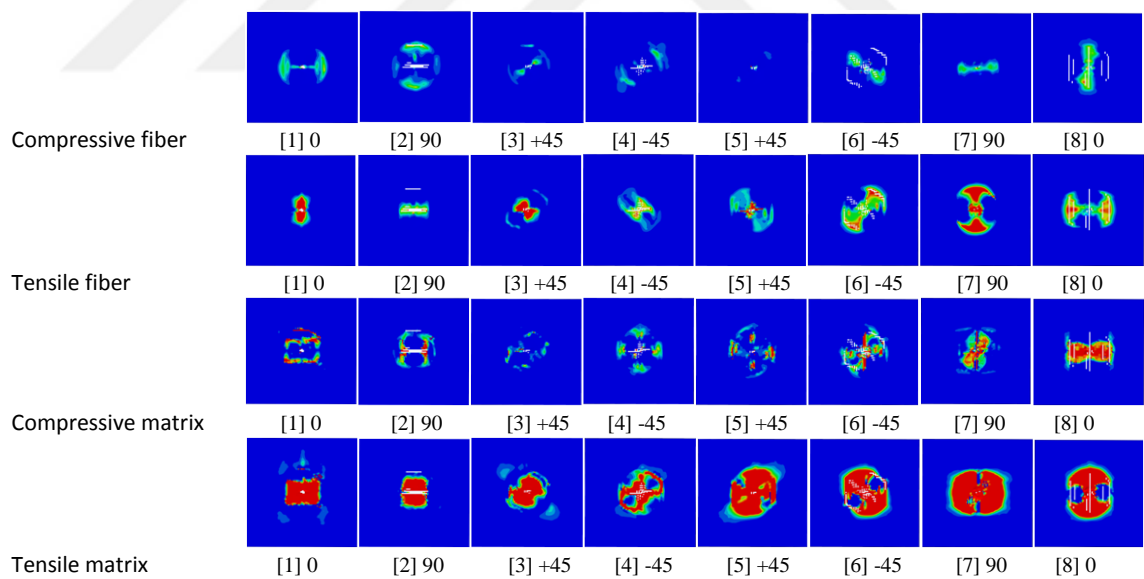| Compressive fiber | [1] 0 | [2] 90 | [3] +45 | [4] -45 | [5] +45 | [6] -45 | [7] 90 | [8] 0 |
Tensile fiber	[1] 0	[2] 90	[3] +45	[4] -45	[5] +45	[6] -45	[7] 90	[8] 0
Compressive matrix	[1] 0	[2] 90	[3] +45	[4] -45	[5] +45	[6] -45	[7] 90	[8] 0
Tensile matrix	[1] 0	[2] 90	[3] +45	[4] -45	[5] +45	[6] -45	[7] 90	[8] 0

Figure 4.17. (d) Hashin fiber- matrix failure evaluation of hybrid unsymmetrical (the impact from carbon layer side) specimen predicted by Finite Element model under 40J impact energy load.

CHAPTER FIVE

CONCLUSION

Low-velocity impacts on unidirectional carbon, E-glass and hybrid fiber/ epoxy laminates composites were studied using experiments and numerical calculations for improving damage mechanisms in new materials. The tests were carried out for various levels of impact energy and in varying experiment designs so that a massive database could be studied, compared, and analyzed.

There are several damage modes after composites are impacted during the experimental tests. These include cracking in the matrix, delamination, and breaking of fibers. They can occur individually or in conjunction

When studying the hybrid samples, it becomes clear that damage is similar to that of the carbon samples. They showed the same levels of: splitting, indentation, and cracks.

The contact force increases by increasing impact energy, the peak of force line from contact force time histories diagrams also increases.

The finite element software was efficient in simulating the necessary situations for the research and predicted the proper modes of failure. A model of 100 x 100 x 2mm carbon/epoxy, E-glass/epoxy and hybrid/epoxy laminate plates with 8 ply and impactor was successfully modelled for the low velocity impact damage analyses.

In the present work, validation and convergence study is carried out by using ABAQUS/explicit software, to simulate the different impact tests with reasonable computational times (a few hours).

Validation study show good agreement in contact force , kinetic energy and time histories graphs between numerical and experimental results.

The parametric study using finite element method with varying impact energy and boundary conditions is helpful to understand the response of composite laminate under low velocity impact.

It seems that impact damage mechanisms are described accurately by the model using finite element method. Moreover, the predictions of impact damage and impact responses obtained with this approach are in good agreement with the available experiments.

The Hashin theory was used with four characteristics to understand the progressive damage initiation: fiber tension and compression, and matrix tension and compression. The prediction of the response and modes of failure from Finite element method agree with the experimentation. The main mode of failure is tension to the matrix which starts at the base and moves to the direction of the fiber. Matrix compression begins at the top and also moves towards the fiber.

REFERENCES

1. Pegoretti A., Fabbri E., Migliaresi C. and Pilati F., (2004). Intraply and interply hybrid composites based on E-glass and poly(vinyl alcohol) woven fabrics: tensile and impact properties, **Polymer International,53**:1929-1297.

2. Shi Y. and Soutis C., (2017). Modelling low velocity impact induced damage in composite laminates, **Mechanics of Advanced Materials and Modern Processes**, 3:14.

3. Grasso M., Penta F., Pucillo G., Ricci F. and Rosiello V., (2015). Low Velocity Impact Response of Composite Panels for Aeronautical Applications, Proceedings of the World Congress on Engineering, WCE 2015, London, U.K., July 1-3.

4. Nisini E., Santulli C. and Liverani A., (2017). Mechanical and impact characterization of hybrid composite laminates with carbon, basalt and flax fibres, **Composite part B, 127**:92-99.

5. Abir M., Tay T., Ridha M. and Lee H., (2017). Modelling damage growth in composites subjected to impact and compression after impact, **Composite Structures, 168**:13-25.

6. Rajesh N. and Jerald J.,(2010). Experimental Investigation of Woven E-Glass Epoxy Composite Laminates Subjected to Low-Velocity Impact at Different Energy Levels, **Journal of Minerals & Materials Characterization & Engineering, 9** (7), 643-652.

7. Singh H., Namala K. and Mahajan P., (2015).A damage evolution study of E-glass/epoxy composite under low velocity impact, **Composite part B, 76**:235-248

8. Duodu E., Gu J., Ding W., Shang Z. and Tang S.,(2017). Comparison of Ballistic Impact Behavior of Carbon Fiber/Epoxy Composite and Steel Metal Structures**, Iran J Sci Technol Trans Mech Eng**, Shiraz University,.

9. Liao B. and Liu P., (2017). Finite element analysis of dynamic progressive failure of plastic composite laminates under low velocity impact, **Composite Structures, 159**:567-578.

10. Feng D. and Aymerich F., (2014). Finite element modelling of damage induced by low-velocity impacton composite laminates, **Composite Structures, 108**:161-171.

11. Li Z., Khennane A., Hazell P. and Brown A., (2017). Impact behaviour of pultruded GFRP composites under low-velocity impact loading, **Composite Structures, 168**:360-371.

12. Singh H. and Mahajan P., (2015). Modeling damage induced plasticity for low velocity impact simulation of three dimensional fiber reinforced composite, **Composite Structures, 131**:290-303.

13. Ahmed A. and Wei L.,(2015). The low-velocity impact damage resistance of the composite structures –A review, **Rev.Adv.Master.Sci, 40**:127-145.

14. Bienias J.,Jakubczak P. and Dadej K.,(2016). Low-velocity impact resistance of aluminum glass laminates –Experimental and numerical investigation, **Composite Structures, 152**:339-348.

15. Chang F.,Choi H. and Jeng S., (1990). Study on impact damage in laminated composites, **MechanicsofMaterials,10**:83- 95.

16. Xu Z., Yang F., Guan Z. and Cantwell W.,(2016). An experimental and numerical study on scaling effects in the low velocity impact response of CFRP laminates, **Composite Structures, 154**:69-78.

17. Caminero M., Moreno I. and Rodríguez G., (2017). Damage resistance of carbon fibre reinforced epoxy laminates subjected to low velocity impact: Effects of laminate thickness and ply-stacking sequence, polymer testing,36:530-541.

18. Cheng X., Du X., ZhangJie, Zhang J., Guo X. and Bao J.,(2018). Effects of stacking sequence and rotation angle of patch on low velocity impact performance of scarf repaired laminates, **Composite part B, 133**:78-85.

19. Lou X., Cai H., Yu P., Jiao F. and Han X.,(2017). Failure analysis of composite laminate under low-velocity impact based on micromechanics of failure, **Composite Structures, 163**:238-247.

20. Jagtap K., Ghorpade S., Lal A. and Singh B.,(2017). Finite Element Simulation of Low Velocity Impact Damage in Composite Laminates, **Materials Today: Proceedings 4**: 2464–2469.

21. LiuP., Liao B., Jia L. andPeng X.,(2016). Finite element analysis of dynamic progressive failure of carbon fibercomposite laminates under low velocity impact, **Composite Structures, 149**:408-422.

22. Ravandia M., Teo W., Tran L., Yong M. and Tay T.,(2017). Low velocity impact performance of stitched flax/epoxy composite laminates,**Composite Part B, 117**:89-100.

23. Antonucci V.,Ricciardi M., Caputo F., Langella A., Lopresto V., Riccio A.and ZarrelliM.,(2014). Low Velocity Impact Response Of Carbon Fibre Laminates Made By Pulsed Infusion, **Procedia Engineering, 88**:230–234.

24. Wang H., Long S., Zhang X. and Yao X.,(2018). Study on the delamination behavior of thick composite laminates under low energy impact, **Composite Structures, 184**:461-473.

25. TirillòJ., Ferrante L., Sarasini F., Lampani L., Barbero E., Sáez S.,Valente T. and Gaudenzi P.,(2017). High velocity impact behaviour of hybrid basalt-carbon/epoxy, **Composite Structures, 168**:305-312.

26. Boria S., Scattina A. and Belingardi G.,(2017). Impact behavior of a fully thermoplastic composite, **Composite Structures,167**:63-75.

27. Camanho P., Arteiro A., Melro A., Catalanotti G. and Vogler M.,(2015). Three-dimensional invariant-based failure criteria for fibre-reinforced composites, **International Journal of Solids and Structures, 55**:92-107.

28. Daniel M D,(2016). Yield and failure criteria for composite materials under static and dynamic loading, **Progress in Aerospace Sciences,81**:18-25.

29. Bienias J., Dadej K. and Surowska B.,(2017). Interlaminar fracture toughness of glass and carbon reinforced multidirectional fiber metal laminates, **Engineering Fracture Mechanics, 175**:127-145.

30. MitchellC.,Dangora L. and Sherwood J.,(2016).Investigation into a robust finite element modelfor composite materials, **Finite Element in Analysis and Design, 115**:1-8.

31. Banerjee S. and Sankar B.,(2014). Mechanical properties of hybrid composites using finite element method based micromechanics, **Composite: Part B, 58**:318-327.

32. Azzam A. andLi W.,(2014). An experimental investigation on the three-point bending behavior of composite laminate, **Materials Science and Engineering,62**: 012-016.

33. Olodo E., Adanhounme V., Adjovi E. and Shambina S.,(2014). Experimental study of a woven fiberglass composite delamination under impact shock, **Engineering Solid Mechanics, 2**:163-172.

34. Reghunath R., Lakshmanan M. and Mini K.,(2015). Low velocity impact analysis on glass fiber reinforced composites with varied volume fractions, **Materials Science and Engineering, 73**:012-067.

35. Mouti Z., Westwood K., Kayvantash K. and Njuguna J.,(2010). Low Velocity Impact Behavior of Glass Filled Fiber-Reinforced Thermoplastic Engine Components, **Materials, 3**: 2463-2473.

36. Bieniaś J. and Jakubczak P., (2012). Low Velocity Impact Resistance Of Aluminum/Carbon-Epoxy Fiber Metal Laminates, **Composites Theory and Practice**,197-3193 :12.

37. Nassr A., Yagi T., Maruyama T. and Hayashi G., Damage and wave propagation characteristics in thin GFRP panels subjected to impact by steel balls at relatively low-velocities, **International Journal of Impact Engineering, 111**:21-33.

38. ParkH.,(2017). Investigation on low velocity impact behavior between graphite/epoxy composite and steel plate, **Composite Structures, 171**:126-130.

39. Dogan A. and Arikan V.,(2017). Low-velocity impact response of E-glass reinforced thermoset and thermoplastic based sandwich composites, **Composite Part B, 127**:63-69.

40. Salvettia M., Sbarufatti C., Gilioli A., Dziendzikowski M., Dragan K., Manes A. and Giglio M.,(2017). On the mechanical response of CFRP composite with embedded optical fibre when subjected to low velocity impact and CAI tests, **Composite Structures, 179**:21-34.

41. Staab GH,(1992).Laminar Composites,Butterworth Heınemann.

42. Richardson, T.,(1987). Composites: A Design Guide. Industrial Press Inc., New York,.

43. DanielI.M. and IshaiO.,(1994). Engineering Mechanics of Composite Materials. Oxford University Press. New York Oxford.

44. Bader M. G., (1994). "Hybrid effect", Handbook of Polymer-fibre Composites, Longman Scientific Technical, pp. 225-230.

45. Schwartz M. M., (1988). "Composite Materials Handbook", McGraw Hill.

46. Durão L.M.,(2005). Machining of Hybrid Composites, PhD. Thesis, University of Porto, Porto.

47. Matthews F. L., Davies.,G.A.O., Hitchings D. and Soutis C.,(2000). Finite element modeling of composite materials and structures, Cambridge: Wood head Publishing Ltd. and CRC Press LLC.

48. Mazumdar,S.K.,(2002). Composites manufacturing: materials product and process Engineering, USA: CRC Press LLC.

49. Ghanbari E.,(2011). Bolt-Hole Tightening Effects in Single lap Composite Bolted Joints, Dokuz Eylül University, Turkey.

50. Keulen, C.,(2006). Design and manufacturing of composite structures using the resin transfer molding technique. M.Sc Thesis, University of Victoria, Canada.

51. Wang H. Y and Shie J. J.,(2009). Effect of autoclave curing on the compressive strength and elastic modulus of light weight aggregate concrete, **Journal of ASTM International, 6**(6).

52. Balya B.,(2004). Design and analysis of filament wound composite tubes.M.Sc Thesis, Middle East Technical University, Turkey.

53. Shukla P.S., (2011). Investigation into tribo potential of ricehusk (RH) char reinforced epoxy composite. M.Sc Thesis, National Institute of Technology Rourkela, India.

54. Grimsley B.W.,(2005). Characterization of the vacuum assisted resin transfer molding process for fabrication of aerospace composites, M.Sc Thesis, Virginia Polytechnic Institute and State University, USA.

55. Bundy C.B.,(2005). Use of pultruded carbon fiber/epoxy inserts as reinforcement in composite structures. M.Sc Thesis, Montana State University, USA.

56. Dhananjayan K. V.,(2013). Design and analysis of acompression molded carbon composite wheel center. M.Sc Thesis, The University of Texas, USA.

57. IpekH.,(2005). Modeling of resin transfer molding for composite manufacturing, M.Sc Thesis, Middle East Technical University, Turkey.

58. Mallick P. K.,(2007). Fiber reinforced composites materials manufacturing and design(3rd ed.). NY: CRC Press.

59. Berk B., (2014). Finite Element Simulation of Ballistic Impact on Composite Plates, M Sc Thesis, DokuzEylül University, Turkey.

60. Paul B., (1960). "Predictions of Elastic Constants of Multiphase Materials," Transact. Metallurg. Soc. AIME, 36-41.

61. Hashin Z.and Rosen B.W., (1965). "The Elastic Moduli of Fiber-Reinforced Materials,' J. Appl. Mech., Transact. **ASME, 31**, 233.

62. J.Halpin C. and Tsai S.W.,(1969). "Effects of Environmental Factors on Composite Materials," AFML-TR 67-423, Dayton, OH.

63. Rosen B.W.,(1964). "Tensile Failure of Fibrous Composites," A/AA J., 2(11), 1985.

64. Broutman L.J.,(1965). "Glass-Resin Joint Strengths and Their Effect on Failure Mechanisms in Reinforced Plastics," Modem Plast.

65. GreszezukL. B.,(1974). "Microbuckling Failure of Circular Fiber Reinforced Composites," AIAA/ ASME/SAE 15th Structure, Structural Dynamics and Materials Conference, Las Vegas, NV.

66. CollingsT.A.,(1974). "Transverse Compressive Behavior of Unidirectional Carbon Fibre Reinforced Plastics," **Composites, 5**(3), 108.

67. Agarwal D., BroutmanJ. and Chandrashekhara K., (2015). Analysis and Performance of Fiber Composites, Third Edition, Reprinted.

68. Kelkar A. D,SankarJ and Grace C.,(1997). Behavior of tensile preloaded composites subjected to low-velocity impact loads. In: Recent advances in solids/structures and application ofmetallicmaterials.**ASME,369**:39–46.

69. Chiu S. T., Liou Y. Y., Chang Y. C. and Ong C. L., (1997). Low velocity impact behavior of prestressed composite laminates. **Mater Chem Phys, 47**:268–72.

70. Babu S. and Shivanand H.,(2008). Impact Analysis of Laminated Composite on Glass Fiber and Carbon Fiber, 9001:2459-2250 .

71. Hashin Z., (1980). "Failure Criteria for Unidirectional Fiber Composites, **Journal of Applied Mechanics, 47**, 329–334.

72. Hashin Z. and Rotem A. , (1973). "A Fatigue Criterion for Fiber-Reinforced Materials," **Journal of Composite Materials,7**, 448–464.

73. Lapczy k. I., and Hurtado J. A., (2007). "Progressive Damage Modeling in Fiber-Reinforced Materials," Composites Part A: **Applied Science and Manufacturing, 38, (**11), 2333–2341.

74. Abaqus Analysis User's Guide (Ver. 6.14), 2014.

75. Lapczyk I and Hurtado J.A. (2007). Progressive damage modeling in fiber-reinforced materials. **Compos A;38**:2333–41.

76.Camanho P.P. and Da'vila C.G. (2002). Mixed-mode decohesion finite elements for the simulation of delamination in composite materials. NASA/TM-2002–211737, pp. 1–37.

77. Rozylo P., Debski H. and Kubiak T.,(2017). A model of low-velocity impact damage of composite plates subjected to Compression-After-Impact **(CAI) testing, composite structure, 181**: 158-170.

78. Aktaş M.,(2007). Temperature effect on impact behavior of laminated composite plates. Phd Thesis. Dokuz Eylül University,.

79. Mater Des, 60 :520–53,1(2014).

CURRICULUM VITAE

PERSONAL INFORMATION

Name , surname   : MOHAMMED MEZHER JABBAR AL-RUBAYE

Nationality   : Iraq

Birth date and place : 17 July 1987, BAGHDAD

Social status   : Marred

Tel   : +9647713317671

E-mail   : mohammedmezher38@gmail.com

Address   : Bahcelievler Mah., Bismil Sok., Aslaner Apt. 1/16 ,

                                        Talas/ Kayseri

EDUCATION

Degree	İnstitution	Date of graduation
MSc	ERU Instituteof Science and Technology	-
License	University of Baghdad.	2009
High school	AL- Jwahrey School	2005

Experiences

Year	Place
2010 – until now	Diyala Governorate

FOREIGN LANGUAGE

English